Nanofinishing of BK7 Glass Using Magnetorheological Finishing Technique with Solid Core Rotating Tool

A dissertation submitted in partial fulfilment of requirement for the award of degree of

Master of Engineering

in

Production Engineering

Submitted by

Sumit Kumar

Roll No.: 801585026

Under the guidance of

Dr. ANANT KUMAR SINGH

Assistant Professor

DEPARTMENT OF MECHANICAL ENGINEERING

THAPAR UNIVERSITY

PATIALA (PB), INDIA, 147004

July, 2017

CERTIFICATE

I hereby declare that the work done in this thesis entitled "**Nanofinishing of BK7 Glass Using Magnetorheological Finishing Technique with Solid Core Rotating Tool**" submitted towards partial fulfilment of requirement for award of degree of **Master of Engineering** in **Production Engineering, Thapar University, Patiala,** is an authentic record of the work carried out by me under the supervision and guidance of **Dr. Anant Kumar Singh, Assistant Professor, Mechanical Engineering Department, Thapar University, Patiala.**

The matter embodied in this report has not been submitted in part or full to any other university or institute for the award of any degree.

Dated: 01/08/2017

Sumit Kumar
(801585026)

This is to certify that above declaration made by the student concerned is correct to the best of our knowledge and belief.

01/08/2017

Dr. Anant Kumar Singh
Assistant Professor
Mechanical Engineering Department
Thapar University, Patiala

Dedicated to

My Father

"Who gave me the greatest gift anyone could give another person,

He believed in me"

ACKNOWLEDGEMENT

First and foremost I express my deepest sense of gratitude and a very sincere thanks to my advisor, **Dr. Anant Kumar Singh** who supported me through the path of this thesis work with his patience, knowledge, and invaluable guidance. His dynamic and diligent enthusiasm has been highly instrumental in keeping my spirits high. His flawless and forthright suggestions blended with an innate intelligent application have crowned my task with success.

I would like to thank **Dr. S. K. Mohapatra**, Head of Mechanical Department, Thapar university for the intellectual support and unyielding encouragement.

I am thankful to Mr. Ravi Bhardwaj owner of Inra Optics who has always been available for discussions about BK7 glass and its applications. I would like to express my gratitude towards my parents for their kind co-operation and encouragement which help me in completion of this research.

I would like to express my special thanks to School of Physics & Materials Science and Metrology Laboratory of Mechanical Department, Thapar University, NRF Laboratory IIT Delhi and School of Mechanical, Materials and Energy Engineering, IIT Ropar for experimentation and testing part of my dissertation.

Sumit Kumar

Abstract

Surface finishing is a promising method to improve the optical characteristics of a crown glass. BK7 finds its applications in transmissive optics i.e. lens of binocular, lens of microscope, lens of telescope and light emitting diodes. The magnetorheological nanofinishing of optical glasses using solid core tool is found more advantageous than the other advance finishing processes in aspects like precision and accuracy. BK7 is a high quality crown glass and is used where additional benefits of fused silica glass such as in temperature sensitive applications are not required. It has low inclusion content and extremely low bubble, also finds application in lens manufacturing. The present work focuses on nanofinishing of the BK7 glass specimen for ratifying its utility in practical application. In this work, programmable logic controlled 3-axis motion are fed to the magnetorheological (MR) tool for finishing the glass specimen. On tool extremity, a hemispherical shape of MR polishing fluid is generated using magnetic control by an electromagnet. MR polishing fluid consists of cerium oxide abrasive powder product of Cepoll with grade 1663, magnetic iron powder and deionised H_2O. Also, it acts as viscoelastic solid under the influence of magnetic field, which assists in reducing the surface roughness of glass upto nano-level range. The magnetorheological (MR) nanofinishing with solid rotating core tool is carried on the BK7 glass of size 10×10×3 mm. Optical properties such as transmittance, absorbance and reflectance of finished BK7 glass are analyzed and found suitable for lens manufacturing. Results of higher quality with excellent finishing are obtained by the present MR finishing process. After 90 minutes of finishing, the surface roughness values Ra and Rq are reduced to 17 nm and 27 nm from the initial values of 41 nm and 57 nm respectively. On considering the results of preliminary experiments and literature survey, the four parameters with three levels design were selected. Response surface methodology is conducted in order to find the optimum process parameters, where box-behnken design (BBD) is applied on those four process parameters and three levels. This research also presents the effects of each process parameters on the percentage change surface roughness such as the effect of composition of CeO_2 abrasives in magnetorheological polishing fluid, effects of magnetising current, effect of tool's (solid core) rotational speed and effects of working gaps. The best surface roughness R_a and R_q values are achieved as 22 nm and 32 nm from the initial of 41 nm and 57 nm at optimum parameters in 30 minutes of finishing time cycle. To study the surface morphology, scanning electron microscopy is performed on BK7 glass with sputter coating of gold on it.

Keywords: Magnetorheological, Nanofinishing, BK7 glass, Optical, Lens, Surface roughness, Optimization.

Table of Contents

List of Figures

List of Tables

Nomenclature

R_a = Average roughness value, µm

R_q = Root mean square value, µm

R_{ai} = Initial average roughness value, µm

R_{af} = Final average roughness value, µm

ΔR_a = change in average roughness value, µm

% ΔR_a = Percentage change in roughness

Acronyms

P = Abrasive concentration

M = Magnetising current

S = Rotation speed of solid core tool

R = Working gap

RMS = Root mean square

DOF = Degree of freedom

2FI = Two factor interaction

S.D. = Standard deviation

C.V. = Coefficient of variance

C.I. = Confidence interval

VIF = Variance inflection factor

CIP = Carbonyl iron particles

AFM = Abrasive flow machining

FMAB = Flexible magnetic abrasive brush

MAF = Magnetic abrasive finishing

MCF = Magnetic compound finishing

MR = Magnetorheological

MRF = Magnetorheological finishing

Chapter 1

Introduction

A good surface finish texture controls the friction during the contact or non-contact machining. Industrial designers are regularly attempting to design machines that can run for longer period without enormous maintenance and preciously operation than ever. Modern engineering has led the development of CNC machines that can work on any geometry. For example parts like guide ways, shafts, dies and optical components, etc. should be specific in terms of dimensions and geometry. But most of the manufacturing processes woefully perform and produce parts that show unsatisfactory results in terms of surface texture quality and dimensional accuracy. Perhaps, solid approach is applied to achieve perfection. Several industries have started focusing on micro/nanofinishing, this performed after the traditional finishing processes. Each and every method of micro-finishing for a precise part is the final operation in machining sequence. Individual method has been designed to develop a particular geometry and to finish the irregularities precisely, therefore these methods must be applied correctly in the machining sequence.

1.1 Traditional Finishing Processes for Optical Glasses

Commonly used traditional finishing processes by the industries are grinding, polishing, etc. The traditional finishing processes are likely not well suited for obtaining high level of finishing because of the constraint of size and profile of the workpiece material, the absence of control of forces exerted by the tool during finishing and the heat generated during the process. Grinding and polishing are two traditional finishing processes which are mainly used for optical glasses.

1.1.1 Grinding Process

It is an abrasive machining process that uses the rotating grinding wheel for material removal. Surface grinding is performed to remove material from the rough surface and making it flat or specular. This finishing technique is found to be the simplest in all aspects when compared with other processes. Ferrous and non ferrous materials both can be finished using the various types of abrasive wheels. The removal of material is obtained through shear action.

Therefore, each abrasive particle gets involved in the material removal by cutting as a small chip.

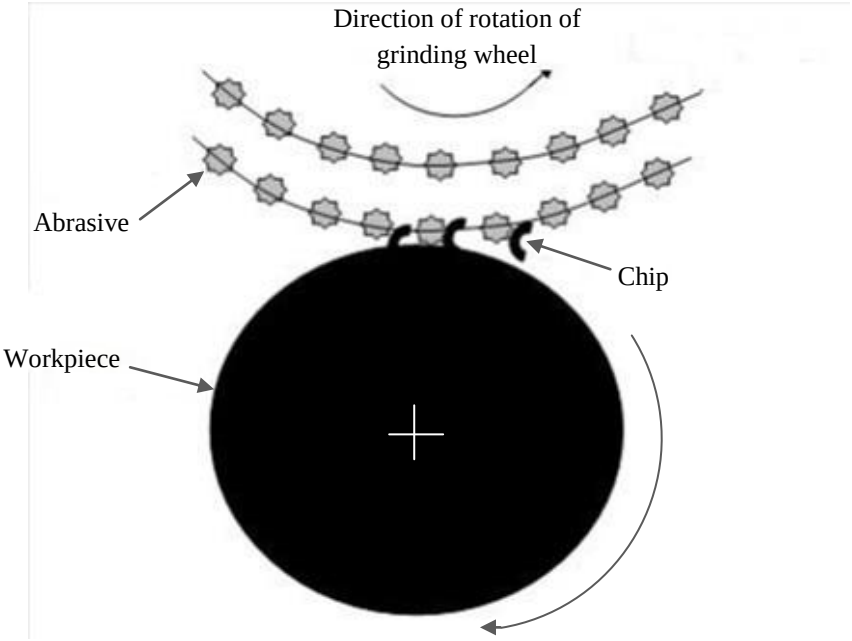

Fig. 1.1 Mechanism of abrasive based grinding process [Jha and Jain, 2005]

1.2 Polishing

Polishing process is applied on glasses to get a smooth and shiny surface. Smooth surface geometry of glass is obtained by some chemical action occurring on the upper most surface and rubbing it with abrasive powder. Thus this results in a significant specularity of the glass surface. For materials like glasses and transparent stones, this technique is capable in reducing diffuse reflectance to lowest values. It has been found in surface analysis that on magnifying till enormous times, peaks and valleys appear. These peaks and valleys are then level by performing abrasion repeatedly. Abrasive polishing is conducted on glass initially with coarse grained abrasive particles and finally with fine grained abrasive particles.

1.2.1 Pitch Polishing

Over the decades, the pitch polishing techniques are being implemented to get precise finish on glass. In this, a visco-plastic lap in spherical shape is used which is nothing but the distilled residue of tar. Usually, the glass workpiece is fitted on the lap and fed with rotational motion. Several different types of abrasives such as silicon carbide, Al_2O_3 and compounds of CeO_2 and ZrO_2 are used to level the peaks and valleys of the rough surface of the glass. High

material removal rate is obtained, but there is chance that the reaction could occur between the glass and the lap used. The key to obtain possible shiny surface of glass, is laid by the well spread polishing agent [Cumbo *et al.*, 1995].

1.2.2 Polyurethane Polishing

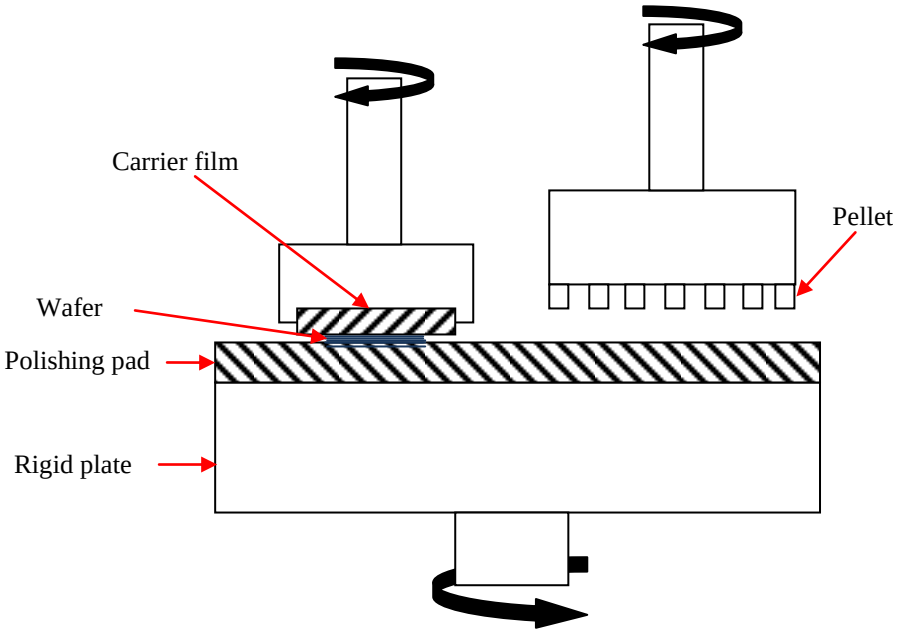

Fig. 1.2: Components of polyurethane polishing [Belkhir *et al.*, 2016]

This process was developed on the basis of manufacturing requirements such as high speed and accuracy. Lap used in this process is made of highly wear resistant polyurethane [Belkhir *et al.*, 2016]. The applied tangential force is same as of pitch polishing. Proper shapes of the glass workpiece get created on the surface of lap, which then copied to the glass surface within a short period of time. The lap material is so rigid that it does change its shape during polishing, therefore, more number of specimens can be polished with a single polyurethane lap. The components used in this polishing are slurry and supporting tool as shown in Fig. 1.2.

1.2.3 Teflon Polishing

It is also a type of chemical-mechanical polishing technique that is used to polish the optical glasses. Instead of lap materials used in pitch polishing and in polyurethane polishing, lap is made up of Teflon. This Teflon lap is fabricated by cutting two parallel grooves at 90° to each other to produce facet and it is installed or fitted on the top of facet. Rubbing with

conditioning plate (70 μm abrasive size) provides a specular reflecting surface and is used to prevent abrasion of lap due to residual of surface roughness. Material is removed at lower rate. Also, pitch abrasives can be used in teflon polishing lap [Faberge, 1968].

1.2.4 Float Polishing

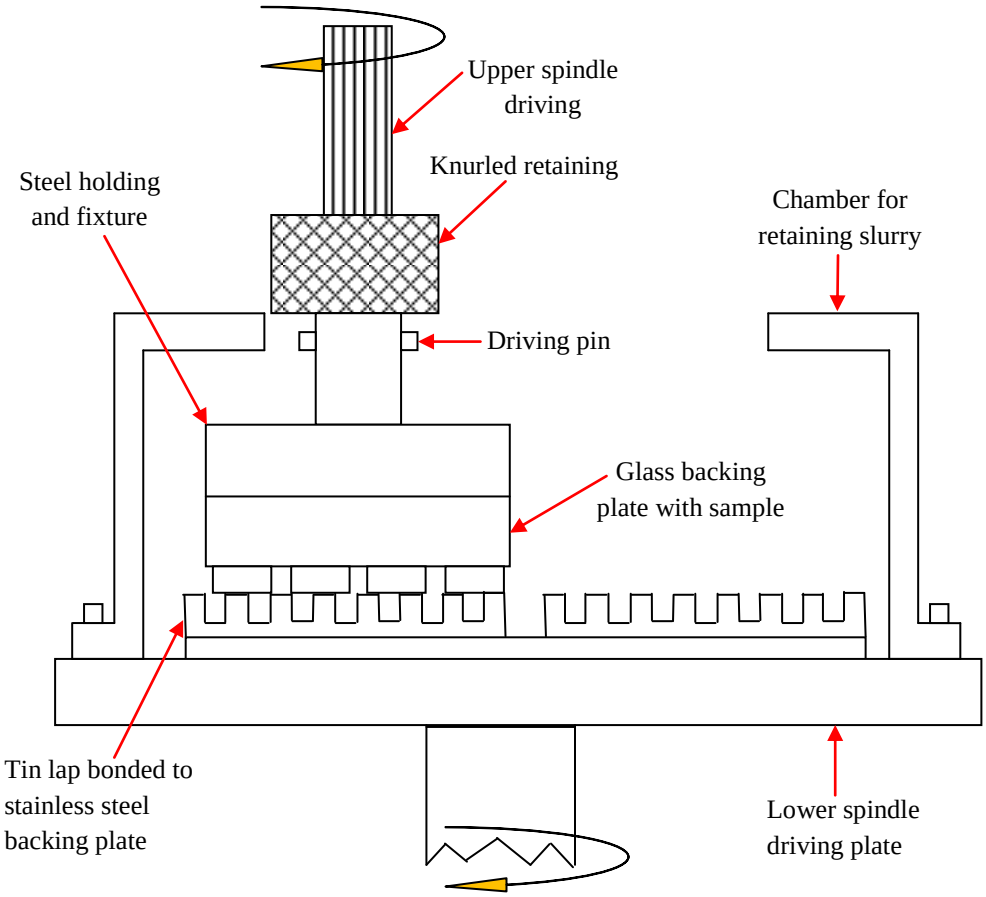

Fig. 1.3: Schematic diagram of float polishing [Bennett *et al.*, 1987]

In float polishing of optical glasses, fast rotating tin lap is used as shown in Fig. 1.3. Where the lap is bonded to stainless steel backing plate and this lap is allowed to float in wet slurry that consists of colloidal silicon oxide. This lap with the wet slurry is kept in a chamber for retaining slurry. The chamber is mounted on the lower spindle driving plate the plate. Materials like glass, aluminium, copper and stainless steel are used as lap material. Power is fed for driving workpiece through the spline of spindle driving. It could be highly reactive with some surfaces but it generates precise surface. It is efficient used for mass production. The float polishing with press process on glass is applied to obtain aspherical microglass lenses and is achieved by using polished mold. An ultra sonic vibration-assisted polishing

machine uses the float polishing technique and can generate the surface profile of a glass upto 7 nm [Suzuki *et al.*, 2006].

1.2.5 Bound Abrasive Polishing

This technique is a type of abrasive based polishing which uses the plastic material lap. Pure water plays two prominent roles in polishing of hard glasses, one for initiating the chemical reaction between the glass and pure water. Secondly, it is used as lubricant. Generally, the bound abrasive polishers available in present day are composed of 60 % to 90 % of polishing agent, 5 – 10 % of binders and 5- 15 % of erosion promoters. CeO_2 is found most functional in polishing of soft and moderately hard glasses. Little work is required in the maintenance point of view, as the tool has to be dressed frequently. Compatibility with CNC machines reduces the production time and high material removal rate is achieved [Gillman and Jacobs, 1998].

1.3 Advanced Finishing Processes for Optical Glasses

Magnetic fluid was discovered in 1948 by Rabinow [Rabinow, 1948]. In 1994, Prof. Steve Jacobs, Don Golini, Lowell Mintz, William I. Kordonski and his colleagues made a "preprototype" finishing machine. Algorithms for deterministic control of magnetorheological finishing (MRF) were developed by Prof. Greg Forbes and doctoral student Paul Dumas. In 1996, Golini and Lowell Mintz formed QED Technologies and the first commercial MRF machine was launched in 1998. Also, for the first time optical glass was considered for finishing using magnetic abrasive based finishing technique.

1.3.1 Magnetic Abrasive Finishing (MAF)

There are two forces named as normal force and cutting force that have direct effect on final finished surface produced. The normal force results in nanoscale/microscale indentation of abrasives particles on the workpiece surface and shearing off the peaks from the workpiece top surface is due to cutting shear force during rotation of magnetic brush. A homogenous mixture of unbounded iron powder and abrasive particles acts as a cutting tool. The bounded type MAP (magnetic abrasive particles) is the mixture of abrasive particles and iron powder which are sintered in furnace followed by sieving and crushing. Sintering is a process by which abrasive particles embedded into the iron particles [Pashmforoush and Rahimi, 2015].

Figure 1.5 presents the MAF setup. In general, mechanism involved in the surface finish of brittle materials like glasses, ceramics and composites are defined as brittle mode and ductile mode. In brittle mode, the surface finish is obtained through lateral cracks that result in chipping. The cracks originate from the ground of the plastic zone just below the abrasives and proliferate towards the workpiece surface. But in ductile mode machining, the material removal involves micro cutting mechanism. Therefore it is highly recommended to use ductile mode for finishing the BK7 glass.

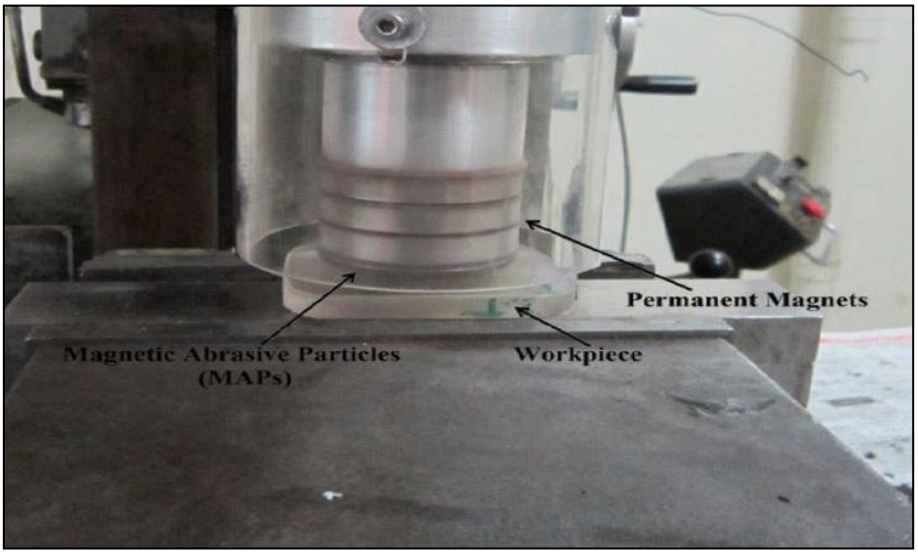

Fig. 1.4: MAF process setup [Pashmforoush and Rahimi, 2015]

1.3.2 Magnetic Compound Finishing

Magnetic compound finishing (MCF) wheel is used for ultra finishing method for optical glass by a new semi-fixed-abrasive [Jiao *et al.*, 2013]. It generates a thin, uniform MCF slurry layer on ring shaped permanent magnet which is placed between two non-magnetic plates. This magnet with feed and rotational motion provides the material removal of optical glass. The MCF slurry is composed of nano-sized magnetite particles, micron sized iron particles, several 10μm-sized α-cellulose fibres and sub micron-sized abrasive particles. The MCF slurry reacts to the magnetic field for obtaining a finished surface of glass. Précised spot depths and surface finish can be achieved by MCF wheel, as the ring shaped non-magnetic plates are installed with same diameter as that of magnet on either side of magnet. Thereby, gets magnetised parallel to the central axis (x-axis) of the annulus as shown in Fig. 1.6.

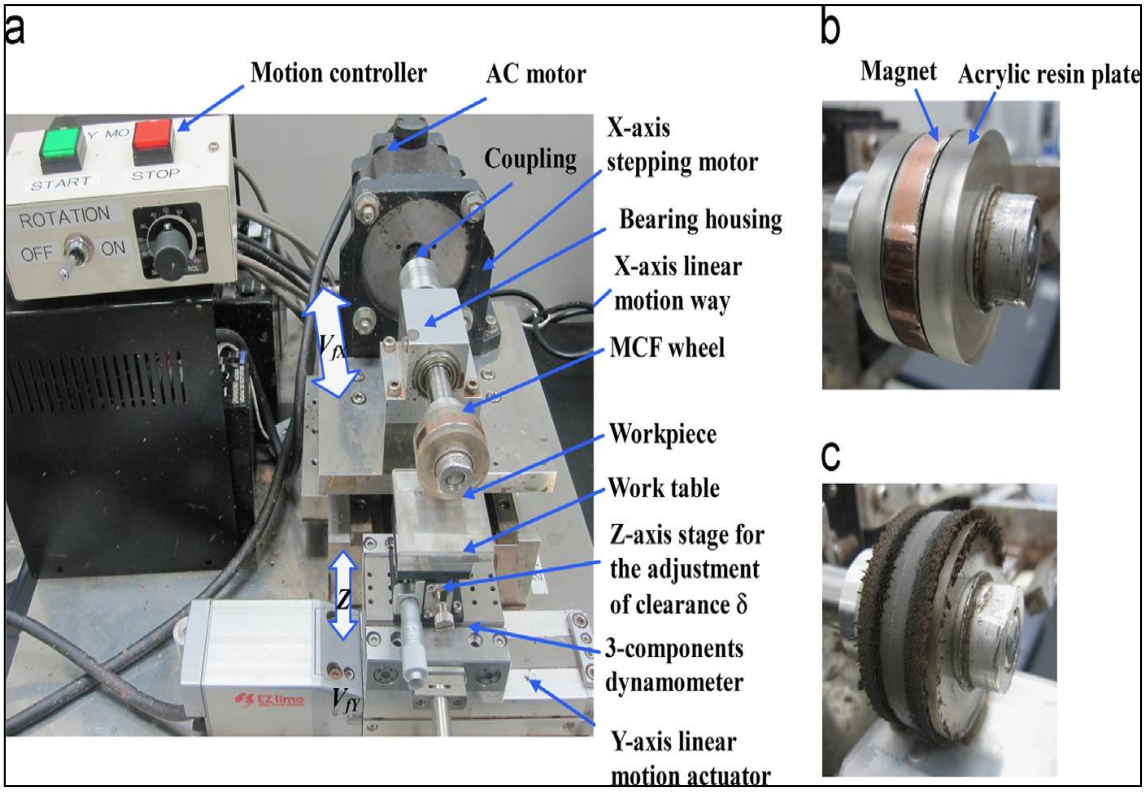

Fig. 1.5: Experimental apparatus with the modified MCF wheel (a) components, (b) MCF wheel without slurry and (c) MCF wheel with slurry [Jiao *et al.*, 2013]

1.4 Magnetorheological Finishing (MRF) Processes

Magnetorheological finishing (MRF) is an advanced finishing process, where the polishing can be performed on different types of materials with variety of tools and various methods. Finishing is obtained on different shapes and sizes of materials without introducing any subsurface damage. Thus MRF is a prominent technique in evolving the precision optics [Jacobs *et al.*, 2007; Kordonski and Golini, 1999]. These processes use magnetorheological (MR) polishing fluid that contains magnetised iron particles, non-magnetic abrasive particles, water or carriers and stabilizers [Singh *et al.*, 2012b]. This fluid gets stiffened under the influence of a magnetic field and helps to remove material. Figure 1.4 shows the MRF set up and the main focus of this process is the lens finishing that is made up of brittle material [Harris, 2011].

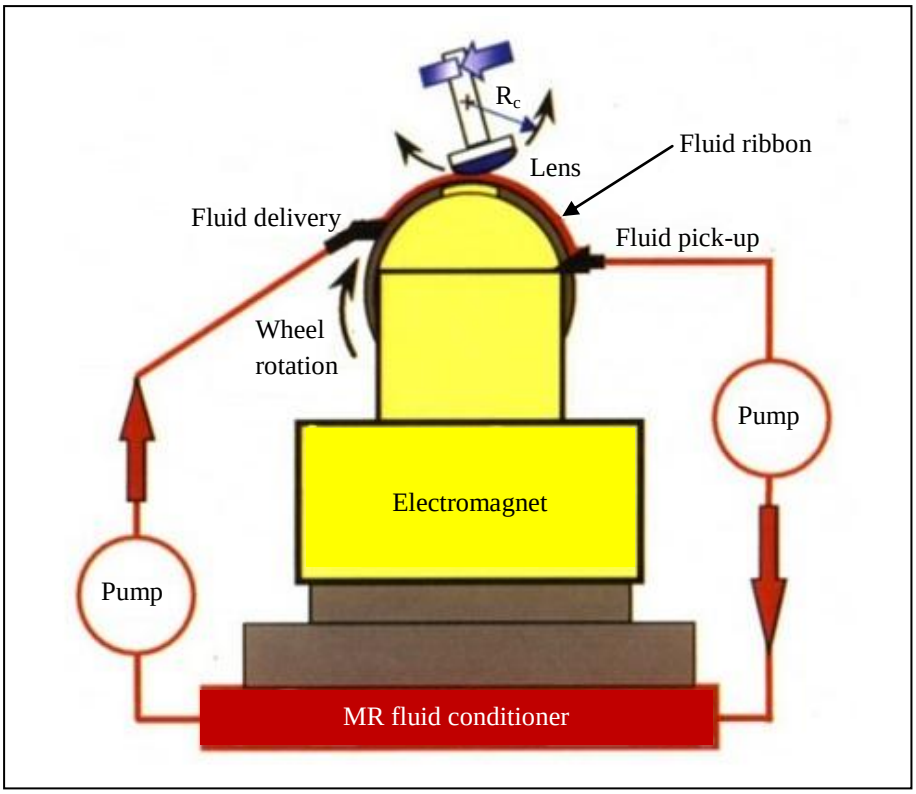

Fig. 1.6: MRF setup for optical glass polishing [Harris, 2011]

1.4.1 Magnetorheological Abrasive Jet Finishing (MRJF)

In jet polishing the energy required for polishing the surface is dependent on kinematic energy of particle impinging on the surface. In this polishing technique, the radial spread of liquid jet supplies the energy to the surface being polished. For material removal the required surface stresses are developed due to the fluid flow caused by liquid jet as shown in Fig. 1.7. Therefore, the nozzle off-set distance is highly sensitive and due to instability of the impinging flow break down of liquid jet occurs at short distance from the nozzle. In MRJF a stable spot is formed which can be utilized to correct surface texture. This unique technique provides the surface finish to the flat optics and conformal optics. Optics with designs such as steep concaves and domes are finished by regulating/controlling the jet velocity, size of the abrasives used and their impact on striking the glass surface. The glass material is held in the aluminium fixture that rotates on an axis with the panoramic motion along its centre, so that the jet remains well maintained normal to the glass surface [Kordonski *et al.*, 2006].

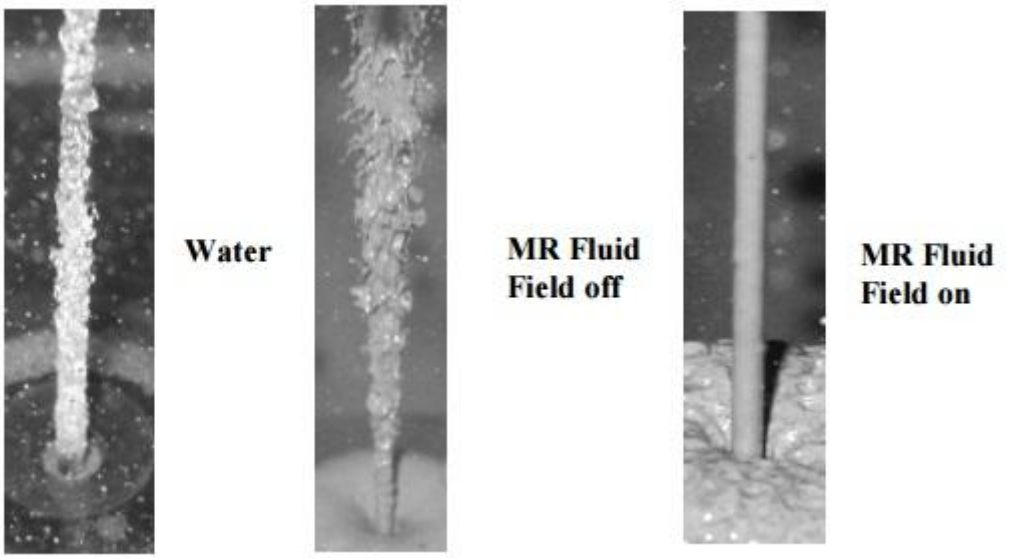

Fig. 1.7: Snapshot images of Jet at velocity = 30 m/s and nozzle diameter = 2 mm [Kordonski *et al.*, 2006]

1.4.2 R-Magnetorheological Abrasive Flow Finishing

R-rotational magnetorheological abrasive flow finishing (R-MRAFF) is a modification of MRAFF. In this process a rotating magnetic field is applied along with reciprocating motion is provided to MR polishing fluid by pistons movement. The MR polishing fluid in top and bottom cylinder is extruded through workpiece superficial surface. The permanent magnet is surrounded over the workpiece fixture as shown in Fig. 1.8. The performance of R-MRAFF is found better than MRAFF. Mirror-like surface finish had been achieved by intelligently controlling the two motions [Das *et al.*, 2010].

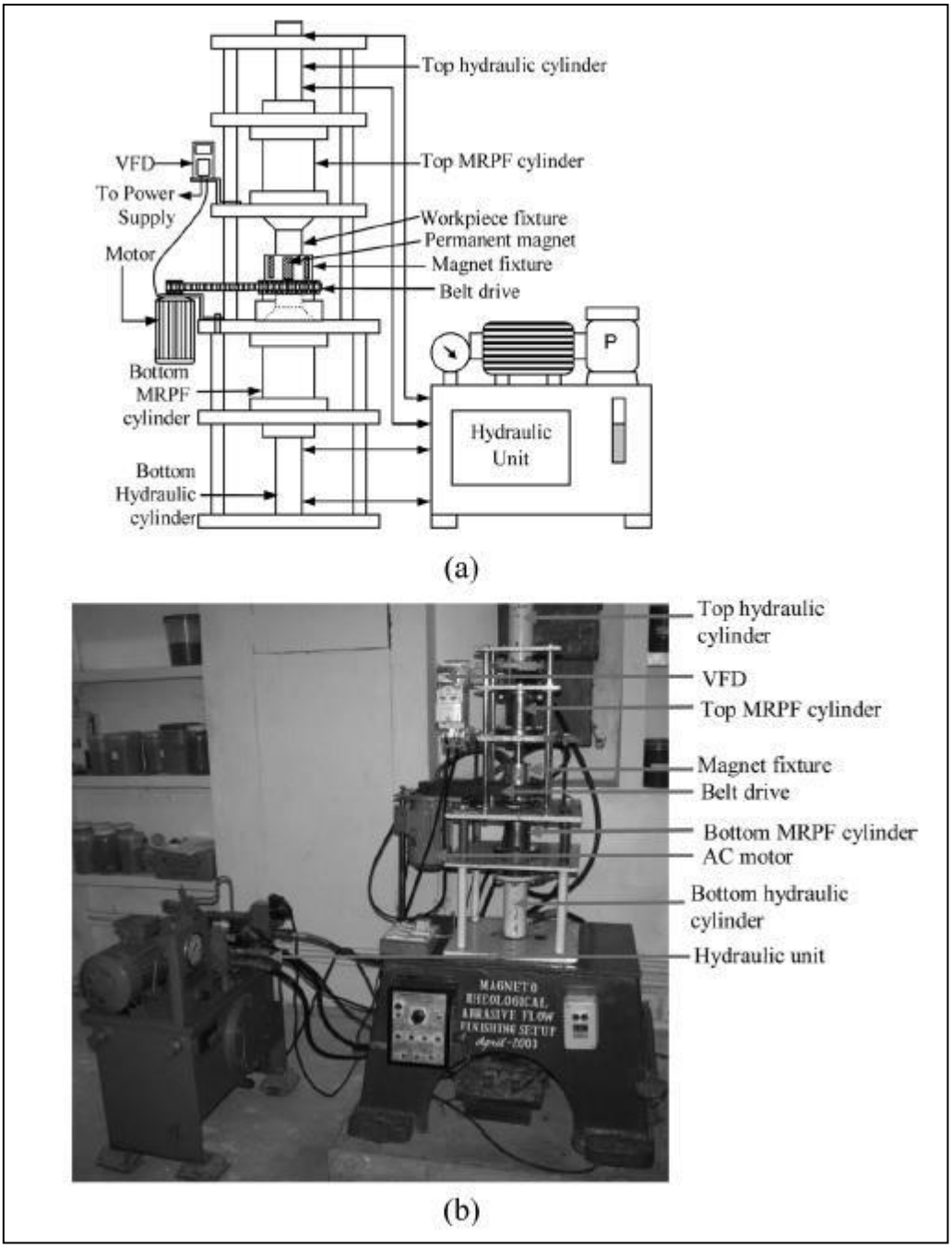

Fig. 1.8: R-MRAFF experiment setup (a) schematic diagram and (b) experimental setup [Das *et al.*, 2010]

1.4.3 Magnetorheological Ball End Finishing

There is a challenge for obtaining defect-free surface and a good surface finish of optical glass that is in the nanolevel range for transmitting high energy laser pulses. For finishing of flat as well as 3-D surfaces of ferromagnetic and non-ferromagnetic materials, a unique process had been developed using ball-end MR finishing tool. The ball end

magnetorheological finishing (BEMRF) setup is a 3-axis programmable computer controlled machine. When magnetic field is applied on the tool tip through electro magnet, a ball shaped spot of the MR polishing fluid is formed at the tip end of central hollow tool. Nanofinishing of optical glasses (fused silica, BK7, etc.) is possible by BEMRF technique using cerium oxide as an abrasive powder [Singh *et al.*, 2011]. This finishing process when applied on optical glass as shown in Fig. 1.9, very low surface roughness value till 0.146 nm can be achieved on fused silica glass [Singh *et al.*, 2012b].

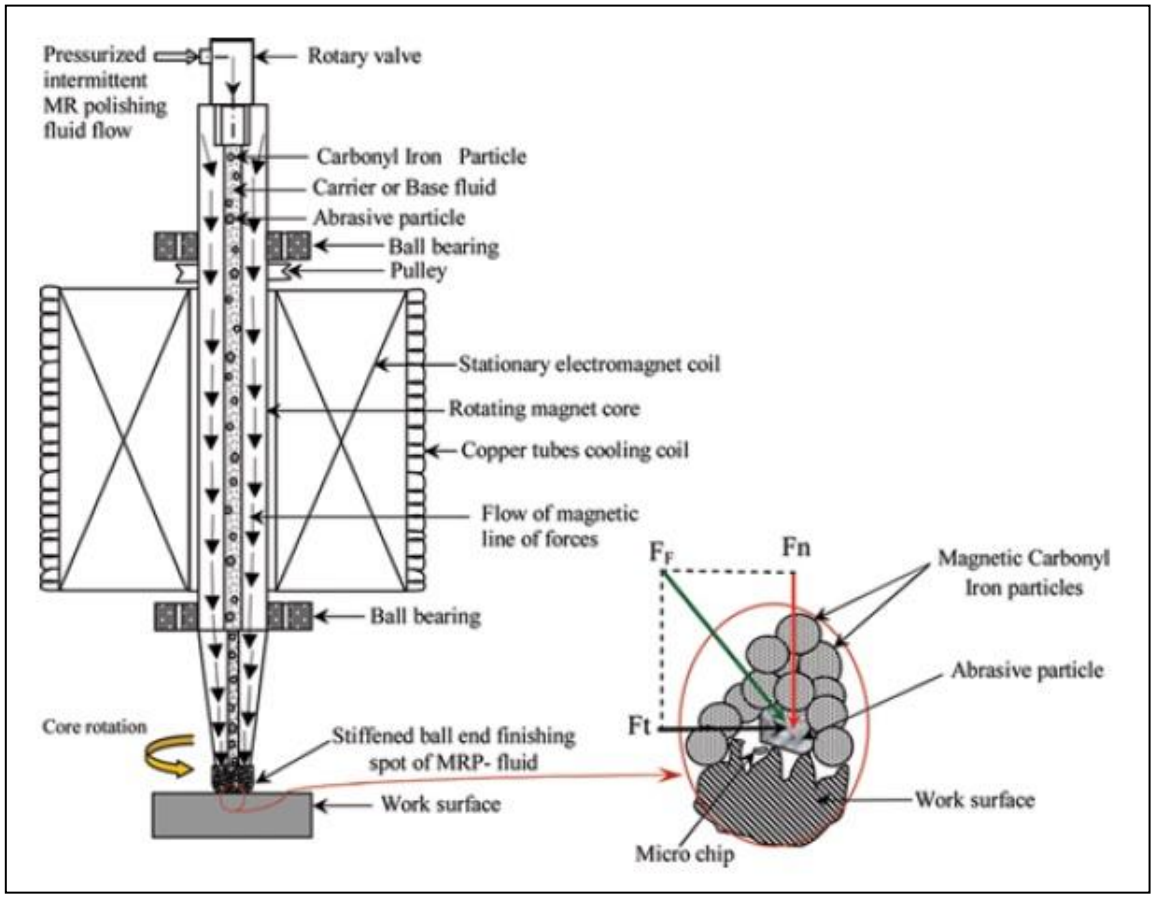

Fig. 1.9: Photograph of BEMRF setup [Singh *et al.*, 2012b]

Over the decades, the lens fabrication has been survived fundamentally unchanged. The traditional finishing methods have employed skilled labours and relatively low cost machineries for manufacturing of lens. While the advanced finishing methods utilized the computer controlled machines to reduce the cost of manufacturing and made the finishing processes for optical glasses a way faster than the traditional finishing techniques. From the initial prototype to the large production, these automated machines have reduced the human efforts for grinding and polishing of glasses. Various methods and techniques for finishing

the optical glasses have been studied. The applications like lens of telescopes, microscopes and freeform surfaces (steep concave and domes) required the surface finishing for optical glasses. Numerous researchers have developed various machines finishing the different shapes and sizes of optical glasses. These developments are made to extract the benefits from the existed glasses i.e. the improvement in optical performance. Recent innovations in magnetorheological setups have clearly justified their capability of finishing of optical glasses and bought the surface profiles in the range of nanolevel. The MRF use the combined effects of magnet field and abrasive actions to remove the material from the surface of optical glasses. All the MR processes stand unique in terms of experimental setup and MR polishing fluid compositions for finishing various specific glass geometries. The idea of replacing the horizontal trough with the vertical wheel in the MRF machine was led by Kordonski in 1996 which got published in 1998. The three objectives in finishing process for optical lens where achieved by deterministic magnetorheological finishing, like (a) subsurface damage removal, (b) smoothing of surface and (c) correction of figure. The traditional pitch and polyurethane polishing techniques were able to achieve both (a) and (b) but figure correction for optical lens cannot be determined. Similarly for ion beam milling, the objective (c) is achieved but not found effective for both objectives (a) and (b) as it cannot provide smooth surface. All the traditional polishing suffered a problem that the abrasives and glass remnants gets ingrained in the tool surface and makes the tool surface glaze.

Chapter 2

Literature Review

2.1 General

This chapter deals with various important researches which had already been carried out on magnetorheological finishing and other techniques used for different applications and manufacturing of optical glasses. Issues related to surface finish are mainly focused under this section. A brief study has been reported on the experiments performed till now and the effects of different conditions and parameters on surface roughness values are discussed.

2.2 Review of the Literature

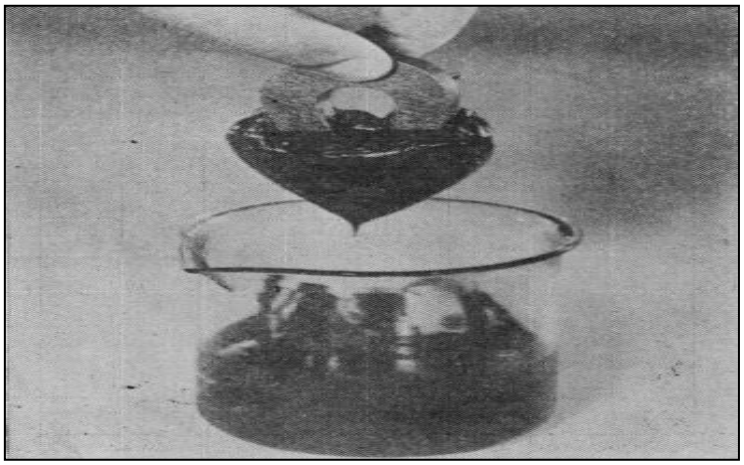

Fig. 2.1: A heart shape of fine iron powder and oil is formed under the influence of magnet field [Rabinow, 1948]

Rabinow [1948] invented the magnetic fluid i.e. magnetorheological (MR) fluid that consisted of fine iron particles with oil. The magnetic fluid clutch was the first application of iron-oil mixture. The magnetic effect on iron particles fluid is shown in Fig. 2.1. Later this concept was accepted by the researchers and implemented in sector of manufacturing engineering. The use of liquid in the mixture was made for smooth functioning of clutch. The difference of kinetic and static friction was removed by this concept. It has been concluded

that the wear occurs during proper functioning is negligible as all surfaces of iron particles and clutch plate are lubricated.

The present technology uses an uncommon fluid which also changes its rheological properties under the influence of magnetic field. It is termed as magnetorheological (MR) polishing fluid and most often used in finishing of optics. The abrasives are added into MR fluid which facilitates the abrasion mechanism on optical glasses. The concentration of abrasives depends on the type of the glass being used for finishing.

Spaggiari [2013] investigated the traditional viscosity based system. The moving parts in traditional system can be replaced easily by varying the properties MR fluid where changing the viscosity as a function of current. These replacements laid a tremendous improvement in functionality of the moving parts and their cost reduction for the viscosity based system. The MR fluid's main features are explained in this study is a fast response, simple interface between electrical power input and the mechanical power output and integration in complex system. A theoretical study was performed on the various modes of MR fluid that are flow mode (used in dampers), shear mode (used in brakes and clutches) and squeeze mode.

Ravishankar and Mahale [2015] presented the current scenario of MR devices and their applications in mechanical engineering. From the initial stage of the commercialization of MR technology which was year 1995, MR fluids have been developing as per the requirement of different applications. This study mainly focuses on the use of rotary brakes in aerobic exercise equipment. The authors stated that the MR technology can be implemented for various applications which included automotive primary suspensions, seat systems in trucks, wire-controlled feedback devices, pneumatic control systems, seismic mitigation and human prosthetics.

Rosenfeld *et al.* [2002] proposed a magnetorheological (MR) fluid based on nanometre-sized powders, micro-sized powders and hybrid scale powder. Yield stress and plastic viscosity were specified by Bingham plastic model. It was clearly observed that nano and hybrid powdered MR fluids have a higher zero field yield stress than micron-sized scale fluids. The plastic viscosity found was similar for all three MR fluids. It was concluded that all these fluids showed signs of shear thinning.

Heslin *et al.* [1974] studied the effects of particle size on the optical properties and surface roughness of glass-balloon-filled with carbon-pigmented paint. This research is done for

developing a diffuse-reflecting, low-total-reflectance and low-outgassing black paint. The particles size of < 20 microns and 74 microns are taken under this study. The surface roughness increased with increase in particles size. Relative total reflectance at near-normal incidence (MgO standard) of the filled paints was found to be less than for the unfilled paint balloon, i.e. between 230 nm and 1800 nm. Total absolute reflectance at 546 nm was decreased with increase in particles size at different grazing angles of incidence. It has been concluded that over a range, the specularity decreased with increasing particles size.

Wang and Meng [2001] analysed the modes of operation of MR fluid devices. The key for achieving success in development of MR fluid technology is the preparation of high-performance MR fluids and designs for MR fluid devices. The first problem encountered in this study was when applying current to MR fluid devices there was a settling instability of MR fluids. The second problem encountered was the initial cost of a controllable MR fluid device compared with conventional passive devices. Therefore, considering these two factors a new method was developed where the fluid was contained in an absorbent matrix.

Kordonski *et al.* [2006] developed a jet stabilization technique, where the round jet of magnetorheological polishing fluid is magnetized by an axial magnetic field when it flows out of the nozzle. It has been experimentally shown that a magnetically stabilized round jet of MR polishing fluid generates a reproducible material removal function (polishing spot) at a distance of several centimetres from the nozzle. MR Jet finishing can produce a high precision surfaces in nanometres with roughness < 1 nm rms. Due to insensitivity to the offset distance this technique may be valuable in finishing complex shapes especially those with steep concaves and parts with a variety of cavities.

Cheng *et al.* [2007] worked on reaction-bonded silicon carbide (RB-SiC) which is used to make optical parts for poor working conditions. The applications like wear resistance and thrust bearings are capable to work in temperature range -200°C to 400°C. This study proceeded with the use of an aspheric manufacturing system equipped with MRF technology. The experiments were carried out on the features of MR fluid by polishing a parabolic SiC mirror with 100 mm diameter aperture. Results obtained were the final surface roughness as 26.74 nm from Ra of 34.39 nm after 20 hours of prepolishing using Al_2O_3 and it was reduced to 1.14 nm after 50 hours of fine polishing using diamond power.

Singh *et al.* [2006] worked on magnetic abrasive finishing (MAF) process. The process parameters such as DC voltage to the electromagnet, working gap, rotational speed of the magnet and abrasive size (mesh number). It is has been reported the experimental findings about the forces acting during MAF process provided the correlation between the surface finish and the forces. A ring dynamometer was designed and fabricated the resistance type force transducer. This was used to measure the normal magnetic force component responsible for micro indentation into the workpiece and tangential cutting force component producing microchips. It was concluded from the study that parameter like voltage and abrasives size contributed more on the change in surface roughness (ΔRa).

Izman and Venkatesh [2007] studied the formation of gelling of the chips with two types of diamond pins which gets loaded on the grinding wheel during grinding operation. First the experiment are performed with regular diamond pin, this generates stalling cracks. The occurrence of these cracks may cause micro cracks and residual roughness, hence it very difficult to remove by lapping and polishing. The cause for these stalling cracks is lack of coolant at machining region during grinding. Dragging marks were also seen on the BK7 glass after grinding performed with the regular diamond pin. These problems were solved by introducing centre cavity on the diamond pin.

Gan *et al.* [2007] applied multi-fractal spectrum theory onto the surface roughness evaluation technique in order to eliminate its heavy dependence on sampling position and sampling size. Also, calculated their partition functions and multi-fractal spectra based on atomic force microscopic (AFM) images of various substrates. Results were obtained as the surface roughness was evaluated in RMS value, i.e. 0.49 nm for a silica wafer, 1.571 nm a quartz substrate, 0.562 nm and 1.189 nm for two different BK7 glass substrate sample, respectively. It has been concluded that on comparing the BK7 glass samples with other substrate samples, the BK7 glass is much better than the slide in surface roughness.

Rahman *et al.* [2007] discussed about the recent achievements in the field of development of machines that are used to produce nanosurface finish on hard and brittle materials. Electrolytic in-process dressing (ELID) grinding and ultra precision machining using single point diamond tool are most widely acceptable techniques that produce nanosurface finish on hard and brittle materials. These techniques are also used for generating nanosurface on silicon wafers. It was thought that this process can be capable of replacing the current chemical mechanical polishing (CMP) process technique. Generally this type of hybrid

machining is performed to produce highly precision micro components. Conclusion made clearly that for a longer life and a well maintained finish on the surface of the components the process of nanosurface finishing with single point diamond tool is recommended. The only condition to achieve this is the proper selection of tool geometry and cutting conditions.

Zhong [2008] discussed the recent advances in polishing of advanced materials. Many "noncontact" processes are developed using magnetic fluids, electrorheological fluids and abrasive flow machining. It is hard enough to polish complicated geometries or difficult-to-approach regions for advance materials by abrasive flow polishing. Automatic polishing technique for polishing the curved surfaces was implemented by using robots and computer numerical controlled (CNC) machines. The polishing advance materials with vibrations and beams are found to be promising. The investigation had become simple as the friction is considered in this study, to understand the polishing mechanisms or control the polishing processes.

Wang *et al.* [2009] investigated the influence of manufacturing defects (that is surface roughness and smooth transition between two discrete sub-surfaces) on the optical performance of two discontinuous freeform lenses. By comparing the experimental results with the numerical simulation results based on Monte Carlo ray trace method. Polymethyl methacrylate (PMMA) lens and BK7 glass lens were used in this study. It had been found that the manufacturing defects induced on the surface profile effects the light output efficiency. The affected uniformity of light pattern was declined from 0.644 to 0.313 for PMMA lens. It was found that the manufacturing defects induced smooth transition surfaces with deviation angle more than 60 degree existing in the BK7 glass lens reduces the light output efficiency from 96.9% to 91.0%.

Heinzel and Rickens [2009] focused on the evaluation of topographical parameters (the specific total grain plateau area and the average grain cutting edge width) and the process results by applying engineered diamond wheels in machining hard and brittle materials. They used coarse-grained, single-layered diamond grinding wheels with electroplated abrasive layers in precision grinding experiments on optical glass. The topographical parameters were determined by 3D-profilometry of replicated layers after each dressing step. Results obtained were surface area roughness Sa = 20 to 100 nm at the end of dressing process from surface area roughness Sa = 885 to 1209 nm using undressed grinding wheel. The extension of R_a to

a surface is Sa. This is a value of the difference in height of each point compared to the arithmetical mean of the surface and generally it is used to evaluate the surface roughness.

Jain [2009] summarized few finishing techniques such as abrasive flow finishing (AFF), magnetic abrasive finishing (MAF), magnetorheological finishing, magnetic abrasive flow finishing (MAFF), elastic emission machining (EEM) and magnetic float polishing. It was suggested that for all processing techniques which use a medium to finish, the properties of that medium used can be controlled externally with the help of magnetic field. The MR polishing fluid medium based techniques were capable to produce surface roughness values of 8 nm or lower. It has been concluded that selection of processes for finishing depends on the type of material used and its shape.

Das *et al.* [2010] introduced a modified polishing method called rotational magnetorheological abrasive flow finishing (R-MRAFF). In this process the rotational motion is provided by AC motor to magnet holding fixture that is used to generate relative motion between MR polishing medium and workpiece. Up and down motions for the MR polishing medium was provided by a hydraulic unit consist of two pistons. R-MRAFF was designed to overcome the problems related to finish internal surface of cylindrical, here stainless steel workpiece were used. The lowest surface roughness value of stainless steel workpiece with this method obtained was 16 nm from the initial 33 nm.

Lilienthal *et al.* [2010] investigated self-organised nanostructures in fused silica and termed it as glass grass directly produced by plasma dry etching methods. These structures appear in shapes of grass, needles, pillars or even tubes depending upon the etching conditions. A study of surface morphology has been performed with various modification done among parameters like reactive ion etching (RIE) and deep reactive ion etching (DRIE). Practical applicable experiments were carried out, such as bonding technologies which support integration into hybrid material systems. It had been concluded that the four different categories of ‘glass grass’ could be differentiated: grass, needle, pillar and tube-like structures, growing in thickness and length on the same order of magnitude, while density decreases in general (from grass to tubes).

Manallah and Bouafia [2011] worked on the method of light scattering. This method was applied to measure the roughness of polished surfaces which was based on the light sent back by the surface. Further, it was also used to characterize the surface as a function of the

distribution of scattered light. These were correlated with the parameters of roughness as the light scattered by rough surface contains information about its quality. For measuring the ratio of scattered light to the total reflected light by the surface, total integrated scattering (TIS) technique was used. The results obtained for BK7 glass were δ = 11,0 nm, average deviation = 2,1 nm and standard deviation = 2,2 nm. Final conclusion stated that the intensity of the scattered light is proportional to the roughness of the surface. If the rms (root mean square) roughness δ is small as compared to the wavelength of light ($\delta << \lambda$), specular reflection and the scattering is low and vice versa depending upon the orientation of the slopes of surface irregularities.

Sidpara and Jain [2012] used the magnetorheological finishing utilizising magnetorheological fluid, which consist of magnetic particles, non-magnetic abrasives, and some additives in water or carrier to polish crystal silicon blank as shown in Fig. 2.2. An experimental study was conducted to predict the effect of process parameters such as concentration of magnetic particles with abrasive particles, carrier wheel speed and initial surface roughness. Results obtained after performing experiments in terms of arithmetical mean roughness (R_a) were as low as 8 nm from 1300 nm in finishing time of 210 minutes [Sidpara and Jain, 2012].

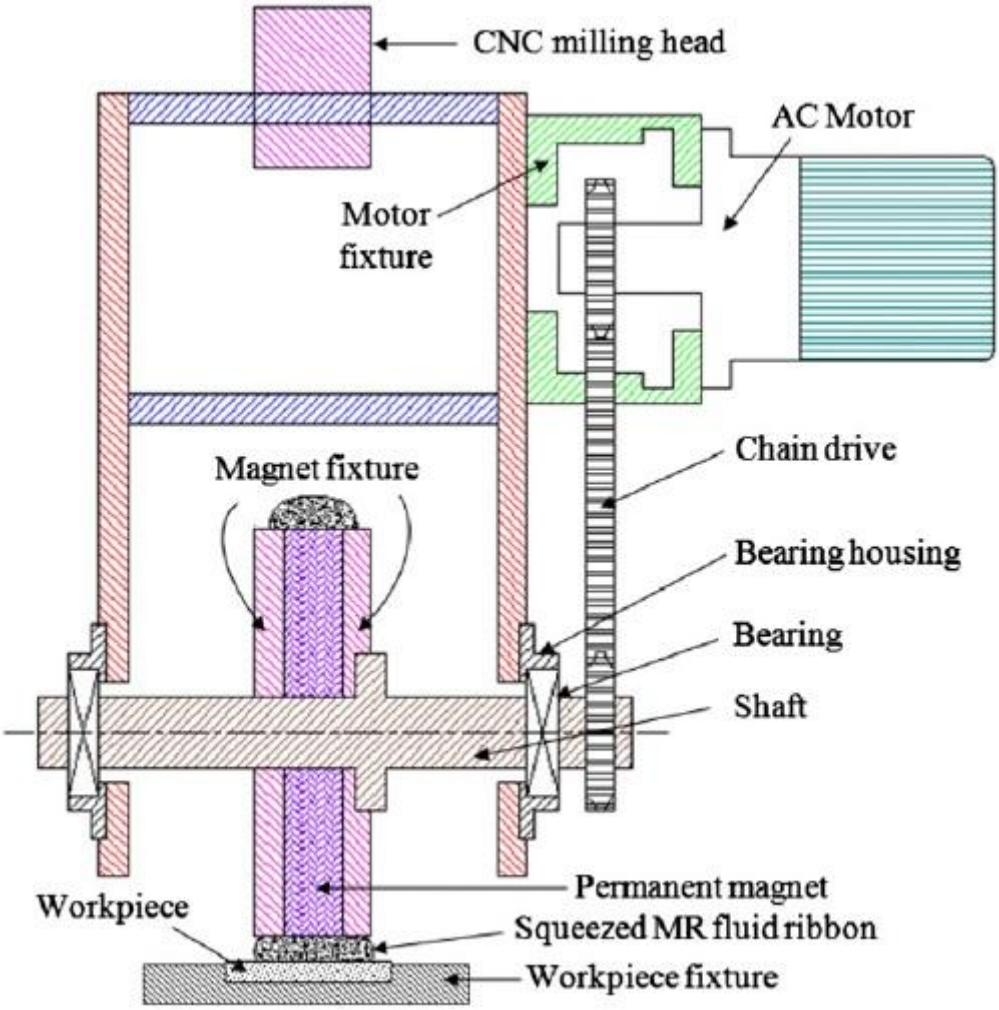

Fig. 2.2: Schematic diagram of experimental setup of magnetorheological finishing (MRF) process [Sidpara and Jain, 2012]

Singh *et al.* [2011] presented a new finishing process to overcome the problem of finishing of 3D intricate shaped surface. A ball-end magnetorheological (MR) finishing tool was developed for flat and as well as for 3D surfaces. This tool was capable of finishing the ferromagnetic and non-ferromagnetic materials. It has been concluded that the shape and the size of the finishing spot were found fluctuating with the distributed range of working gap under the same magnetizing current. The concept of newly developed MR finishing process was implemented on 3D surfaces of ferromagnetic material. The ball-end MR finishing tool successfully demonstrated its capability as the surface finish achieved was 70.0 nm from 414.1 nm on ferromagnetic EN31 workpiece in finishing time of 100 minutes. The surface roughness for non ferromagnetic copper specimen was reduced to 102 nm from the initial of 336.8 nm in 60 minutes of finishing time.

Singh *et al.* [2012a] worked on the finishing of 3D workpiece surfaces using ball-end magnetorheological finishing process. The workpiece was made using milling process at various angles of projections like flat, 30°, 45° and curved surfaces. The centre line average (CLA) R_a values obtained after milling were 1334.1 nm, 1452.3 nm, 2739.3 nm and 1754.7 nm respectively, further the R_a value of 142.9 nm was obtained after grinding. The experiments were performed at rotational speed of tool of 500 rpm, magnetising current of 4 ampere and working gap of 0.66 mm. The final R_a value of ground flat surface achieved was 19.7 nm from initial R_a value 142.9 nm after 120 minutes of finishing time.

Singh *et al.* [2012b] carried research on fused silica glass. Where the BEMRF process was implemented on fused silica glass, in order to reduce the surface roughness and get a defect free surface after finishing. Experimental set up used for this research consisted of an electro magnet, cylindrical hollow tool, servo motors for three axis and tool's rotational motion. The mechanism of MR polishing fluid was explained using Fig. 2.3. After 90 minutes of MR finishing, the final surface roughness value achieved was 0.146 nm from the initial of 0.74 nm.

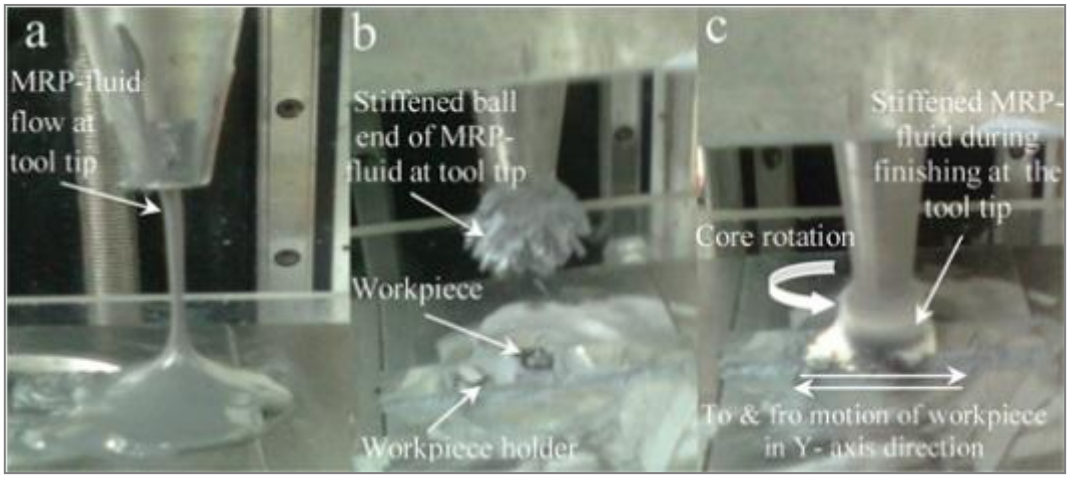

Fig. 2.3: MR polishing fluid at the tool tip (a) when electromagnet is OFF, (b) stiffened hemispherical shape when electromagnet is ON and (c) during finishing operation [Singh *et al.*, 2012b]

Jiao *et al.* [2013] used magnetic compound fluid (MCF) wheel for finishing the optical glass. This method is a 'semi-fixed-abrasive' and an 'ultra-fine' finishing method that can be used for achieving precision surface finish of optical glass. Certain modifications were made in the existed setup to evaluate the performance of the modified wheel in spot-polishing of fused

silica glass. Experiments were performed to evaluate the material removal and the surface roughness of the glass specimen with the modified wheel. Results of these experiments showed better material removal. The modified MCF wheel performed much better than the unmodified wheel. The material removal and the surface roughness found for both modified and unmodified MCF wheel were 0.04 mm^3 vs. 0.0088 mm^3, R_a = 5.624 nm and 14.67 nm. Therefore this study showed better work surface and greater material removal with smaller working clearances or working gap and higher wheel rotational speeds.

Baranwal and Deshmukh [2012] presented the prominent features of magnetorheological finishing (MRF) technology. It is concluded that main features of this technology were the sudden and fast responses, a straight-forward interface between electrical input and mechanical output and finally an intelligent controllable system. According to the commercial point of view, the MRF system need to be made more sensitive, possibly by introducing the uses of sensors and feedback system i.e. closed loop systems.

Guo *et al.* [2014] investigated the effect of micro-structures on surface roughness and subsurface damage. This paper focus on a series of micro-structured coarse-grained diamond wheels used for surface grinding of optical glass and its aim was to improve the grinding performance, especially for subsurface damage. Comparison was made with the conventional coarse-grained diamond wheel where the subsurface damage depth was reduced effectively from 5 to 1.5 μm. Perhaps the better surface roughness was not obtained by the new micro-structured coarse-grained diamond wheel.

Guo *et al.* [2014] investigated the distribution of material removal rate through spot polishing of borosilicate glass. ANOVA worked was performed by considering three process parameters such as magnet revolution speed, MCF carrier rotational speed and working gap on pressure. Where the response measured was in terms of shear stress and MRR. Results illustrated that the pressure was found higher near the centre of interacting area which was the polishing spot centre. Final observation revealed that the material removal is minimal at the spot centre and maximum value was achieved at approximately 8.2 to 10.2 mm away from the spot centre.

Pattanaik and Agarwal [2014] developed a method called flexible magnetic abrasive brush. This FMAB is a combination of MRF with the pillar drill machine. It was developed to finish objects of freeform surfaces. Further the experiments were performed by varying the slurry

composition. It has been concluded that the surface finish obtained by this method also depends on the type of vessel used for storing MR fluid. Results improvement of finishing the copper workpiece for flat surface is found in terms of 77% whereas 67% for cylindrical surface.

Zhou *et al.* [2014] recently revised a concern of a fixed-abrasive polishing process. This study considers the different kinds of pellets used in the polishing process. Water reacts with the glass to produce smooth surface as it forms sol-gel layer which is conductive in nature. The surface roughness was improved sharply for pore-free pellet, that is from >80 nm to <1 nm (average). The results suggest that on applying ultrasonic unit to the system, the "G-ratio" of polishing process can be increased and effectively alleviate the wear loss of pellet. G-ratio is defined as the ratio of the removed thickness of glass to the wear thickness of pellet.

Blaineau [2015] used wet etch technique for measuring subsurface damage (SSD). These SSD are introduced during the bound abrasive grinding of fused silica glass. To attain defect free surface of fused silica glass, an investigation between the relationship of SSD depth and forces applied by the grinding wheel on the sample. The results of investigation revealed a relation between the SSD depth and the grinding forces. It has been concluded that this relation can be normalized by the abrasive concentration.

Pashmforoush and Rahimi [2015] utilized the magnetic abrasive finishing (MAF) method for finishing the BK7 optical glass. Already defined that the BK7 is hard-to-machine material and difficult to store in safe manner, smart precautions were taken to reduce the chance of forming defects on surface. A statistical approach was made to obtain the optimum process conditions and investigated the effect of various process parameters on surface roughness using response surface methodology. Various finishing parameters such as the abrasive size, rotational speed, and percentage weight of binding agent were considered for this study. The plot of Fig. 2.4 illustrates the relation between R_a value with finishing time and the best surface roughness value achieved was 23 nm.

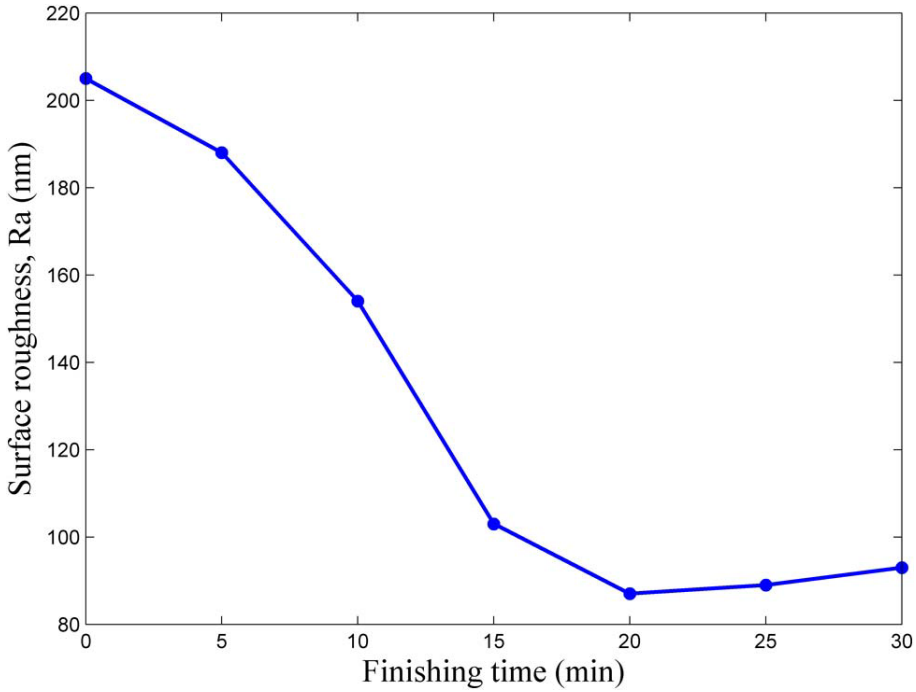

Fig. 2.4: Plot of surface roughness with finishing time where rotational speed is 800 rpm, abrasive size is 1 μm, magnetic abrasive particle (MAP) size is 50 μm and percentage weight of binder is 25 % [Pashmforoush and Rahimi, 2015]

Onwuka and Abou-El-Hossein [2016] worked on borosilicate (BK7) that is widely used in automotive and optics industries, for the production of a number of critical optical components. In this study, an ultra-high precision grinding process was applied to machine flat surfaces of BK7 by mounting a spindle on the tool. Considering three grinding parameters such as depth of cut, feed rate and wheel speed, the experiments were carried out. It was observed that the effect of varying the feed rate was more noticeable than that of depth of cut and wheel speed. Final results obtained with developed response surface model after the optimization of model were 320 nm to 80 nm. Conclusion stated that the better surface finishes can be achieved by using low values of feed rate, cutting depth and high wheel rotation.

2.3 Research Gap

Observations are made from the literature available regarding the precise surface finish of BK7 optical glass using MR techniques. It reveals that a lot of work has been done on finishing of optical glasses such as Zerodur, soda lime and fused silica glass but no such work is reported in literature on precise surface finish of BK7 optical glass by using

magnetorheological finishing process using solid core rotating tool. The research gap follows as:

- Numerous researches performed till now on surface finishing of BK7 optical glass that have used various methods like ultra-precision grinding, magnetic compound fluid (MCF) wheel and magnetic abrasive finishing (MAF).
- Statistical regression analysis has not been performed for finishing BK7 glass with solid core rotating tool using parameters such as composition of abrasives in MR polishing fluid, magnetising current, rotational speed of solid core rotating tool.

2.4 Objectives of the Present Research

Based on the subsequent analysis of research gaps and after the survey of the available literature, the present research aims to provide better results with improved optical performance of BK7 glass. To fulfil the aim of present research the following objectives were planed.

- To demonstrate the capability of solid core rotating tool equipped on magnetorheological finishing (MRF) computer controlled setup in finishing the surface of BK7 glass at nano-level range.
- To optimize the process parameters for finishing of BK7 glass with MRF process using the solid core rotating tool.
- To demonstrate the feasibility of present MRF process with solid core rotating tool in practical application of surface finishing in optics industries.

2.5 Material and Methodology

BK7 glass is being broadly used in lens manufacturing as shown in Fig 2.5. This crown glass material is a type borosilicate glass, having boron tri-oxide and silica as the main constituents. Low co-efficient of thermal expansion makes it thermal shock resistant on comparing with other glasses. The presence of these properties in BK7 makes its use in astronomical reflecting glass mirrors telescope [Tsegaw *et al.*, 2015].

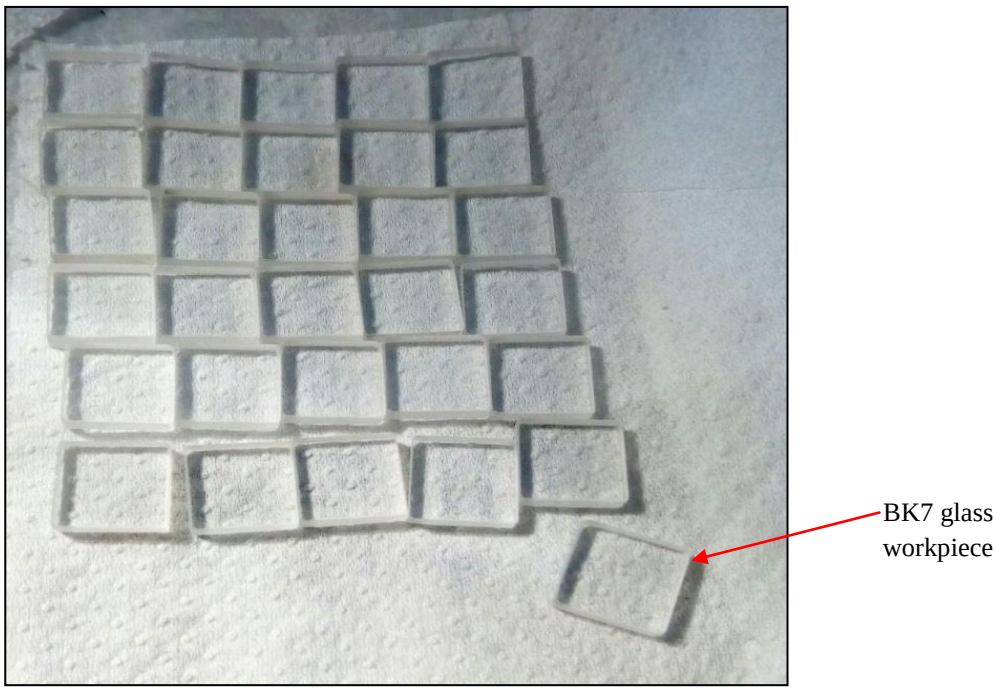

Fig. 2.5: BK7 glass workpieces obtained after pitch polishing

From the literature survey, it has been made clear that surface finishing can be done on optical glass using BEMRF process. It is the most suitable finishing process for producing nanolevel surface profiles of glass [Singh *et al.*, 2012b].

Under favourable conditions, the MR solid core rotating tool is also capable to finish BK7 glass and generate nano range surface profile. But the process parameters depends on the type of material used, therefore preparative experiments are conducted in order to get optimum conditions and parameters. On the basis of these preparative experiments, RSM was applied to the design of experiments and optimum combinations of parameters were known.

2.5.1 Experimental Setup

The MR solid core rotating tool was mounted on the Z-axis slide of the present magnetorheological finishing (MRF) setup. The MRF setup is a 3-axis programmable computer controlled machine as shown in Fig. 2.6. BK7 glass specimen was held in aluminium fixture and further was tightened in the modular precision vice mounted on Y-axis slide. All the motions are provided by the four servo motors fixed at each slide and for tools rotary motion. This computer controlled MR finishing setup is operated with the help of

combination of graphical user interface (GUI) with human machine interface (HMI). The tool is composed of a solid core and electromagnet.

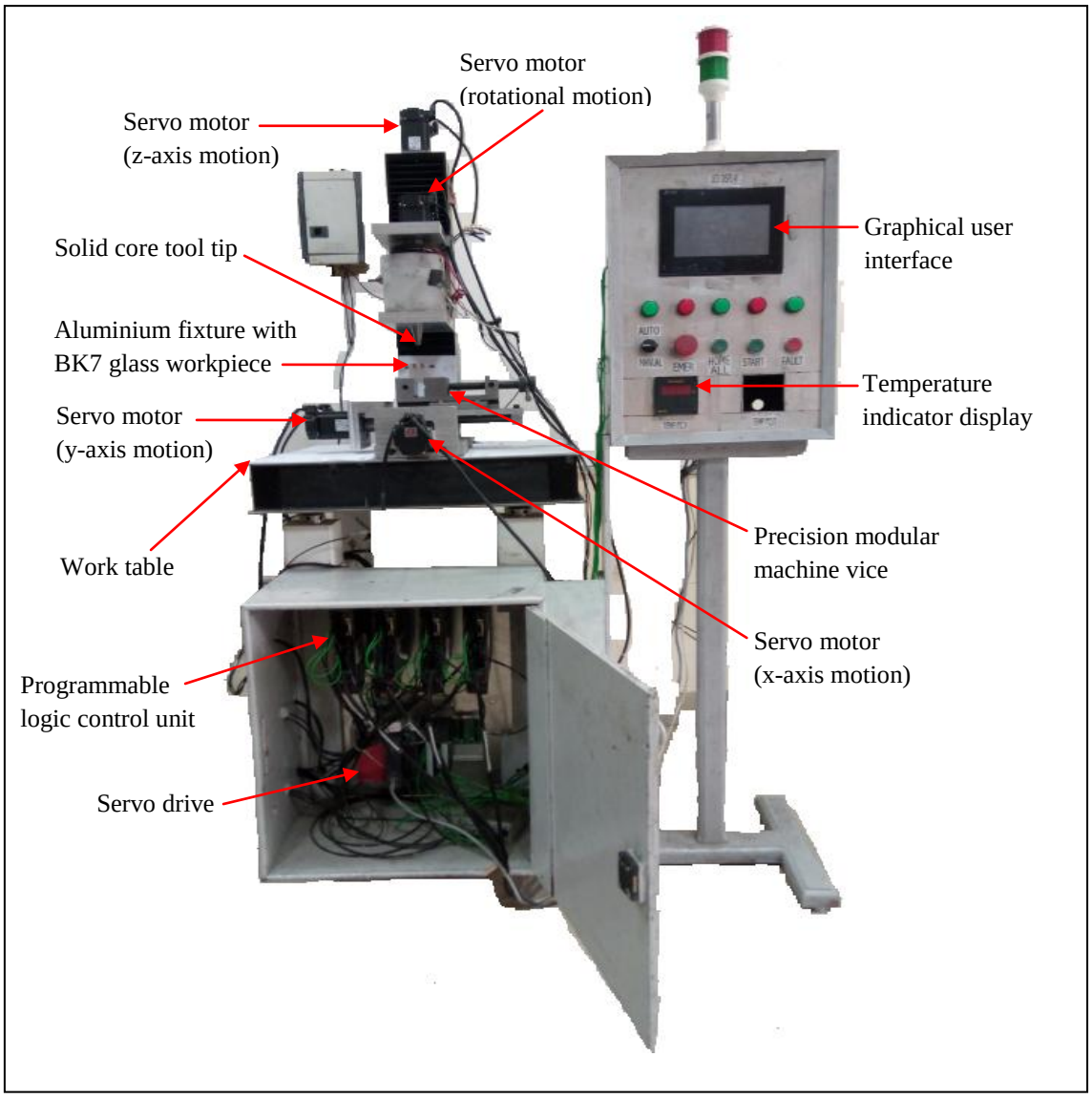

Fig. 2.6: Photograph of the set up of magnetorheological finishing with solid rotating core tool [Khurana *et al.*, 2017]

2.5.2 Materials Selection

The extensively used material for lens manufacturing is BK7 which is a high quality optical glass. BK7 works competently in all chemical tests and there is no additional or special handling requirement for this type of crown glass, hence the processing and manufacturing costs are minimized. In real, BK7 glasses are available with different compositions. Spectroscopy is performed to get the compositions of the BK7 glass as listed in Table 2.1.

Table 2.1: Composition of BK7 glass

Element	BK7 workpiece composition (%)
SiO_2	70
B_2O_3	11.5
Na_2O	9.5
K_2O	7.5
BaO	1
TiO_2, CaO and other foreign bodies	0.5

2.5.3 Methodology

The prime objective of this research is to improve the optical performance of BK7 glass using magnetorheological finishing (MRF) with solid core rotating tool technique and demonstrate the material removal mechanism of silica based glass. Certain procedures are followed to meet the industrial standards for lens manufacturing. Efforts are made to show the capability of solid rotating core tool in optics.

1. Related literature survey for determining the exigency of surface finishing, methods of surface finishing being applied in optics and the exigency for recently developed advanced methods and techniques
2. Detailed investigation of various advanced finishing processes for optics and selecting a feasible process from them
3. Selection of material based on practical applications in optics industries
4. Plan of preparative experiments for deciding the range for main experiments
5. Preparation of fixture and glass specimens
6. Performing the preparative experiments
7. Analysing the results and selecting process parameters
8. Design of experiments
9. Performing the designed experiments
10. Analysis of finished surface characteristics and surface roughness profiles
11. Conclusion for the results
12. Optimizing process parameter

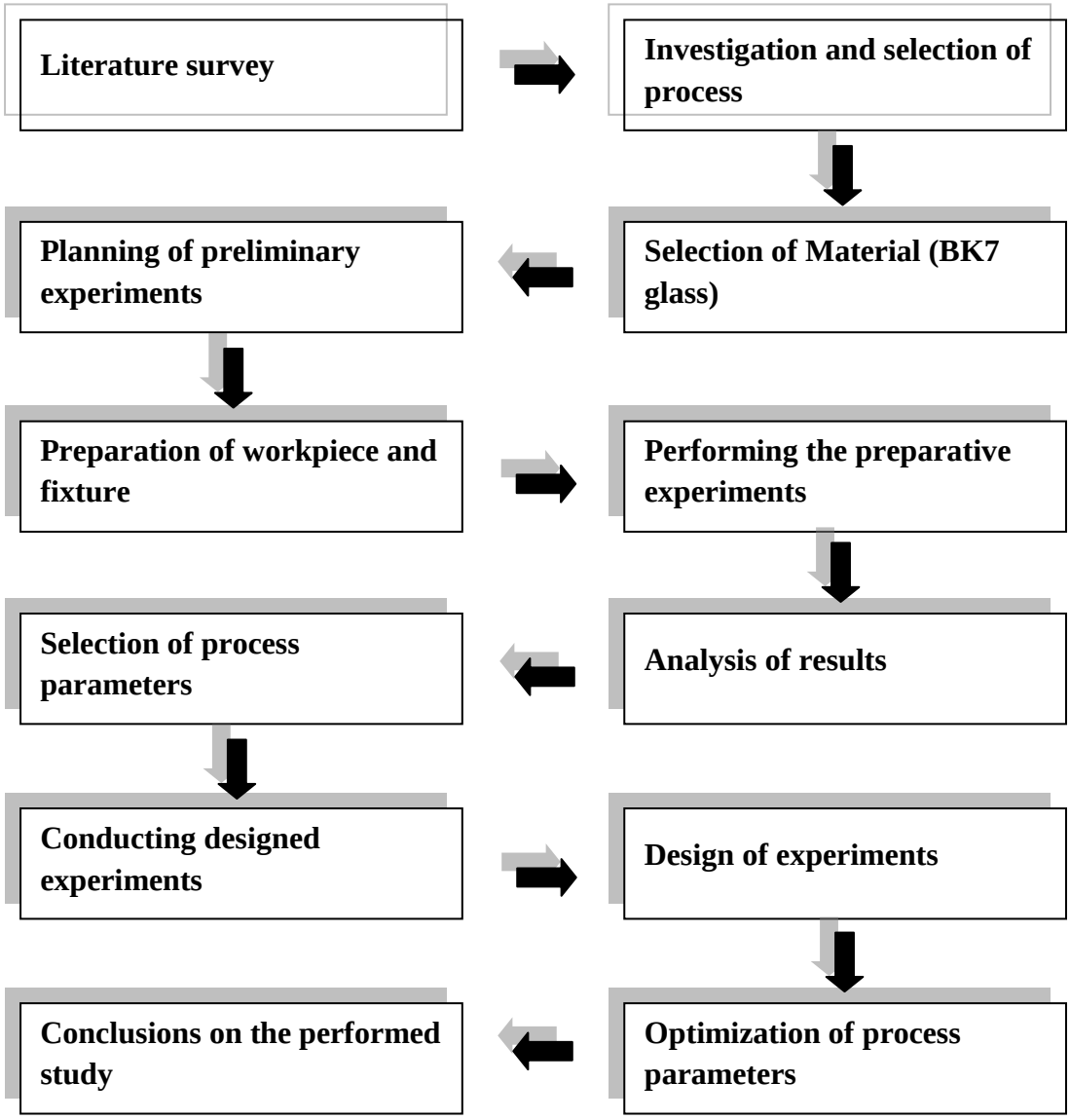

Fig. 2.8: Flow chart of methodology being followed in the present research work

Chapter 3

Preliminary Experiments on BK7 Glass

3.1 Chapter Overview

The extensively used material for lens manufacturing is borosilicate glass which is a crown glass with SiO_2 and B_2O_3. Also, it is having very low co-efficient of thermal expansion (approx. 3×10^{-6} K^{-1} at $68^{\circ}F$). Due to these properties, it is used in manufacturing of astronomical reflecting telescope glass mirrors [Tsegaw *et al.*, 2015]. Because of high normal forces in conventional lap polishing, it leads to the development of damage sites on both surface as well as sub surface [Lee *et al.*, 2011]. In 1988, Q22 MRF (magnetorheological finishing) system is introduced by QED technology which could eliminate subsurface damage. A multi axis and computer-controlled machine is capable of polishing of optical glass upto 200 mm in diameter [Kordonski and Jacobs, 1996]. A new method for finishing optical glass is developed called ball end magnetorheological finishing which is capable of obtaining surface roughness values at lowest in nanometer range [Singh *et al.*, 2011]. The MR polishing fluid for finishing of optical glass is based on magnetorheological phenomenon that consists of magnetic iron particles, abrasives and de-ionised water (H_2O) [Sidpara *et al.*, 2009]. L M Cook proposed mechanic-chemical model, the chemical reactions which occurs in interaction of glass surface and abrasive particles with H_2O [Cook, 1990]. Use of deionised water plays a major role in material removal rate from the borosilicate glass, as the balanced pH of the solution is directly proportional to the log of the non-linking oxygen ions [Das, 2014]. Last step is the release of SiO_2 particle from the particles of CeO_2, where initially the SiO_2 film and CeO_2 particles reacts with each other and cleaving of Si-O-Si occurs to take off the SiO_2 lumps with CeO_2 particle from the film surface [Hoshino *et al.*, 2001]. Using modified Preston's equation, with increase of drag force (F_d/A) and with increasing the abrasives concentration provides higher material removal rate (MRR) for optical glass [DeGroote *et al.*, 2007]. The material removal rate through spot polishing of borosilicate glass considered the parameters such as magnet revolution speed, gap and magnetic compound finishing carrier rotational speed. Using magnetostatic simulation and varying the working gap under the same magnetising current, the appearance and the size of the finishing

spot is found [Guo *et al.*, 2014; Singh et al., 2012b]. The R_a value of finished BK7 glass totally depends on its machining system and its material properties. In general for the finishing of brittle materials, the involved material removal mechanisms are classified as the ductile mode and the brittle mode. During brittle mode, occurrence of the chipping is through lateral cracking but this mode provides excellent quality surface with less number of damage and low surface roughness. Observation says that brittle materials like borosilicate with higher fracture toughness still can provide relatively high machinability if parameters related to machining are selected carefully. Therefore, it is mostly recommended to process BK7 glass in ductile mode [Feng *et al.*, 2012; Malkin and Hwang, 1996; Pashmforoush and Rahimi, 2015; Onwuka and Abou-El-Hossein, 2016]. Magnetic assisted electrochemical finishing prevents electrolytic agents to get attach to the electrode material, and also, provides sudden discharge dregs from tool gap. For the improvement by finishing, the distance is kept shorter between the two magnets which provide large magnetic force [Pa, 2009]. [Qwen *et al.*, 2015] reported the work on micrometric measurement of forces of orthogonal cutting and turning.

Over the decades, remarkable improvements have been made in high resolution of linear, rotary motions (nanometric length for linear motion) and thermal stability [Zhang, 2015]. Complex components developed by additive manufacturing technique can be finished by recent developed abrasive fine finishing technology [Hahimoto, 2016]. It is possible to finish the optical polymers such as PMMA, BK7 and H_2O soluble with moderation in MR polishing fluid. Materials like $CuSO_4$, $NiSO_4$, $(H_2O)_6$ and optical glasses that are difficult to process, but can be polished by altered the composition of MR polishing fluid [Jacobs, 2007]. In present work, a modified solid rotating magnetorheological tool is used [Maan *et al.*, 2016]. The tool is comprised of solid core which rotates with the help of programmable servo motor, and capable to finish both ferromagnetic and non ferromagnetic materials. At the extremity of the solid rotating core tool, provided with uniform magnetic flux density [Maan *et al.*, 2016; Singh *et al.*, 2016; Khurana *et al.*, 2017] and it can find its application in nanofinishing of optical glasses. Therefore, the solid rotating core tool used in the present manufacturing process leads to nano-finish and it can be highly capable in precision engineering. The aim of the present work is to achieve and withstand the standards required by [LARAMY-K optical lab, 2010], improving the optical performance, and better surface profile of BK7 glass by using the present MR finishing process with the solid rotating core tool.

3.2 Experimental Methods

BK7 glass workpiece is selected for confirming its utility in practical application after finishing using the present MR fluid based process with solid rotating core tool. The material's composition is validated by using spectroscopy. The material compositions of the BK7 glass is found as SiO_2 = 70 %, B_2O_3 = 11.5 %, Na_2O = 9.5 %, K_2O = 7.5 %, and BaO = 1 %, 0.5 % of TiO_2, CaO and other foreign bodies. The BK7 glass specimen dimensions were taken as 10×10×3 mm. Initial surface roughness values of the BK7 glass workpiece is measured by using Surfcom 130A surface roughness tester and found as R_a = 41 nm and R_q = 57 nm. Scanning electron microscopy completes the study of finished surface characteristics of BK7 glass.

The requirement for holding the workpiece on the working table is accomplished by cuboidal shape fixture. The fixture for holding the workpiece is made with dimensions of 40×40×40 mm. The material used to fabricate the fixture is aluminium, which is fabricated by using vertical milling machine and surface grinder. The milling machine after machining on the surface of aluminium fixture may leave back many cut marks by milling cutter. This milled surface cannot suit for holding the soft BK7 glass workpiece as it can create scratches on the contacted surface of the glass. The surface finish achieved by grinding process is better than the milling process which can remove milling cut marks and achieve acceptable surface finish on the soft ductile aluminium fixture. This results in smooth holding of BK7 glass workpiece onto the ground ductile aluminium fixture.
The magnetorheological polishing fluid was made for this work composed of iron particles, cerium oxide and deionised H_2O. As water softens the surface of BK7 glass, pH is to be maintained below 9 to achieve high polishing rate and avoid leaching, a type of corrosion on glass that is visible to the unstrained eye (white spots). The reactions [Das, 2014] that occurs on the surface of BK7 glass with water at equilibrium pH is given in Eq. (3.1),

$$(OH-)L = K\ (= Si - O-)G \qquad (\mathbf{3.1})$$

Where, $(OH^-)_L$ is the active OH^- ions in the solution, $(= Si\text{-}O^-)_G$ presents the action performed by non-bonding O_2 ions at the surface of glass and K is equilibrium constant. According to the law of mass action, K depends on the concentrations unit used.

The specifications of abrasive powder are dusty white appearance with average particle size of 1.5 to 1.7 micron. As it is designed to produce high quality and scratch free surface with low level value of surface roughness. Mixing of Cepoll 1663 abrasive powder and

carbonyl iron particles with deionised H_2O is done by stirring machine. The total volume is 0.02 L = 20 cm^3 of MR polishing fluid, which contained CIPs 30 % by total volume = 6 cm^3, and by weight = 6 cm^3 × 7.8 gm/cm^3 = 46.8 gm. The cepoll 200 powder is 10 % by volume = 2 cm^3 and by weight = 2 cm^3 × 7.65 gm/cm^3 = 15.3 gm. Deionised H_2O used as carrier fluid is 60 % by volume = 12 cm^3 and by weight = 12 cm^3 × 1.0 gm/cm^3 = 12 gm. The process parameters and conditions are listed in Table 3.1.

Table 3.1: Process parameters selected for finishing of BK7 glass

Process parameters	**For BK7 glass workpiece**
Cerium oxide abrasive (by volume %)	10
Magnetic iron powder (by volume %)	30
Deionised water (by volume %)	60
Working gap (mm)	0.8
Magnetising current (A)	1.0
Rotational speed of tool (rpm)	400
Finishing cycle time (min)	90
Each finishing cycle time(min)	30
Feed rate (mm/sec)	2

A fixture made of aluminium is used for holding the flat surface glass workpiece which is gripped in a precision vice as shown in Fig. 3.1(a). With the use of feeler gauge, the working gap is maintained at 0.8 mm from tool tip to the flat surface glass workpiece. The feed rate of 2 mm/sec is given to the workpiece which followed horizontally to and fro motion along Y-axis. As soon as the current applied to the electromagnetic coil wounded on the core, a uniform magnetic flux generated on the core tool tip made of mild steel as shown in Fig. 3.1 (b).

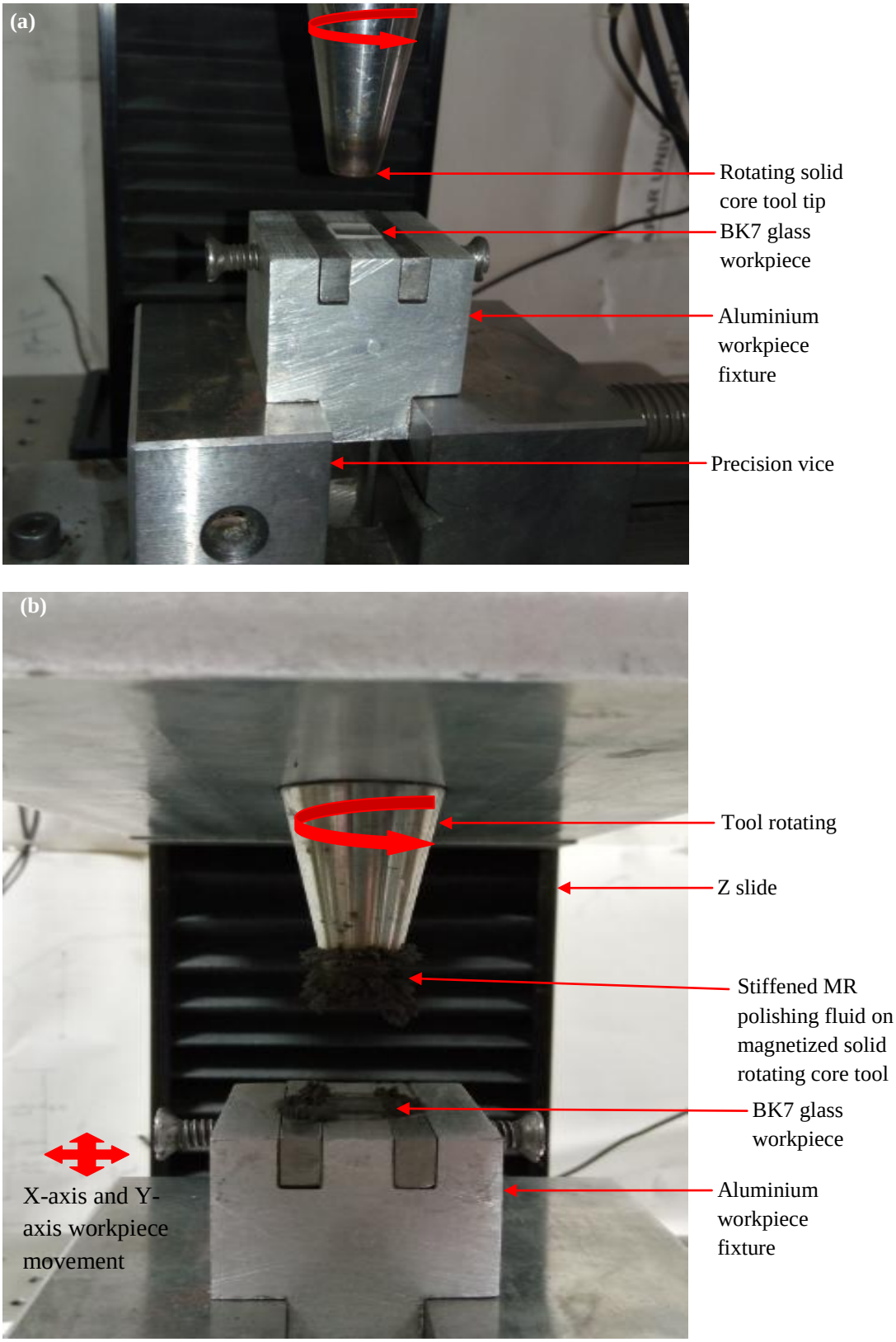

Fig. 3.1: (a) Workpiece held in fixture of aluminium material and (b) MR polishing fluid on magnetised solid rotating core tool under magnetic field for finishing of BK7 glass workpiece

Due to this uniform magnetic flux, the magnetic iron particles of MR polishing fluid forms chain like structure and providing uniform gripping to the abrasive particles which get gripped between them as shown in Fig. 3.2. For the creation of smooth and finish surface, there are two kinds of forces that directly affect the surface geometry of workpiece. Nanoscale and microscale indentation of abrasives on the workpiece surface is carried out by magnetic normal force where as cutting force during rotation of magnetorheological finishing tool, does the trimming off the crest of the ridge surface [Pashmforoush and Rahimi, 2015].

3.3 Surface Finishing Mechanism of BK7 Glass

The material removal rate (MRR) is obtained with the help of cook's equation as represented in Eq. (3.2),

$$MRR\ \alpha\ 1/\ Log\ (sbs\ |pH - IEP|) \qquad (\mathbf{3.2})$$

where, sbs = single bond strength of abrasive particle, pH = potential of hydrogen, and IEP = iso-electric point of the polishing abrasive (the pH of a host solution at a particular particle which carries no net electrical charge).

The maximum removal according to Cook's equation is obtained by maintaining the slurry's pH as close as to the IEP values of the abrasives (for cerium oxide generally ranges from 7 to 9). As the slurry's pH is close to IEP of abrasive particle, the abrasive particles tend to bunch up which increases material removal rate. The chemical and mechanical action of reaction of SiO_2 with deionised water is given in Eq. (3.3),

$$SiO2 + H2O \rightarrow Si(OH)4 \qquad (\mathbf{3.3})$$

where, SiO_2 is silicon dioxide and $Si(OH)_4$ is silicic acid. As mentioned in above reaction in Eq. (3.3), a rate constant exists which rapidly increases with increase in temperature. The MRR is directly proportional to the rate constant in prospective of reaction occurring chemically. As the upper most surface is removed mechanically by abrasion, the SiO_2 remaining gets exposed to the MR polishing fluid and chemical reaction continues. This step by step mechanism of material removal process, first chemical reaction occurs and then mechanically removal of material through abrasion from the surface of the BK7 glass workpiece as shown in Fig. 3.2.

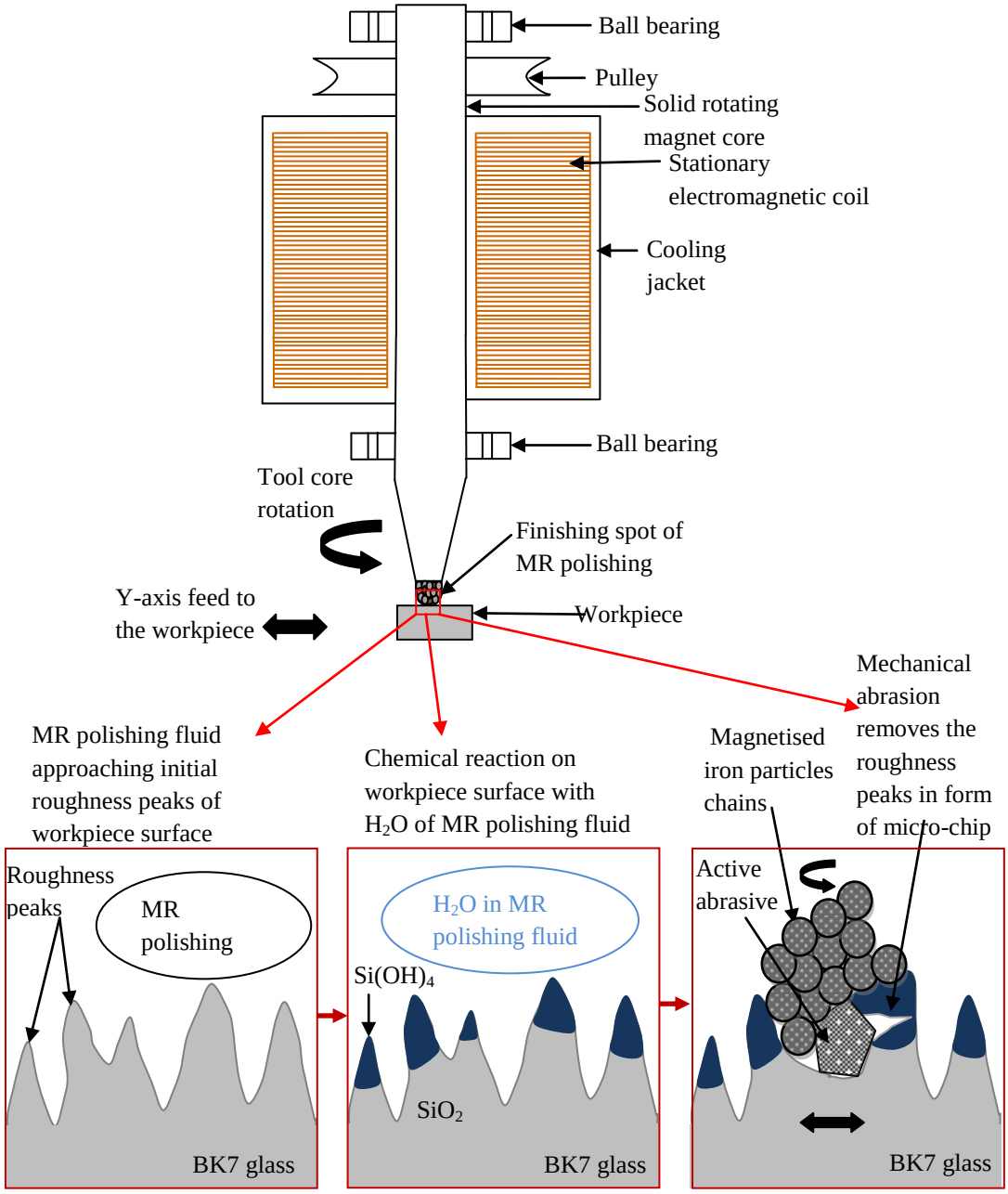

Fig. 3.2: Schematic diagram of solid rotating core tool with chemical and mechanical abrasion mechanism of material removal on the surface of BK7 glass workpiece

As soon as the current is supplied to the electromagnetic coil, a stable and uniform magnetic flux density is obtained at the tip of solid rotating core tool. Due to this uniform magnetic flux density, a chain-like structure of magnetisable iron particles is generated at the tool tip surface which holds the CeO_2 abrasive particles with consistent strength as shown in Fig. 3.2. On the finishing surface of the BK7 glass workpiece, these chain-like structures apply indent force through CeO_2 abrasive particles of MR polishing fluid. When tool rotates, the tangential force is exerted on the surface of BK7 glass workpiece by the magnetised iron

particle. The resultant force initializes the formation of cracks and further resulting in removal of micro-chipping. Thus, abrasion mechanism is obtained as the MR polishing fluid along with solid tool tip rotates with horizontal feed to the workpiece as shown in Fig. 3.2. The present solid rotating core tool has added benefits by providing uniform magnetic flux density [Maan *et al.*, 2016; Singh *et al.*, 2016; Khurana *et al.*, 2017]. Because of the flow of direct current in the stationary electromagnetic coil, heat is generated from the electromagnet. A refrigerated bath is used to supply constant flow of coolant over the electromagnet coil surface through the cooling jacket which dissipated the heat generation from electromagnet coil. As solid rotating tool core is rotated coaxially inside the electromagnet coil, heat is also dissipated on a solid rotating tool core from the electromagnet coil. Therefore, when cooling is done to the electromagnet coil, heat is not dissipated to the solid rotating tool core and it maintained constant low temperature at the solid rotating core tool tip during the finishing operation. Also, it prevents the variation in rheological properties of MR polishing fluid at tool tip surface which mainly affected by the rise in temperature.

The values of optical properties such as absorbance, transmittance, diffuse reflectance and total reflectance are obtained using UV-2600 SHIMADZU spectrophotometer. For the measurement of transmittance, an integrating sphere collects all the light which is transmitted in forward direction. As scattering through the sample, causes an amount of deviation of transmitted beam from optical path of the spectrophotometer, avoiding those beams to the lead sulphide detect also known as galena or resulting in value of transmittance lower than the original one. The reflectance of BK7 glass workpiece is measured by placing the workpiece at the back of the integrating sphere as shown in Fig. 3.3.

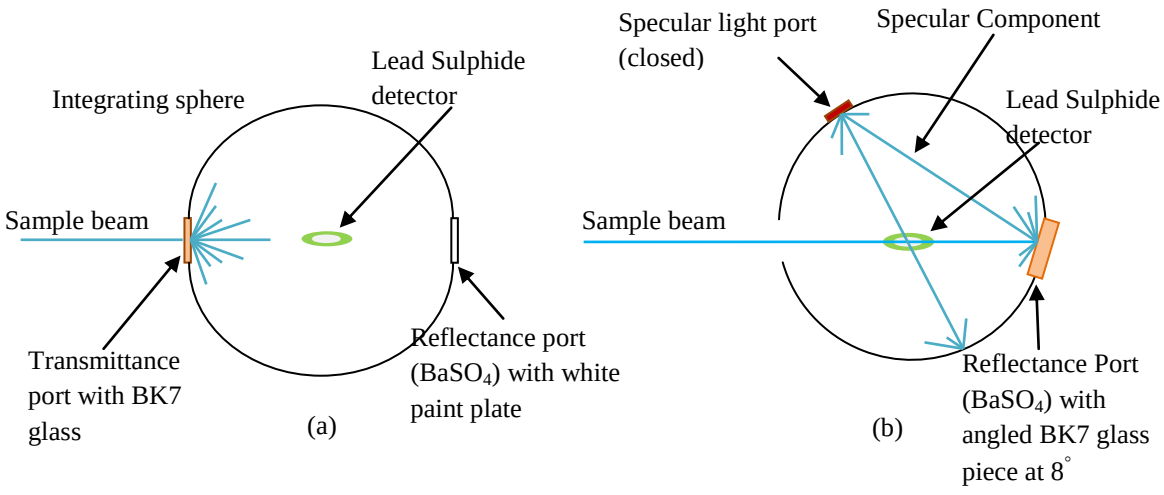

Fig. 3.3: Measurement by spectrophotometer for (a) transmittance and (b) reflectance

3.3 Results and Discussion

Surfcom 130A surface roughness tester is used for providing the surface roughness profiles for the experiments conducted. The surface roughness profiles for unfinished and finished BK7 glass workpiece with present MR finishing process are shown in Fig. 3.4. The reduction in profile of surface roughness of BK7 glass workpiece from 41 nm to 17 nm demonstrated the capability of the present solid rotating core magnetorheological finishing process. This is achievable due to uniform and high bonding strength of magnetic iron particles under the influence of magnetic field.

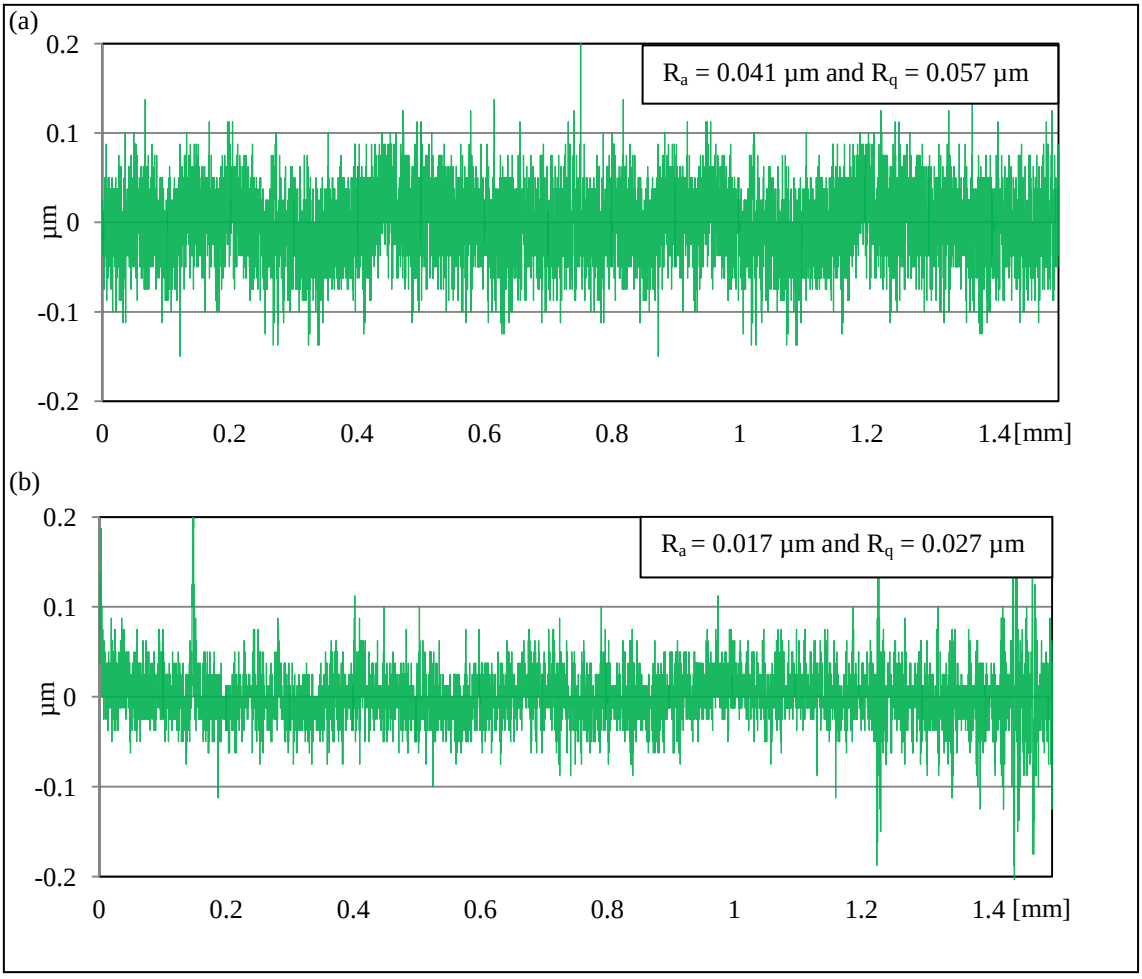

Fig. 3.4: Surface roughness profiles of BK7 glass workpiece (a) unfinished surface and (b) finished surface

The present work mainly focuses on the nanofinishing process to obtain desired surface profile of the BK7 glass. With solid rotating core tool, the magnetorheological finishing process is carried out step by step, started with the initial surface roughness values of Ra = 41

nm and Rq = 57 nm of BK7 glass. The 30 minutes of time interval is considered for each cycle of nanofinishing. After obtaining the Ra and Rq values at different time intervals of magnetorheological nanofinishing, the results are plotted on graph as shown in Fig. 3.5. The plot showed the uniform decreasing trend till 90 min of magnetorheological nanofinishing. There is a large amount of reduction in roughness values during the period of 0 to 30 min of finishing. The R_a value after magnetorheological nanofinishing of 30 min is reduced to 19 nm from 41 nm and R_q value reduced to 29 nm from 57 nm. But the rate of reduction of surface roughness values slowed down as the finishing time is extended to 60 min (Fig. 3.5). The final surface roughness values R_a and R_q are reduced to 17 nm and 27 nm in 90 minutes of finishing.

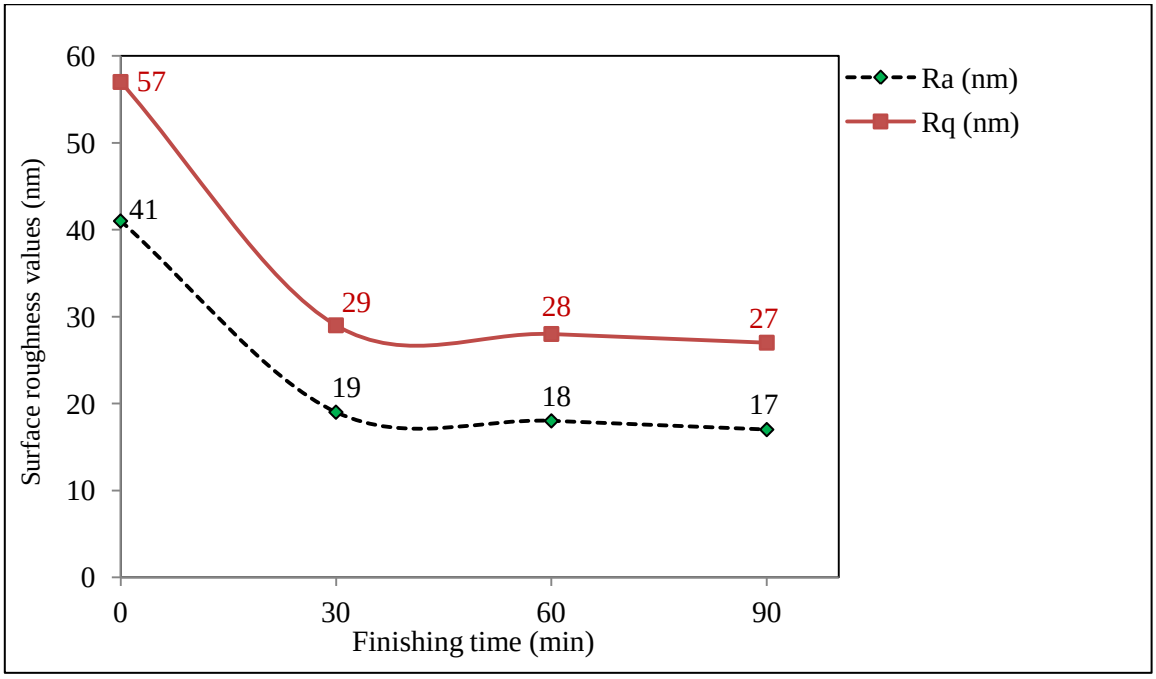

Fig. 3.5: Plot between the finishing time versus surface roughness values of BK7 glass workpiece

The factors responsible for slowing down the rate of reduction in the surface roughness values after 30 min of nanofinishing are the sharp cutting edges of abrasive particles and area of removal roughness peaks of the surface. The sharp edges of abrasive particles reduced with the increase in finishing time as the fracture occurs on the glass surface and the abrasive particles surface. Due to the continuous contact of abrasive particles with the glass surface during the rotational motion of tool, the sharp cutting edges of abrasive particles may start blunting. The abrasive particles without sharp cutting edges may cause for slowing down the rate of reduction in surface roughness values after 30 min of nanofinishing on the surface of

the BK7 glass. But in the present research, the MR polishing fluid is frequently changed manually after every 15 minutes of finishing time, so this may not be caused much for slowing down the rate of reduction in surface roughness values after 30 min. Therefore, another reason such as modulus of elasticity of roughness peaks may be considered for the slowing down the rate of reduction in surface roughness values. The modulus of elasticity of upper part of the roughness peaks is very less as compared to modulus of elasticity of base area of the peaks. The upper part of the roughness peaks with low modulus of elasticity gets trimmed off easily which led to more reduction in roughness values in the beginning of the finishing time. Rate of reduction in surface roughness values slowed down at the base area of roughness peaks because of comparatively its higher modulus of elasticity. The percentage reduction in R_a values for each 30 min of finishing till 90 minutes were found as 53.66 %, 5.26 % and 5.56 % respectively. R_q calculated as root mean square of surface measured of peaks and valleys, and used to characterise the material for optical applications. R_q value from initial value 57 nm reduced to 29 nm after 30 minutes of finishing. R_q values achieved by present magnetorheological finishing process after 60 and 90 minutes are 28 nm and 27 nm as shown in Fig. 3.5. The percentage reduction in R_q values for each 30 min of finishing till 90 minutes were found as 49.12 %, 3.45 % and 3.57 % respectively.

The effect of rotational speed of tool (rpm) and magnetising current (Amp) on percentage change in surface roughness is shown in Fig. 3.6. The magnetising current is related to magnetic flux density. Because, when direct current is supplied to electromagnetic coil it induces magnetic fields. Current at 1 Amp during finishing is found to be best process condition value that reduces the surface roughness R_a value to 17 nm (Fig. 3.5).

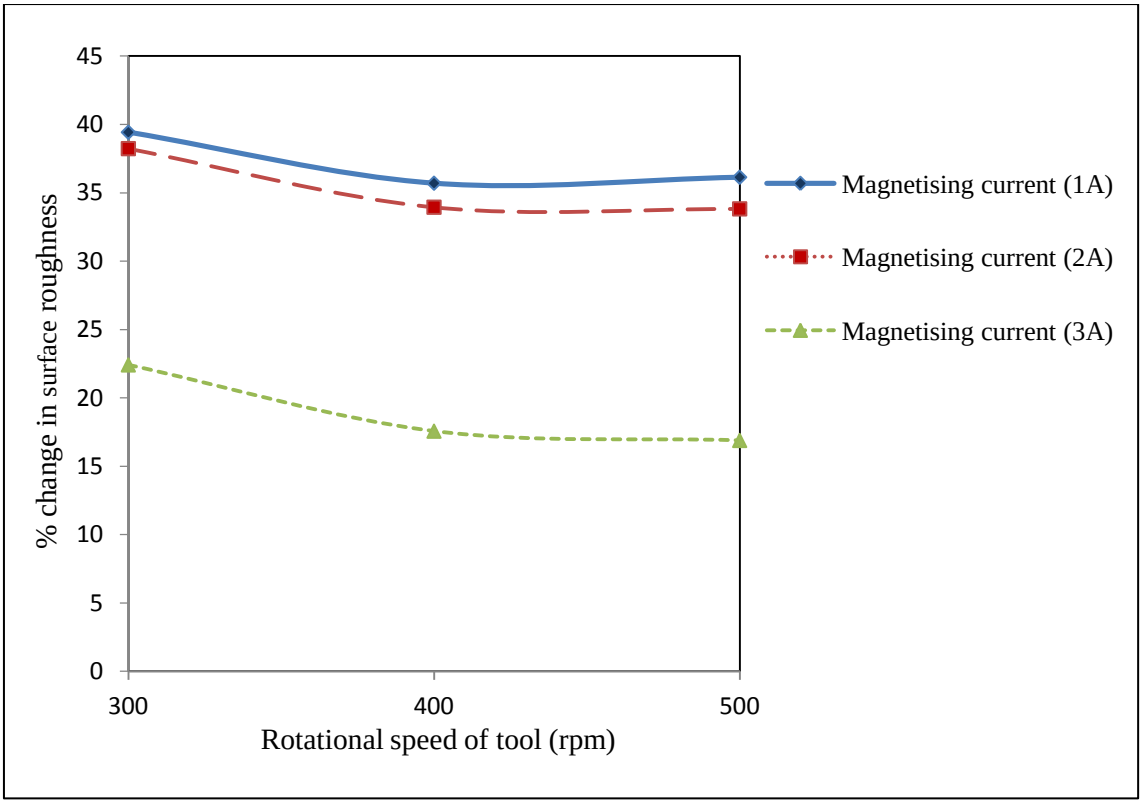

Fig. 3.6: Effect of rotational speed of tool (rpm) and magnetising current (A) on percentage change in surface roughness (%ΔR_a)

As seen in Fig. 3.6, rotational speed also affects the surface roughness profile of the BK7 glass workpiece. On increasing the rotational speed of the solid core tool from 300 rpm to 500 rpm it is found that the percentage change in surface roughness values decreased. It is due to increase in centrifugal force over the range of magnetic force. This centrifugal force results in weak bonding between the magnetised iron particles and CeO_2 abrasive particles. Due to this weak gripping, the abrasive particles gets misplace from the allocated area of finishing. As magnetorheological finishing with solid rotating core tool is a super finishing process, the obtained material removal rate (MRR) is quite low, therefore in the present work, the MRR is not considered.

The optical properties such as transmittance %, absorbance % and reflectance % of the present BK7 glass are plotted with UV-2600 SHIMADZU spectrophotometer. The results of ultraviolet-visible-infrared (UV-VIS-IR(A)) spectroscopy with the wavelength range of 190 nm to 1400 nm are presented as a function of surface roughness in Figures 3.7(a), 3.7(b) and 3.7(c) respectively.

Any light which is not reflected or absorbed by the glass is transmitted through the glass. Fig. 3.7(a) illustrates the effect of transmittance which increases with decrease in surface

roughness values. The increase in transmittance percentage after the present MR finishing on BK7 glass provided better results for the transmissive optics. The transmittance unit measured with the spectrophotometer were taken at 110-nm increments from 190 to 1400 nm of wavelength. For short wavelength ultraviolet B (UVB) region, 30.5 % of transmittance is required for lens manufacturing with the crown glass as material [LARAMY-K optical lab, 2010]. Initially the transmittance % lies between 2-3 % for unfinished BK7 glass at 190-228 nm, whereas for the finished BK7 glass, the % transmittance showed more than 4 % resulting in improvement in transmittance % of a material from the beginning itself (Fig. 3.7a). For the UVB region from 320 to 380 nm, the unfinished BK7 glass taken is not well suited for the lens manufacturing as transmittance percentage lie in range of 25-26 %. Because borosilicate glass used does not allow the desired amount of limit through it and can affect the image quality that is blurring effect. This is often occurred due to the uneven surface profile of the glass workpiece. Nanofinishing of the unfinished BK7 glass workpiece enhanced the transmittance % to approximately 42 %. This results in transmitting large amount of light through the finished BK7 glass. After finishing of BK7 glass by the present magnetorheological finishing process with solid core rotating tool, the transmittance percentage at wavelength 380 nm achieved is 41.9717 from the initial 26.1411 % transmittance. Also, for the long range wavelength 380 to 1400 nm, there is a significant improvement in transmittance percentage till 43.4278 % from 30.5454 %. Hence, the present finished BK7 glass can be extensively used in manufacturing of lens.

When light travels through a glass, the intensity of the light is typically reduced. This takes place when the energy of a photon of light matches the energy needed to excite an electron to its higher energy state within glass. Thus, the photon is absorbed by the BK7 glass. Absorbance (Au) is calculated with the Beer lamber law and verified with spectrophotometer readings. This is found a decreasing pattern with the decrease in R_a value shown in Fig. 3.7(b). The finished BK7 glass absorbed less than 1.35 % in UV wavelength range of 190 to 220 nm with respect to unfinished BK7 glass absorbing 1.49 %, following the design of spline the percentage absorbance gradually decreased to 0.5 % from 270 to 300 nm. This results in less absorption of light by the material. Results obtained from UV-VIS-IR (A) spectroscopy for both of the unfinished BK7 glass and finished BK7 glass shows a constant plot for the wavelength region from 300 to 1400 nm. The best absorbance is found in VIS wavelength range at 787 nm which is 0.3629 Au and calculated as 3.629% of finished BK7 glass workpiece. This range of absorbance is acceptable in lens manufacturing and often assumed as negliable.

The total reflectance increases with specularity of the surface, and diffuse reflectance reduces with the specularity of the surface. Results showed the relation between the surface profiles with the reflectance in plot of Fig. 3.7(c). At 190 nm in vacuum UV range, the percentage reflectance is more than 36 % for finished BK7 glass. Gradually decreasing pattern, for both unfinished and finished BK7 glasses indicates that the present nanofinishing process does not disturb the spectra of the material used. Wavelength range from 300 to 1400 nm, the percentage reflectance remains constant for both unfinished and finished BK7 glass approximately between 8 to 13 %. Best reflectance value achieved of finished BK7 glass at 192 nm is 37.9791 % from 37.9993 % of unfinished glass. This percentage reflectance can be removed using anti reflective coating for the implementation of this material in lens manufacturing or directly can be used as mirrors too.

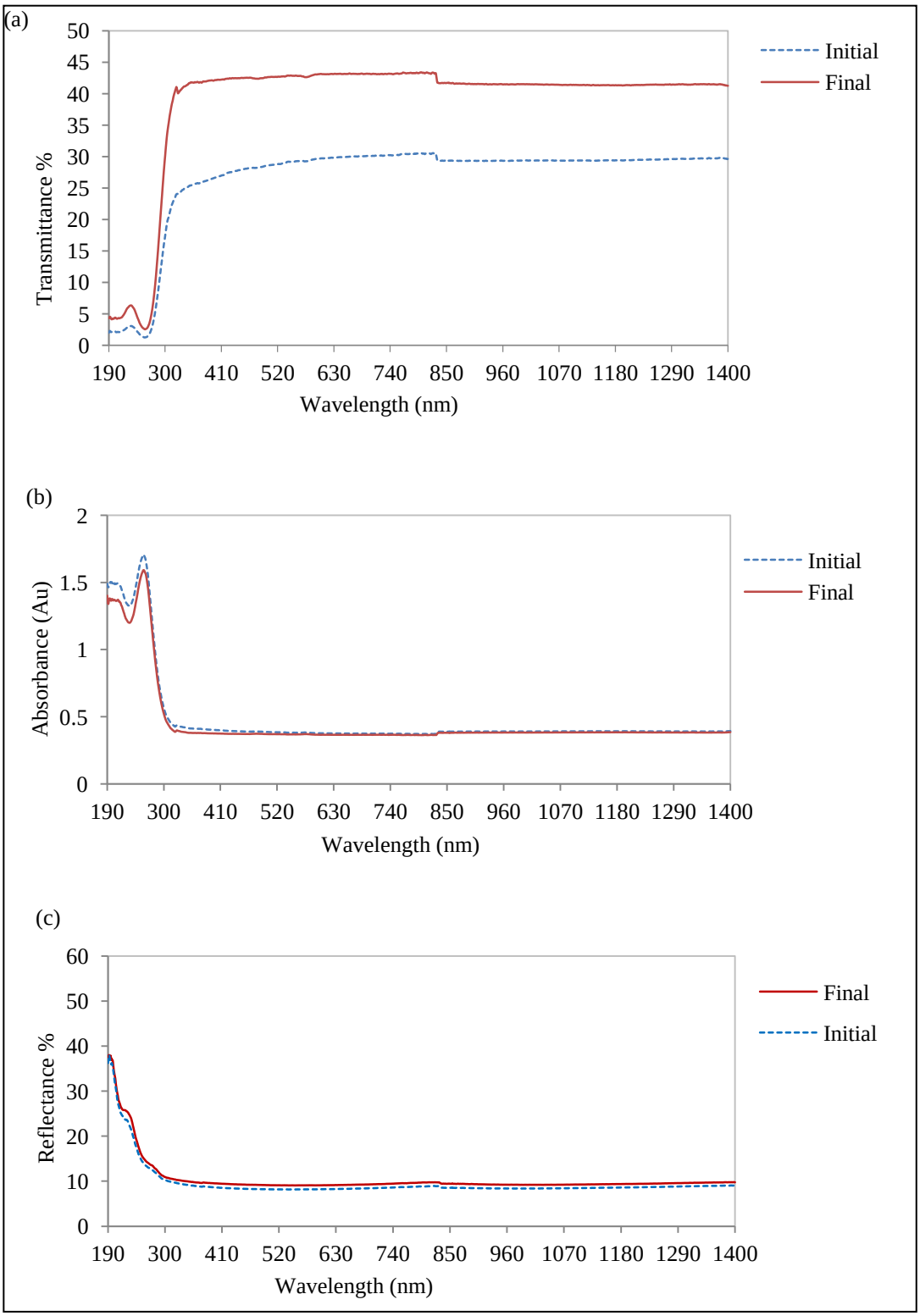

Fig. 3.7: Effect of surface roughness on optical properties of BK7 glass workpiece (a) transmittance, (b) absorbance and (c) reflectance

The scanning electron microscopy (SEM) analysis of both the unfinished and finished surface of BK7 glass is also carried out with the help of JEOL JSM-6510LV scanning electron microscope. This SEM measurement clearly visualized the surface morphology of BK7 glass before and after magnetorheological nanofinishing. After 90 min of finishing, the SEM analysis at 6000× is carried out on the unfinished surface and finished surface of BK7 glass workpiece shown in Figures 3.8(a) and 3.8(b) respectively. Multiple number of debris can be seen on the unfinished surface of BK7 specimen. These crags like peaks were removed by present magnetorheological finishing process with solid rotating core tool. This results in finished BK7 glass without any scratches as shown in Fig. 3.8(b).

(a)

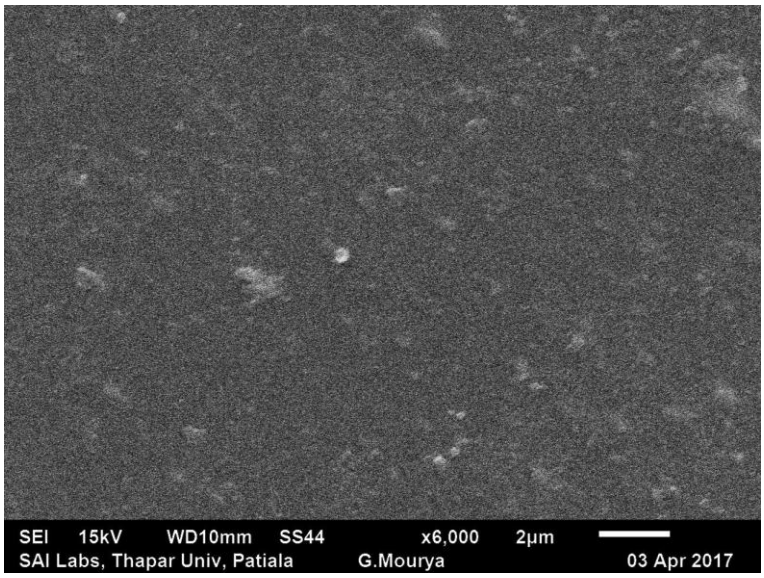

(b)

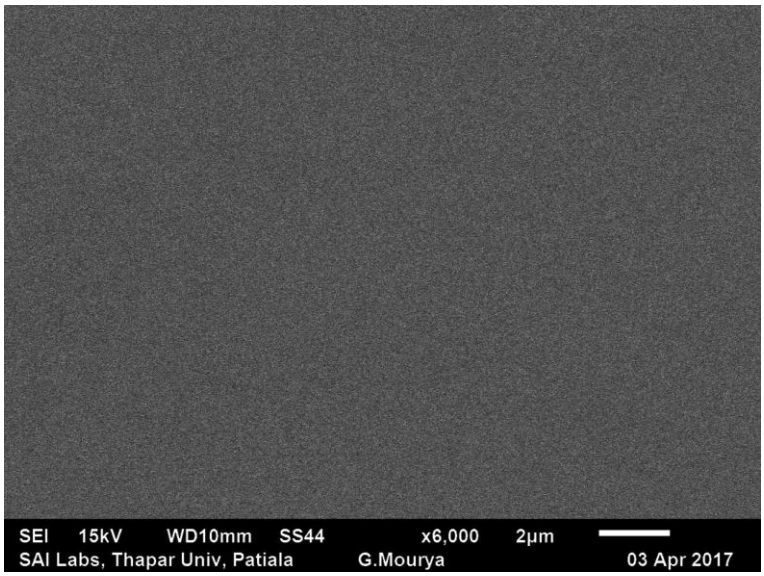

Fig. 3.8: Scanning electron microscopy (SEM) at 6000× of (a) unfinished BK7 glass and (b) finished BK7 glass

The BK7 glass with transmittance more than 30.5 % is required as optical property for lens manufacturing material as crown glass, offers a boost to transmissive optics as per the LARAMY-K optical lab. Therefore, the present finished BK7 glass with transmittance value of 43.4278% confirmed that it is useful in lens manufacturing. Hence, the present finished BK7 glass can find its relevance in transmissive optics such as telescopes, microscope, light emitting diodes and binocular. The characteristics like scratch resistance, hardness and cost, the BK7 glass showed more satisfactory results than fused silica glass as used for UV, visible and near infrared optics.

3.4 Conclusions

The present work demonstrated the MR finishing process with the solid rotating core tool on the BK7 glass. Cerium oxide is used as abrasive powder in the magnetorheological fluid. Finishing without any scratches on the BK7 glass surface has been achieved using appropriate composition and size of abrasives in MR polishing fluid. Based on the results obtained from the present work, the following conclusions are drawn.

- The MR finishing process with the solid rotating core tool is found to be more successful in improving the optical properties of BK7 glass.
- Surface roughness values Ra and Rq of BK7 glass workpiece is reduced to 17 nm and 27 nm from 41 nm and 57 nm by using uniform magnetic flux density at the end of solid rotating core tool.
- Scanning electron microscopy showed the better results in surface morphology of finished BK7 glass.
- Result obtained from Photospectroscopy fulfilled the optical properties such as transmittance percentage, absorbance percentage and reflectance percentage required for lens manufacturing.
- Present work illustrated that both the transmittance and reflectance increased with the decreased in surface roughness value.

Chapter 4

Parametric Analysis of Magnetorheological Nanofinishing on BK7 Glass Using Solid Core Rotating Tool

4.1 Chapter Overview

Surface finish is a significant requirement for optics. The current research focuses on the nanofinishing of BK7 glass by solid rotating core tool using indigenously made MR polishing fluid. Magnetorheological finishing is a process that can be performed in both the ways; either it is loose abrasive polishing or flexible abrasive polishing. The plasma dry etching method is used to produce these glass grasses structures. And these structures are differentiated into four different categories, such as grass structures, needle structures, pillar structures and tube-like structures. Many workers have observed a presence of a thin layer that is generated on the surface of glass during the polishing process. Later, this thin layer was termed as 'polish layer'. Polish layer stands different with respect to structure and physical properties from the bulk glass [Yokota *et al.*, 1969]. Because of high normal forces in conventional lap polishing which leads to the development of damage sites on both surface as well as sub surface [Lee et al., 2011]. Polishing of optical materials is benefited using MR finishing techniques, as polishing is performed without generating subsurface affected layer [Kordonski and Jacobs, 1996]. While comparing MR finishing techniques with conventional polishing techniques, the force acting on each abrasive particle is relatively very small. This means that the shear force is used determine the material removal rate [Shorey *et al.*, 2001]. Forces acting on each particle on the ribbon of MR fluid is calculated and normal force is found to near about 1×10^{-07} N [Shorey, 2000]. The force acting on individual abrasive particle is resulted as 5-200 $\times$ 10^{-03} N for conventional polishing [Bulsara *et al.*, 1998]. A programmable numerically controlled MR finishing machine, the Q22 in commercial, recently came in optics industry to produce precision spherical surface components, flat surface components and aspheric surface components. Abrasives are the basic element for MR polishing fluid in the optics industry [Kordonski *et al.*, 1998]. MR finishing is

implemented on optical components of different types of surface such as flat, concave, convex and aspheric; to obtain precision finishing [Golini *et al.*, 1999].

Several "non-contact" finishing processes are developed, and are providing high level finishing using various compositions of abrasives in magnetic and electro rheological fluids. Polishing various complicated geometries abrasive flow finishing is used which is also a non-contact finishing process [Zhong, 2008]. With certain alterations in the chemistry of MR fluid, MR finishing is capable to finish difficult surface of different optical materials. Soft optical materials like single crystal, PMMA and ZnS; can be polished [Jacobs, 2007].

Nanofinishing process must be capable of providing precision, good quality surface finish and defects free surface. The time from the commercialisation of magnetorheological finishing in the world, new techniques and new methods have developed using smart MR fluid and magnetic field. BEMRF process is capable to finish both ferromagnetic and non-ferromagnetic materials. Conditioning can be provided to the MR polishing fluid, as the flow of MR polishing fluid is not continuous at the tool tip. The flow is regulated with the help of a peristaltic pump, or else continuation with already formed MR polishing fluid spot may affect material removal rate [Singh et al., 2011].

In present work, latest magnetorheological nanofinishing with solid rotating core tool is performed. This solid core tool comprises of a stationary electro-magnet coil and Cu cooling coils, wound over the stationary electro-magnet coil for providing constant chilling [Khurana et al., 2017]. Cooling jacket is provided to maintain the temperature of electromagnetic coil below room temperature which allows coolant to flow around that electro-magnet coil with the help of a pump from coolant tank. The MR polishing fluid is applied manually by the worker at the solid core tool tip, resulting in less wastage of MR polishing fluid.

Photograph of an improved BEMR finishing set-up is shown in Fig. 4.1. The new solid rotating core tool is mounted on the vertical slide (Z-axis) of the 3-axis motion platform. Four servo motors are used and are driven by programmable devices. One servo motor is used for providing rotational motion to the solid core tool and remaining three does the work of providing movement to the workpiece and tool in XYZ direction. An RTD is inserted between the windings of electromagnet coil which reports the variation in temperature during the process of finishing.

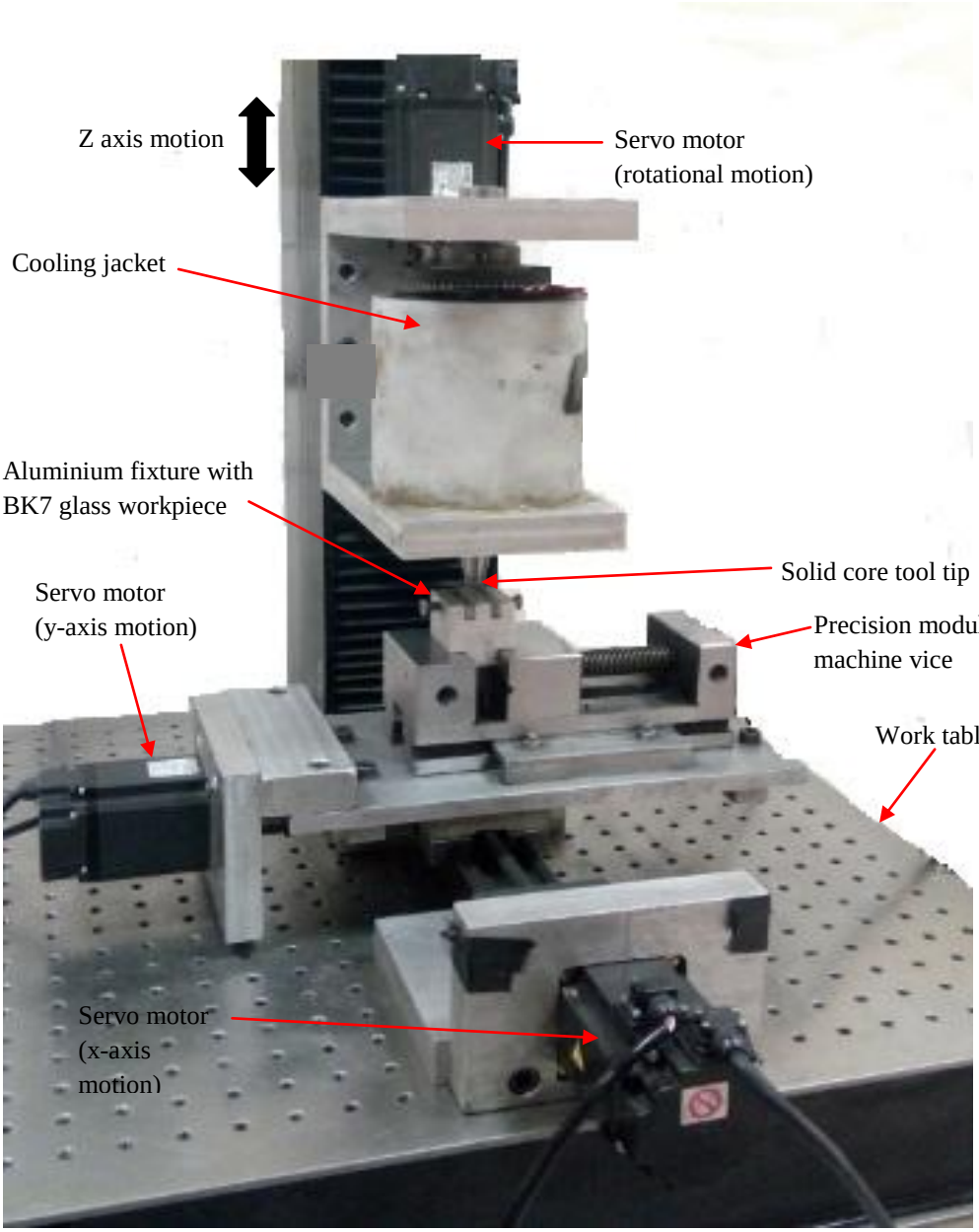

Fig. 4.1: Photograph of the set up of magnetorheological finishing with solid rotating core tool.

4.2 The Process Variables

From the initial stage of engineering, lot of finishing methods and processes have developed and implemented for various applications. Comparatively, MRF process with solid core tool is a recently developed and there is a deficiency of data available in literature on this finishing process. Thus on similarity basis with the other MRF processes, both the

controllable and un-controllable variables are identified. Table 4.1 list out the variables and the controlled variables are selected for parametric study.

Table 4.1: Process variables MRF process with solid rotating core tool

Independent controllable variables	Dependent uncontrollable variables
Rotational speed of tool core Magnetizing current Working gap Abrasive type, concentration, and mesh size Carbonyl iron particle size and Concentration Base medium volume percentage and Viscosity Initial surface roughness	Ambient temperature

4.2.1 Cerium Oxide as Abrasive Powder

Cerium oxide (CeO_2) is the basic ingredient in making MR polishing fluid. CeO_2 is world widely accepted for using as abrasive powder in precision finishing of optical glasses, as it reduces the chances in generating defects like cracks, sub-surface damage and glass corrosion. Cepoll product of grade 1663, cerium oxide powder manufactured by RCMPA Polishing Technologies Pvt. Ltd. is used in this study. Average abrasive particles taken for this research were 1.5 to 1.7 microns. MR polishing fluid consists of CeO_2 particles, carbonyl iron particles and de-ionised water. This combined form of particles in de-ionised water will get stiffen under the influence of magnetic field. Due to the rotational motion provided by servo motor, the CeO_2 abrasive particles are expelled towards the superficial surface of the MR polishing fluid as shown in Figure 2. It may occur because the centrifugal force exceeds the magnetic force of attraction between the magnetised iron particles under the influence of magnetising current. As the feed rate of 2 mm/sec is given through X-slide, these particles contact the glass specimen and they are returned back, so forces between the magnetised iron particle and CeO_2 particles are very small. Resulting as an organised system, providing every CeO_2 abrasive particles to involve in abrasion mechanism i.e. contact with the glass specimen and enhance material removal. CeO_2 by percentage volume in MR polishing fluid is taken in range from low to high i.e. 5 to 15 %.

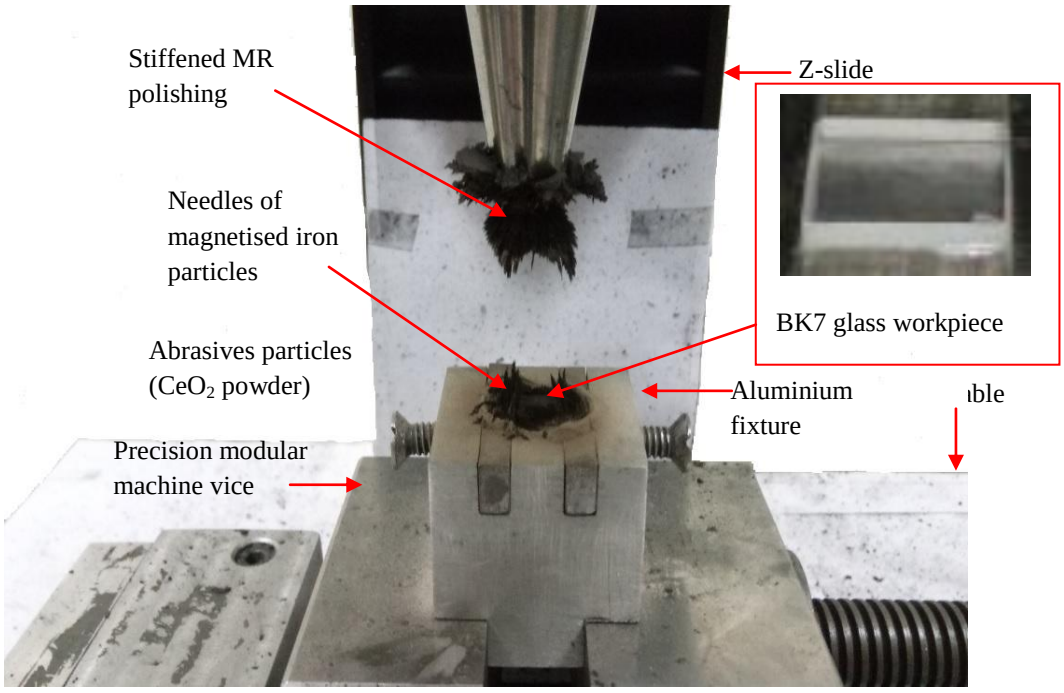

Fig. 4.2: Dusty white appearance of abrasive (CeO_2) particles observed on and near to the finishing region.

4.2.2 Magnetizing Current

Magnetorheological phenomenon occurs at tip of the solid rotating core tool, these rheological properties of ball nose finishing region totally depends on magnetic flux density and as well as its uniformity. Also, it depends on the supply of the current i.e. magnetising current to a stationary electromagnetic coil. The actual strength of finishing region of MR polishing fluid at the solid core rotating tool tip is governed by providing the supply of direct current to stationary electromagnetic coil. During the time of abrasion, the removed material from top surface of the glass specimen directly depends on bonding strength of magnetised iron particles at finishing region. As per the design of electromagnet, the values of magnetising current were selected which lie in range from low to high i.e. 1.0 Amp to 3.0 Amp and experiments were performed.

4.2.3 Rotational Speed of Solid Core Rotating Tool

Removal of peaks from the surface of the glass workpiece is achieved by the rotational motion of the solid core rotating tool with the finishing region of MR polishing fluid. Material removal originates from a crack and ends at micro-chipping. This is governed by the

shear force during the rotation of solid core tool with a finishing region of MR polishing fluid. Considering the statistical design of 3-level, experiments are conducted at three different level such as 300, 400 and 500 revolutions per minute (rpm). These values of rotational speed were selected on the basis of preparative experimentation.

4.2.4 Working Gap

Distance between the tool facing workpiece surface and the solid core tool tip end surface which is generally termed as 'working gap'. By varying the gap distance, the effectiveness of finishing region of MR polishing fluid at the solid core tool tip can be controlled. Meanwhile a constant direct current supply is provided to the stationary electromagnet coil. This means, on keeping the tool end tip closer to the glass specimen for current constant supply, magnetic field will increase at the tool end tip. Result in more material removal from glass workpiece surface (facing tool) by stiffening the MR fluid at the finishing region. Similarly for the same supply of current with the tool tip surface kept functioning comparatively away from the glass specimen, the magnetic field gets decreased at the solid core tool end surface. This results in less stiff finishing region of the MR polishing fluid. Less number of peaks are removed. Experiments are conducted at different working gaps such as 0.60 mm, 0.8 mm and 1.00 mm respectively. These working gap distance values are chosen on available literature basis.

4.3 Design of Experiments

Experimental investigation is carried out on the basis of design of experiments and a study is conducted which shows the effects of the selected process variable on improvement in surface quality in terms of surface roughness values. A MRF method using solid core rotating tool [Khurana et al., 2017] is implemented on the BK7 glass to conduct the designed experiments successfully, as shown in Fig. 4.1. Flat BK7 glass specimens of dimension 10×10×3 mm are taken for experiments and this cuboidal shape is obtained by pitch polishing. The initial surface roughness value was 0.041 μm. Percentage change in surface roughness ($\%\Delta R_a$) for each experiment is calculated using Eq. (4.1) and is given as,

$$(\%)\Delta Ra = [(Rai - Raf)/Rai] \times 100 \qquad (\mathbf{4.1})$$

An aluminium fixture was made in cuboidal shape after performing several precision machining operations such as milling, surface grinding, etc. Square shape slot of dimension 10×10×3.5 mm is cut from the aluminium fixture for holding the BK7 glass specimen. Programmable servo motors for X-Y linear motion provides movement to fixture held in precision vice. Y axis slide provides the reciprocating movement to the fixture for performing finishing, as the solid core tool tip diameter, workpiece length and width are same. Response surface methodology (RSM) is a statistical approach which is employed to increase the production of final product by optimizing the selected process parameters. This method is used for analysing and solving engineering related problems. Considering the case of full factorial experiment with all combinations of levels, the responses are measured. This fusion of levels represents the requirements and responses, at which they are, performed [Montgomery, 2001]. To study the importance of regression equation, analysis of variance (ANOVA) is performed. 'F' test value is taken to study relationships between controllable process parameters and explaining the cause for improvement in response. Using full factorial design, the effects on $\%\Delta R_a$ with four process variables are investigated. The actual values and coded values of different process parameters used in nanofinishing of BK7 glass workpiece with solid rotating core tool are listed in Table 4.2. Table 4.3 lists out the various experimental conditions. MR polishing is prepared by mixing the magnetised iron particles, CeO_2 abrasive particles and de-ionised H_2O (by percentage volume). Table 4.4 lists the range of composition of ingredients used in making MR polishing fluid. Random order experiments were conducted on BK7 glass specimen, according to the plan of experiments listed in Table 4.5.

Table 4.2: Coded levels and corresponding actual values of process parameters

S. No.	Parameter	Units	Low actual	High actual	Low coded	High coded
1.	Abrasive (P)	% V	5.00	15.00	-1	1
2.	Magnetising Current (M)	Amp	1.00	3.00	-1	1
3.	Rotational speed of solid rotating core tool (S)	Rpm	300.00	500.00	-1	1
4.	Working gap (R)	mm	0.60	1.00	-1	1

Table 4.3: Experimental parameters and conditions

Parameters	**Conditions**
Finishing cycle time	30 min
Constant feed rate to workpiece for to and fro motion	2 mm/min
Workpiece material	Borosilicate glass (BK7)
Bonded type cerium oxide powder	1.5 to 1.7 micron

Table 4.4: Composition of MR polishing fluid

Constituents	**% volume concentration**
Carbonyl iron powder	25-35
Bonded type cerium oxide powder	5-15
Deionised water as base fluid	60

Table 4.5: Plan of experiments

Run order	Standard order	Coded values				Actual values			
		A	B	C	D	P	M	S	R
7	1	-1	1	1	-1	5	3	500	0.6
16	2	1	1	1	-1	15	3	500	0.6
22	3	0	-1	1	0	10	1	500	0.8
25	4	0	0	0	0	10	2	400	0.8
21	5	0	0	0	0	10	2	400	0.8
23	6	0	0	0	-1	10	2	400	0.6
15	7	-1	1	1	1	5	3	500	1
2	8	1	-1	-1	-1	15	1	300	0.6
20	9	1	0	0	0	15	2	400	0.8
19	10	-1	0	0	0	5	2	400	0.8
12	11	1	1	-1	1	15	3	300	1
17	12	1	0	0	0	15	2	400	0.8
6	13	1	-1	1	-1	15	1	500	0.6
29	14	0	0	0	0	10	2	400	0.8
13	15	-1	-1	1	1	5	1	500	1
30	16	0	0	0	0	10	2	400	0.8
10	17	1	-1	-1	1	15	1	300	1
14	18	1	-1	1	1	15	1	500	1
1	19	-1	-1	0	-1	5	1	400	0.6
26	20	0	0	0	0	10	2	400	0.8
11	21	-1	1	-1	1	5	3	300	1
5	22	-1	-1	1	-1	5	1	500	0.6
9	23	-1	-1	-1	1	5	1	300	1
3	24	-1	1	-1	-1	5	3	300	0.6
27	25	0	0	0	0	10	2	400	0.8
4	26	1	1	-1	-1	15	3	300	0.6
28	27	0	1	0	0	10	3	400	0.8
24	28	0	0	0	1	10	2	400	1
8	29	0	1	1	-1	10	3	500	0.6
18	30	0	0	1	0	10	2	500	0.8

4.4 Surface Finishing Mechanism on BK7 Glass Workpiece with the Present MR Finishing Process

Removal of material from BK7 glass is achieved by chemical action and mechanical action as shown in Fig. 4.3. When the water molecules present in the MR polishing fluid gets in contact with the BK7 glass, the reactions start to occur on outer most surface of BK7 glass workpiece. The hydration that takes place on the outer most surface of BK7 glass is given in Eq. (4.2) as

$$SiO2 + H2O \rightarrow Si(OH)4 \qquad (\mathbf{4.2})$$

Where water molecule (H_2O) reacts with silicon dioxide (SiO_2) to give silicic acid [$Si(OH)_4$] which is a weak acid. Material is removed from the surface of BK7 glass workpiece by mechanical abrasion, as the rotation motion of the solid core tool facilitates the breaking of hydrated surface roughness peaks. After the removal of the hydrated surface, the surface below it gets exposed to the MR polishing fluid. This bit by bit removal continues to achieve low surface finish.

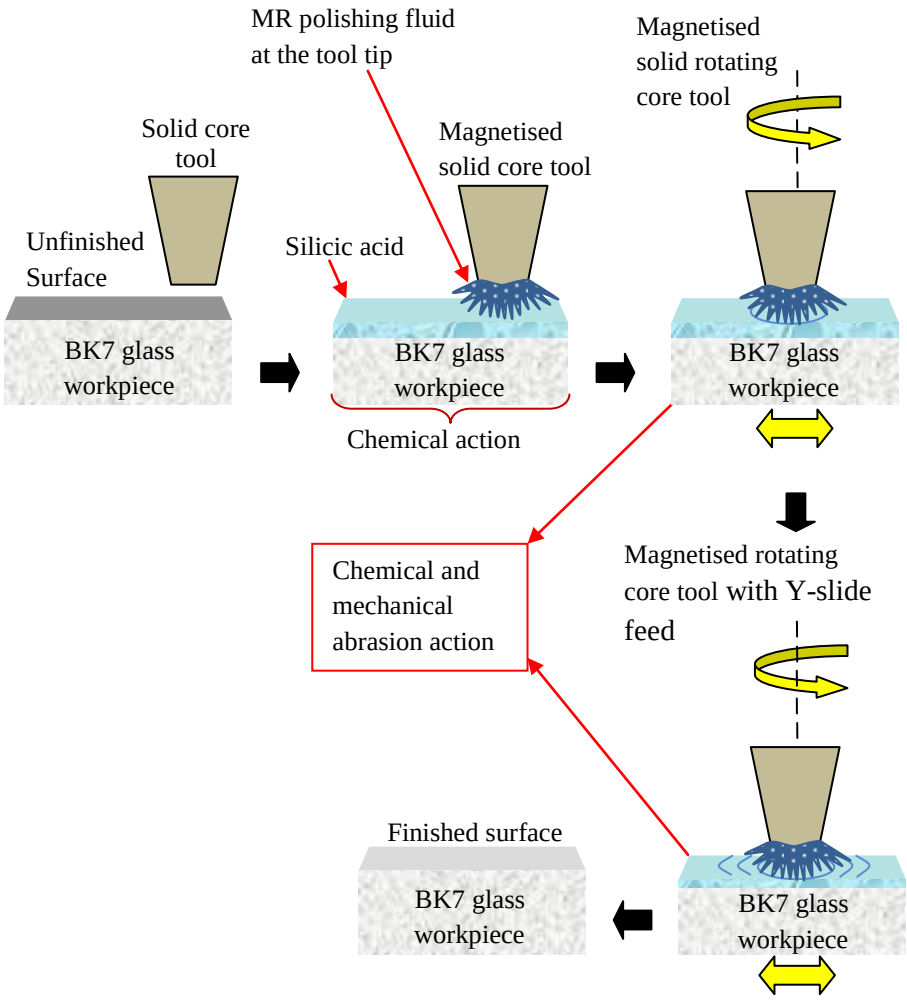

Fig. 4.3: Material removal mechanism through chemical and mechanical action

4.5 Response Surface Regression Analysis

All the surface responses are listed in Table 4.6, responses are absolute value R_a and $\%\Delta R_a$.

Table 4.6: Summary of responses

Std order	Factors				Initial average roughness value (μm) R_{ai}	After finishing average roughness value (μm) R_{af}	% change in roughness values ΔR_a (%)
	P	M	S	R			
1	5	3	500	0.6	0.041	0.027	32.426
2	15	3	500	0.6	0.041	0.026	35.191
3	10	1	500	0.8	0.041	0.030	25.389
4	10	2	400	0.8	0.041	0.028	30.682
5	10	2	400	0.8	0.041	0.028	31.382
6	10	2	400	0.6	0.041	0.027	32.387
7	5	3	500	1	0.041	0.033	18.441
8	15	1	300	0.6	0.041	0.026	35.664
9	15	2	400	0.8	0.041	0.027	33.207
10	5	2	400	0.8	0.041	0.027	31.736
11	15	3	300	1	0.041	0.029	27.363
12	15	2	400	0.8	0.041	0.028	30.207
13	15	1	500	0.6	0.041	0.028	31.101
14	10	2	400	0.8	0.041	0.028	31.112
15	5	1	500	1	0.041	0.033	18.486
16	10	2	400	0.8	0.041	0.028	31.282
17	15	1	300	1	0.041	0.028	30.184
18	15	1	500	1	0.041	0.030	25.332
19	5	1	400	0.6	0.041	0.029	27.726
20	10	2	400	0.8	0.041	0.028	30.882
21	5	3	300	1	0.041	0.028	30.371
22	5	1	500	0.6	0.041	0.030	25.151
23	5	1	300	1	0.041	0.028	30.006
24	5	3	300	0.6	0.041	0.022	46.068
25	10	2	400	0.8	0.041	0.028	31.682
26	15	3	300	0.6	0.041	0.022	46.063
27	10	3	400	0.8	0.041	0.028	31.597
28	10	2	400	1	0.041	0.031	22.654
29	10	3	500	0.6	0.041	0.027	33.019
30	10	2	500	0.8	0.041	0.028	30.599

For selecting the highest order polynomial, the sequential model sum of squares is calculated. The additional terms are significant and non-aliased model, terms with increase in complexity contribute to total model as shown in Table 4.7. Lack of fit for all tests is presented in Table 4.8. As linear terms are the highest and p-value is least, suggests the

model suitability for addition of quadratic terms to 2FI (two factor integration). For the selected quadratic model "Lack of fit" is found insignificant. Considering Table 4.7 and Table 4.8, a quadratic model is selected.

Table 4.7: Sequential model sum of squares

Source	**Sum of squares**	**DOF**	**Mean square**	***F*-value**	***p*-value Prob > *F***	**Remark**
Mean	28054.28	1	28054.28			
Linear	796.75	4	199.19	23.22	< 0.0001	
2FI	150.63	6	25.11	7.48	0.0003	
Quadratic	43.66	4	10.91	8.13	0.0011	Suggested
Cubic	15.00	9	1.67	1.94	0.2158	Aliased
Residual	5.14	6	0.86			
Total	29065.45	30	968.85			

DOF: degrees of freedom; 2FI*: two factor interaction.

Table 4.8: Lack of fit tests

Source	**Sum of squares**	**DOF**	**Mean square**	***F*-value**	***p*-value Prob> *F***	**Remark**
Linear	209.28	19	11.01	12.85	0.0023	
2FI	58.65	13	4.51	5.26	0.0258	
Quadratic	15.00	9	1.67	1.94	0.2158	Suggested
Cubic	0	0				Aliased
Pure Error	5.14	6	0.86			

DOF: degrees of freedom; 2FI: two factor interaction.

For response surface model at initial stage, all terms were include such as P, M, S, R, P^2, M^2, S^2, R^2, PM, PS, PR, MS, MR and SR. Where process parameter 'P' stands for composition of abrasive in MR polishing fluid by percentage volume, 'M' for magnetising current, 'S' for rotational speed of solid core tool and R stands for working gap. ANOVA for this selected model is given in Table 4.9.

Table 4.9: ANOVA for percentage change in R_a

Source		Sum of squares	DOF	Mean square	*F*-value	Prob > *F*	Remark
Model		991.04	14	70.79	52.72	< 0.0001	Significant
	P	8.50	1	8.50	6.33	0.0238	
	M	41.80	1	41.80	31.13	< 0.0001	
	S	309.18	1	309.18	230.28	< 0.0001	
	R	462.73	1	462.73	344.65	< 0.0001	
	P^2	3.08	1	3.08	2.30	0.1506	
	M^2	5.04	1	5.04	3.76	0.0717	
	S^2	19.37	1	19.37	14.43	0.0017	
	R^2	26.52	1	26.52	19.75	0.0005	
	PM	3.86	1	3.86	2.87	0.1107	
	PS	16.64	1	16.64	12.39	0.0031	
	PR	0.062	1	0.062	0.046	0.8322	
	MS	3.62	1	3.62	2.70	0.1213	
	MR	58.87	1	58.87	43.85	< 0.0001	
	SR	1.17	1	1.17	0.87	0.3647	
Residual		20.14	15	1.34			
Lack of Fit		15.00	9	1.67	1.94	0.2158	not significant
Pure Error		5.14	6	0.86			

DOF: degrees of freedom.

Where process parameter ‘P’ stands for composition of CeO_2 abrasives in MR polishing fluid by percentage volume, ‘M’ for magnetising current, ‘S’ for rotational speed of solid core tool and R stands for working gap. ANOVA for this selected model is given in Table 4.9. Where F-value of model is 52.72 which states that model obtained is significant. Only 0.01% chance is there which can arise due to noise. And if the values of "Prob > F" are below than 0.0500, it means all the terms in model are significant. In this case model terms such as P, M, S, R, S^2, R^2, PS and MR are significant. Values higher than 0.1000 indicates that the terms of model are insignificant. Values of α are 0.1, 0.05 and 0.01 and for the hypothesis test the significant level (0.05) is α value. If p-value ≤ α value, then it is treated as significant and for this case p-value is significant. This level α corresponds to the value, which determine the rejection and acceptance of null hypothesis H_0. Value of $\alpha = 0.05$ which signifies true result for null hypothesis. This is denoted as Type I error according to decision theory. Probability to cause an Type I error = significant level α. Small α is selected to lessen the probability that Type I error will occur. Significant terms in this case are P, M, S, R, S^2, R^2, PS and MR. If p-values > 0.05 indicating that the terms for fit is not significant. For improvement of the model, the model reduction is done in order to remove the insignificant terms. Variation of the selected data near around the fit data is termed as “Lack of fit”. F-value for ‘Lack of fit’ is

1.94 and signifies that 21.58% chance which may arise due to noise. Table 4.10 list out the other ANOVA parameters.

Table 4.10: Other ANOVA parameters

Std. Dev.	1.16	R^2	0.9801
Mean	30.58	Adj R^2	0.9615
C.V.	3.79	Pred R^2	0.8708
PRESS	130.62	Adeq Precision	35.063

Coefficient of Variation (C.V.); Press: predicted residual sum of squares; Std. Dev.: standard deviance.

Table 4.11: Factor coefficients (coded form)

Factor	**Coefficient Estimate**	**DOF**	**Standard Error**	**95% CI Low**	**95% CI High**	**VIF**
Intercept	30.99823	1	0.373589	30.20194	31.79451	
P-abrasive	0.719185	1	0.285862	0.109885	1.328484	1.095532
M-current	1.609564	1	0.288483	0.994677	2.224451	1.115715
S-rpm	-4.74529	1	0.312704	-5.4118	-4.07878	1.216255
R-gap	-5.39016	1	0.290346	-6.00902	-4.77131	1.121802
P^2	0.87726	1	0.579049	-0.35695	2.111473	1.798057
M^2	-1.61263	1	0.832083	-3.38617	0.160915	3.712847
S^2	3.269867	1	0.860893	1.434916	5.104817	4.066405
R^2	-3.01905	1	0.679271	-4.46689	-1.57122	2.474344
PM	-0.61065	1	0.36028	-1.37857	0.157266	1.446926
PS	1.3359	1	0.379468	0.527084	2.144716	1.487176
PR	-0.07769	1	0.36028	-0.84561	0.69023	1.446926
MS	-0.60617	1	0.369031	-1.39274	0.180402	1.609356
MR	-2.36433	1	0.357048	-3.12536	-1.6033	1.506539
SR	0.3513	1	0.375837	-0.44978	1.152377	1.546527

DOI: degree of freedom; CI: confidence interval; VIF: variance inflation factor.

How feasible the model predicts the response value? For this, 'predicted R^2' is a measured. As predicted R^2 and adjusted R^2 must be within the range of 0.20 to 0.16 [Jha and Jain, 2008]. The predicted R^2 value is 0.8708 and adjusted R^2 value obtained is 0.9615, resulting in accepatable range. The signal to noise control are meausred by 'adequate precision'. The ratio of 35.063 indicates a type of signal which is in adequate level, desirable ratio should be more than 4. To navigate the design space this model can be used. The top and bottom bound of 95% confidence interval (CI) which rings up the coefficient estimate for that factor are the 95% CI high and low values. Table 4.11 lists out the true coefficient range which must be found within the 95% of time. If this range lies between upper limit and lower

limit then the coefficient of 0 is true, therefore no effect has been shown by the factor. Variance inflation factor (VIF) quantifies that till what extent the model variance is magnified by inadequacy of orthogonality in the design. The VIF is one in model, if and only if the factor is perpendicular to all other factors. Values > 10 indicates that the factors tally each other, i.e. factors are not independent. Coded factors final equation depending upon the calculated coefficient in Table 4.11 is given by Eq. (4.3)

$$\begin{aligned}&\%\text{ change in surface roughness } (\%\,\Delta Ra)\\&= +31.00 + 0.72A + 1.61B - 4.75C - 5.39D + 0.88A^2 - 1.61B^2 + 3.27C^2 - 3.02D^2\\&- 0.61AB + 1.34AC - 0.078AD - 0.61BC - 2.36BD\\&+ 0.35CD \end{aligned} \quad (\mathbf{4.3})$$

Actual factors final equation is given by Eq. (4.4)

$$\begin{aligned}&\%\text{ change in surface roughness } (\%\,\Delta Ra)\\&= +57.43392 - 1.32028P + 21.16339M - 0.33769S + 111.20559R + 0.035090P^2\\&- 1.61263M^2 + 0.000326987S^2 - 75.47635R^2 - 0.12213PM + 0.00267180PS\\&- 0.077689PR - 0.00606169MS - 11.82167MR\\&+ 0.017565SR \end{aligned} \quad (\mathbf{4.4})$$

Table 4.12: ANOVA for percentage change in surface roughness (%ΔR_a) after dropping the insignificant terms

Source	**Sum of squares**	**DOF**	**Mean square**	***F*-value**	**Prob > *F***	**Remark**
Model	970.51	8	121.31	62.65	< 0.0001	Significant
P	11.66	1	11.66	6.02	0.0230	
M	40.49	1	40.49	20.91	0.0002	
S	338.81	1	338.81	174.98	< 0.0001	
R	453.11	1	453.11	234.01	< 0.0001	
S^2	32.62	1	32.62	16.85	0.0005	
R^2	43.87	1	43.87	22.65	0.0001	
PS	30.39	1	30.39	15.69	0.0007	
MR	69.12	1	69.12	35.70	< 0.0001	
Residual	40.66	21	1.94			
Lack of Fit	35.52	15	2.37	2.76	0.1084	not significant
Pure Error	5.14	6	0.86			

DOF: degrees of freedom.

Model terms are insignificant as p-value is found above 0.05. There are eight insignificant model terms from Table 4.9. Further, contraction of model by removing those eight insignificant terms can do improvement in the model. After removing those eight insignificant terms from the model, ANOVA is listed in Table 4.12 and Table 4.13.

Table 4.13: Other ANOVA parameters after model reduction

Std. Dev.	1.39	R^2	0.9598
Mean	30.58	Adj R^2	0.9445
C.V.	4.55	Pred R^2	0.9020
PRESS	99.13	Adeq Precision	36.124

Coefficient of Variation (C.V.) Press: predicted residual sum of squares; Std. Dev.: standard deviance.

The F-value of model is 62.65 which hint to significant model. Only 0.01% chance is there for F-value of model that may arise due to noise. Values lower than 0.05 of 'prob > F' indicates that the terms in model are significant. Model terms P, M, S, R, S^2, R^2, PS and MR are significant for this case. Range is acceptable for 'predicted R^2 of 0.9020 with the 'adjusted R^2' of 0.9445. "Adequate Precision" quantifies the S/N ratio (signal to noise). If S/N ratio is higher than 4, it is acceptable for the model. The S/N ratio of 36.124 point out an adequate signal. To navigate the design space this model may be used. Table 4.14 represents the range that the true coefficient must be found to 95% of the time after the reduction of the model.

Table 4.14: Factor coefficients (coded form) after model reduction

Factor	**Coefficient Estimate**	**DOF**	**Standard Error**	**95% CI Low**	**95% CI High**	**VIF**
Intercept	31.069	1	0.42	30.1	31.93	
P-abrasive	0.83	1	0.34	0.13	1.53	1.06
M-current	1.54	1	0.34	0.84	2.25	1.06
S-rpm	-4.84	1	0.37	-5.60	-4.08	1.16
R-gap	-5.24	1	0.34	-5.96	-4.53	1.08
S^2	2.95	1	0.72	1.46	4.45	1.97
R^2	-3.44	1	0.72	-4.94	-1.93	1.94
PS	1.51	1	0.38	0.72	2.30	1.04
MR	-2.17	1	0.36	-2.93	-1.42	1.08

DOI: degree of freedom; CI: confidence interval; VIF: variance inflation factor.

The coded factors final equation is given by Eq. (4.5)

$$\%\ change\ in\ surface\ roughness\ (\%\ \Delta Ra) = +31.06 + 0.83A + 1.54B - 4.84C - 5.24D + 2.95C^2 - 3.44D^2 + 1.51AC - 2.17BD \quad (\mathbf{4.5})$$

The actual factors final equation is given by Eq. (4.6)

$$\%\ change\ in\ surface\ roughness\ (\%\ \Delta Ra) = +53.56704 - 1.03971P + 10.23753M - 0.31459S + 132.92688R + 0.000295031S^2 - 85.88119R^2 + 0.00301339PS - 10.86568MR \quad (\mathbf{4.6})$$

% contributions of each process parameter and conditions in terms of on the final response of R_a values are shown in Table 4.15.

Table 4.15: Percentage contribution of process parameters and conditions in final response of R_a value

Source	Sum of squares	Percentage contribution
P	11.66	1.14
M	40.49	3.97
S	338.81	33.21
R	453.11	44.42
S^2	32.62	3.19
R^2	43.87	4.30
PS	30.39	2.98
MR	69.12	6.77
Pure error	5.14	1.14

4.6 Results and Discussion

Considering regression analysis of the surface response, the results of effect of process parameters and conditions are checked. And the effects of composition of CeO_2 abrasives (P) in MR polishing fluid, magnetising current (M), rotational speed of solid core tool (S) and working gap (R) on the percentage change in surface roughness (% ΔR_a) values has been discussed in this section.

4.5.1 Effect of Composition of CeO_2 Abrasives in Magnetorheological Fluid

The effect of composition of abrasives in magnetorheological fluid on the % ΔR_a is shown in Fig. 4.4. With an increase in percentage volume of abrasive particles, the % ΔR_a values increases. On increasing the number of abrasive particles, the numbers of cutting edges are also increased at the allocated region for finishing. These cutting edges facilitate the material removal of the peaks on the surface of BK7 glass by action of lateral crack to the micro chipping. Hence, on increasing the concentration of CeO_2 in the MR polishing fluid the R_a values are reduced.

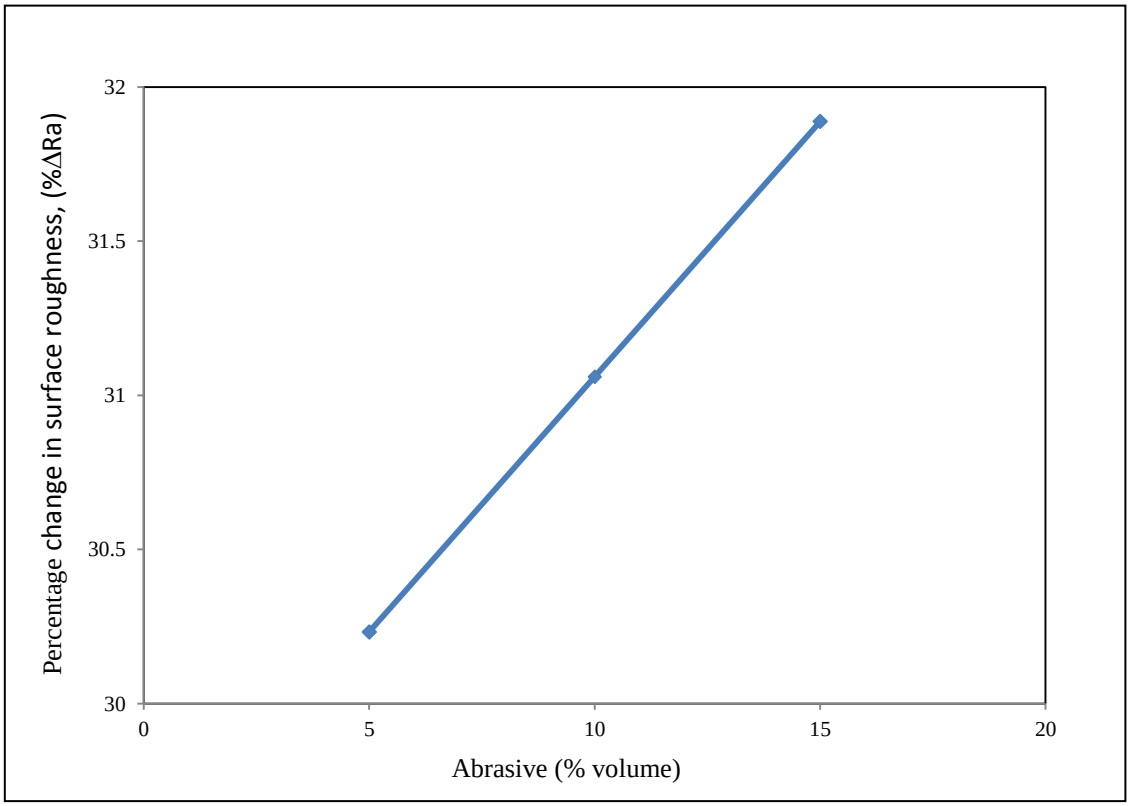

Fig. 4.4: Effects of concentration of CeO_2 abrasives by % volume on the percentage change in surface roughness at magnetising current of 2 Amp, rotational speed of solid core tool of 400 rpm and working gap of 0.8 mm

The value of optimum parameter cannot be determined from plot as shown in Fig. 4.4. Therefore, this research is further extended to study the effects of abrasive concentration on % ΔR_a values. Only CeO_2 concentration (by % volume) is altered and the other process parameters are taken as constant with respect to optimum values. Figure 4.5 shows the effects of high concentration of abrasive by % volume on percentage change in surface roughness

(magnetising current = 3 Amp, rotational speed of solid core tool = 300 rpm and working gap = 0.6 mm). This reveals that the optimum value of CeO_2 concentration is 15 (by% volume).

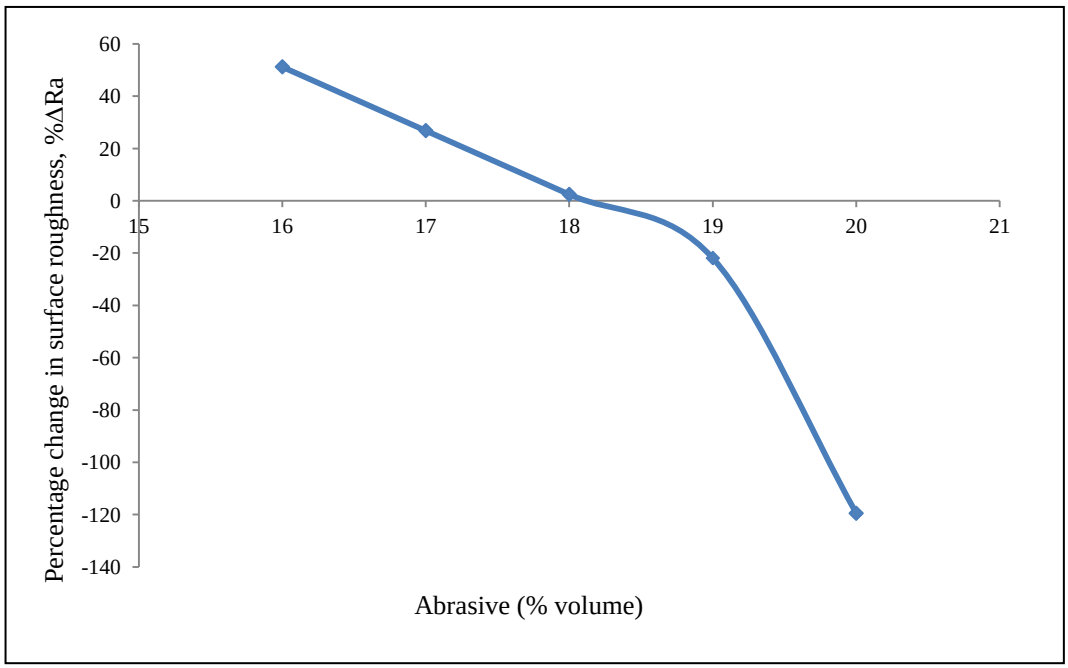

Fig. 4.5: Effects of high concentration of CeO_2 abrasives by % volume on percentage change in surface roughness (magnetising current = 3 Amp, rotational speed of solid core tool = 300 rpm and working gap = 0.6 mm)

4.5.2 Effects of Magnetising Current

The effect of magnetising current on the % ΔR_a values is shown in Fig. 4.6. It has been observed that % ΔR_a increases with increase in magnetising current. As on increasing the magnetising current i.e. the direct current supply to the electromagnetic coil, magnetic flux density increases during the finishing at the terminus of the solid rotating core tool. This results in holding the CeO_2 abrasive particles tightly by the magnetised iron particles. For a particular time period, continuous finishing of BK7 glass with high bonding strength of the magnetised iron particles rapidly increases the % ΔR_a values.

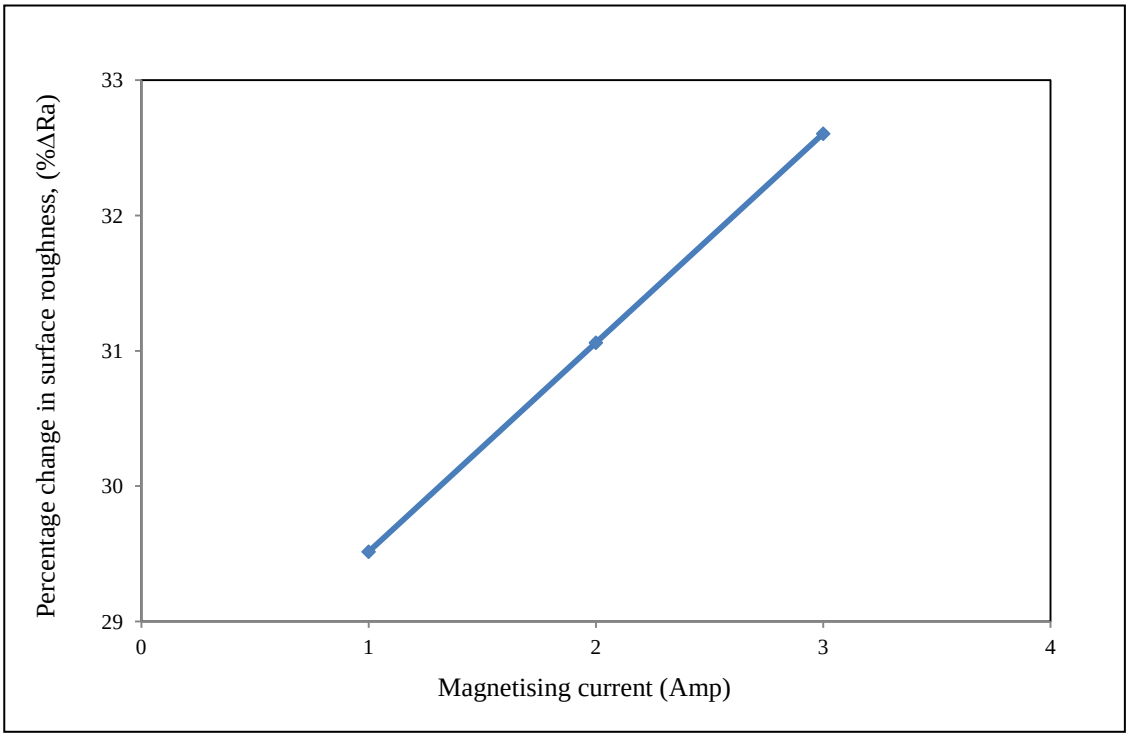

Fig. 4.6: Effect of magnetising current on percentage change in surface roughness (%ΔR_a) at CeO_2 abrasives of 10 % by volume, rotational speed of solid core tool of 400 rpm and working gap of 0.8 mm

4.5.3 Effects of Rotational Speed of Solid Core Tool

Figure 4.7 shows the effect of rotational speed of solid core tool on % ΔR_a values. Increase in rotational speed of the solid core tool causes reduction % ΔR_a values. It mainly occurs due to the effects of centrifugal force acting on magnetised particles of iron rises above the magnetic force of attraction between those particles at higher rotational speed. It results in loosening the grip of magnetised iron particles over the abrasive particles. Due to decrease in magnetic force of attraction and the loose grip of magnetised iron particles, few abrasive particles are pushed away from the allocated region of finishing. Therefore, magnetic force of attraction must be greater than the fictitious force so as to obtain required strength of magnetised iron particles chain and proper griping for CeO_2 abrasive particles.

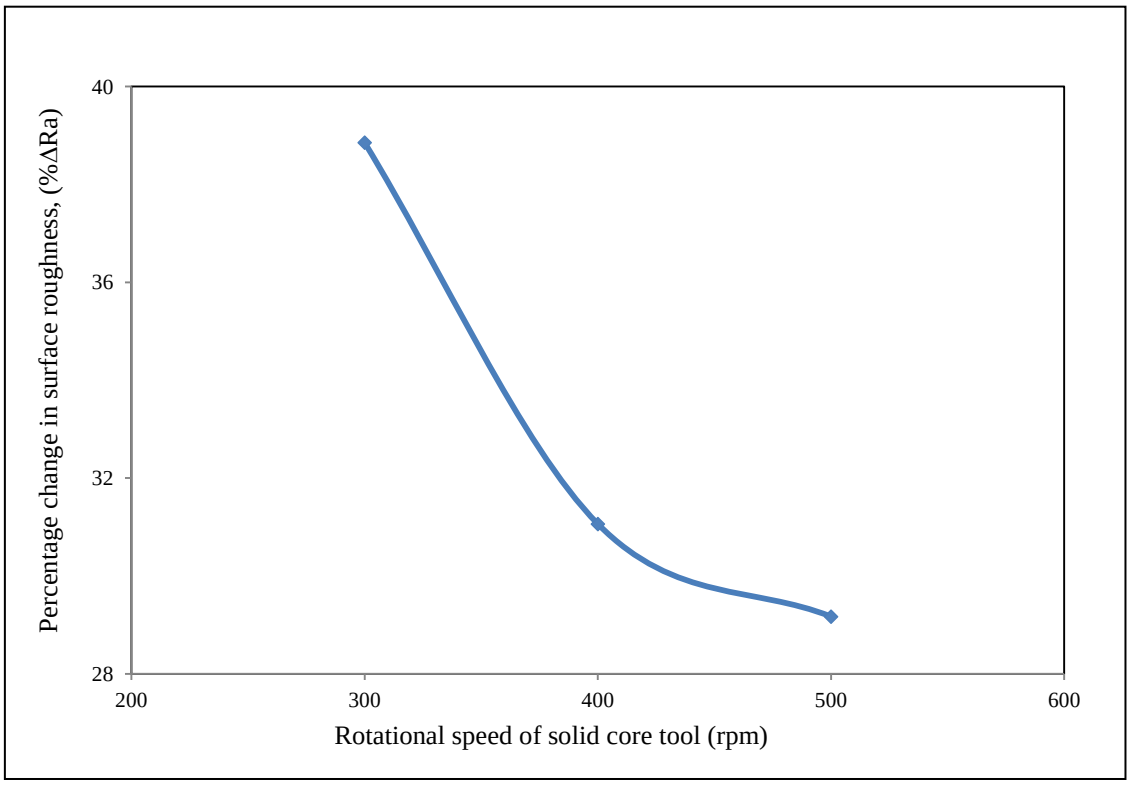

Fig. 4.7: Effect of rotational speed of solid core tool on percentage change in surface roughness (%ΔR_a) at CeO_2 abrasive of 10 % volume, magnetising current of 2 Amp and working gap of 0.8 mm

4.5.4 Effect of Working Gap

The influence of working gap distance on the % ΔR_a values is shown in Figure 4.8. It has been noticed that on increasing the working gap during finishing, the % ΔR_a values gets decreased. The magnetic flux density is inversely proportional to the gap. If the working gap is reduced, the magnetic flux density is increased in the finishing region of MR polishing fluid [Sidpara and Jain, 2011]. Due to this, strong magnetic field is generated at tool extremity surface if BK7 glass comes closer to the solid core tool tip. When the distance of BK7 glass surface and tip of the tool is increased, the strength of MR polishing fluid finishing region is decreased. Because of this the magnetised iron particles could not able to grip the abrasives firmly. This results in decreased % ΔR_a values. It has been interpreted from the Figure 4.8 that the % ΔR_a values reduce throughout the selected range of the working gaps. But this reduction in the change in surface roughness is not uniform. As this MRF process implemented on the finishing of optical glass, the chemical reactions also plays an extensive role in removing the peaks of the surface profiles. Firstly, the peaks get rot due to the

interaction of SiO_2 particles of BK7 glass workpiece surface with the water molecule present in MR polishing fluid. Second step is the mechanical abrasion from the surface of BK7 glass by the CeO_2 abrasive particles provided by rotational motion of the solid core tool. Thus, the chemically reacted peaks may get trimmed off easily at shorter working gap. This result in less % ΔR_a values from the working gap of 0.6 mm to 0.8 mm and more % ΔR_a values from the working gap of 0.8 mm to 1.0 mm.

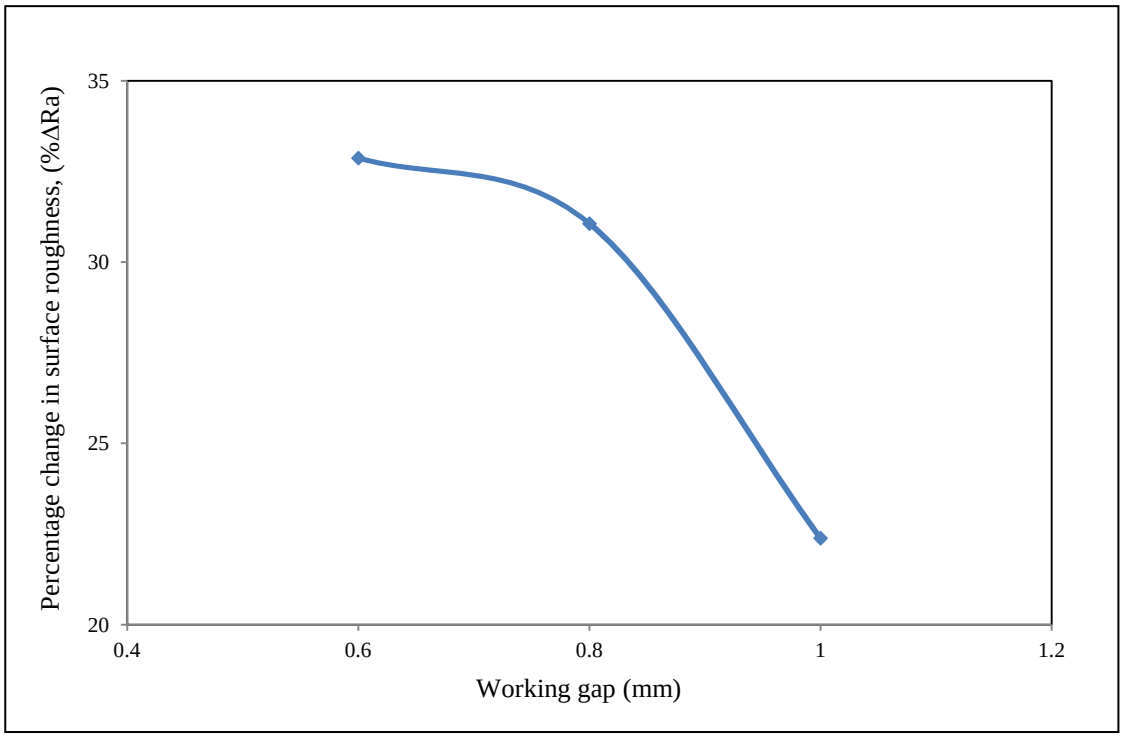

Fig. 4.8: Effect of working gap on percentage change in surface roughness (%ΔR_a) at CeO_2 abrasives of 10 % by volume, magnetising current of 2 Amp and rotational speed of solid core tool of 400 rpm

4.5.5 Effect of Interaction of Process Parameter on the % ΔR_a Values

There are two interactions that are found to be significant in the model. Both the parameters like abrasive composition (% volume) in MR polishing fluid and rotational speed of solid rotating core tool (rpm) together influences the percentage % ΔR_a values with 2-D and 3-D plot is shown in Figures 4.9(a) and 4.9(b) respectively.

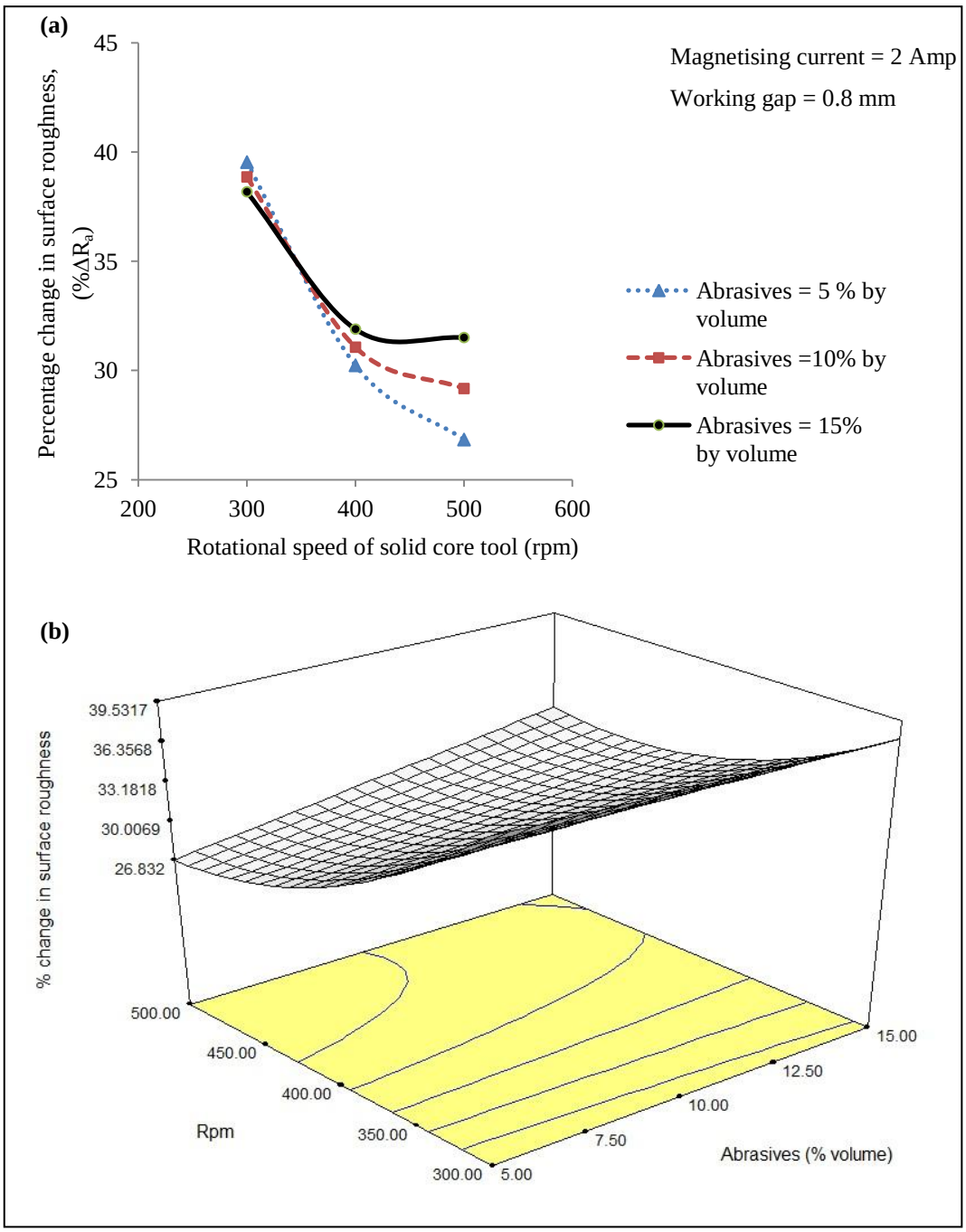

Fig. 4.9: Plots for percentage change in surface roughness (a) 2-dimensional and (b) 3-dimensional with CeO_2 abrasives composition in MR polishing fluid and rotational speed of solid core tool

At low concentration of abrasives with increase in rotational speed of the solid core tool, the % ΔR_a values decreases. This may be due to the increasing centrifugal force beyond a limit of magnetic force that results in throwing out the abrasive particles from the grip of magnetised iron particles chain. Perhaps at high concentration of CeO_2 abrasives (% volume)

with increasing rotational speed of the solid core tool, the % ΔR_a values increased as shown in Fig. 4.9(a). As the number of cutting edges are increased at high concentration of CeO_2 particles in MR polishing fluid which results in large material removal from the BK7 glass work piece.

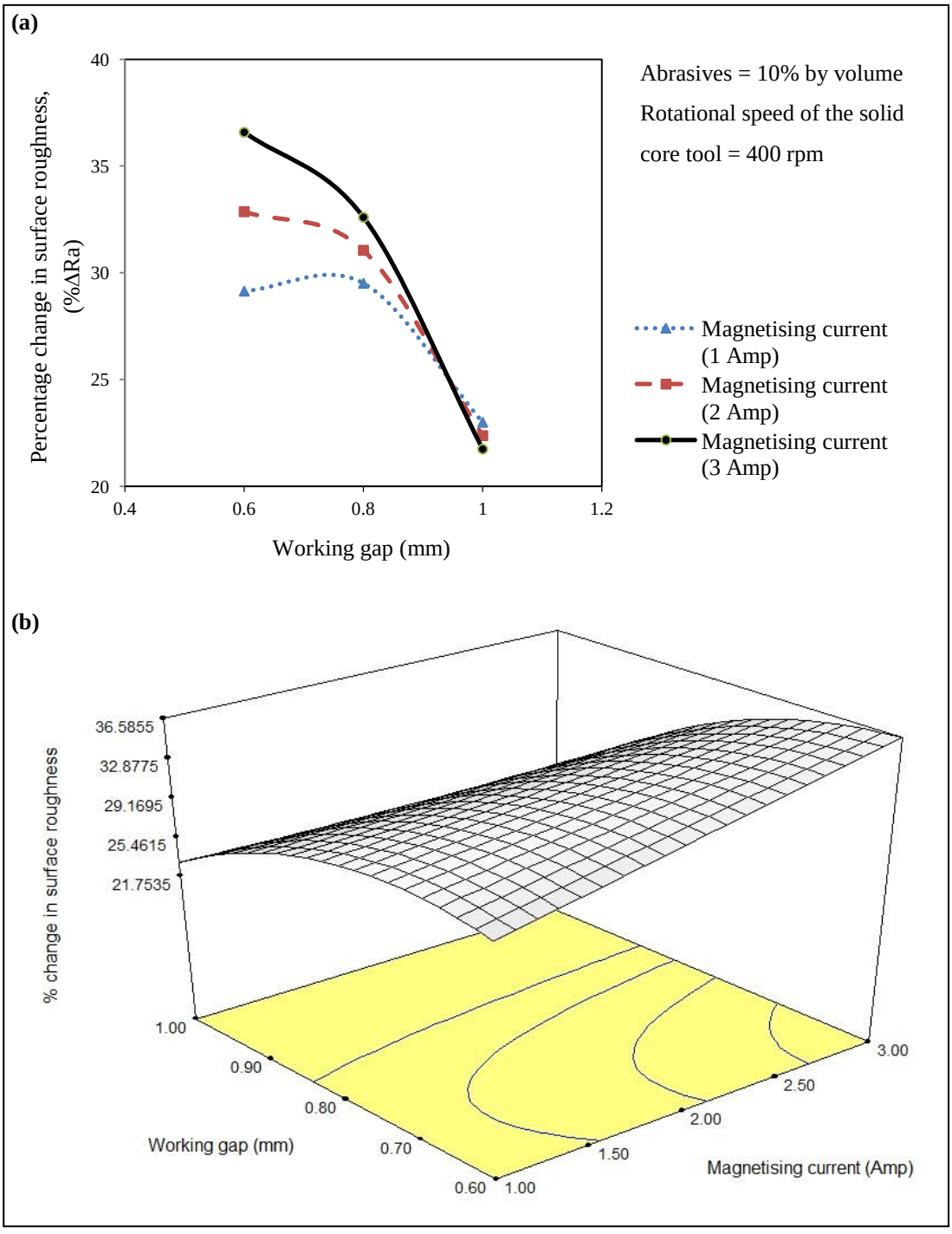

Fig. 4.10: Plots for percentage change in surface roughness (a) 2-dimensional and (b) 3-dimensional with magnetising current and working gap

The other interaction between magnetising current and working gap that effect the % ΔR_a values are shown as 2-D plot and 3-D plot in Figures 4.10(a) and 4.10(b) respectively. As the magnetising current increases along with the working gap, both together reduce the % ΔR_a.

6. Confirmation Tests for Comparison and Validation of the Results

The optimum process parameters are taken from the solutions of the quadratic model and conformation tests were performed. To verify the validity of surface response Eq. (4.5), three experiments are performed and their R_a values are measured. Table 16 shows the comparison and validation of the results of the confirmation tests with the predicted % ΔR_a values. After performing the analysis, it has been observed that % error between experimental and predicted values of % ΔR_a values lies in the range from -5.49% to 1.48%. Hence it confirms that the model is acceptable.

Table 4.16: Comparison and validation of the results of confirmation tests

S. no.	**Experimental conditions**				**Experimental values of %ΔR_a**	**Predicted values of %ΔR_a**	**% Error**
	P	**M**	**S**	**R**			
1	10	2	400	0.8	32.5	31.06	-1.44
2	15	2	500	0.6	38.8	33.3097	-5.49
3	10	3	400	0.8	35.9	32.605	-3.29
4	5	1	300	1	30	31.4819	1.48
5	15	3	500	1	24	22.1958	-1.80

The optimum finishing conditions are recorded within the experimental range of process parameters and lies at P = 15 (% volume), M = 3 (Amp), S = 300 (rpm) and R = 0.6 (mm). The surface roughness profiles of unfinished and finished BK7 glass specimen are shown in Figures 11(a) and 11(b). The surface roughness value of the BK7 glass workpiece achieved at optimum finishing conditions is R_a = 22 nm from the initial R_a = 41 nm.

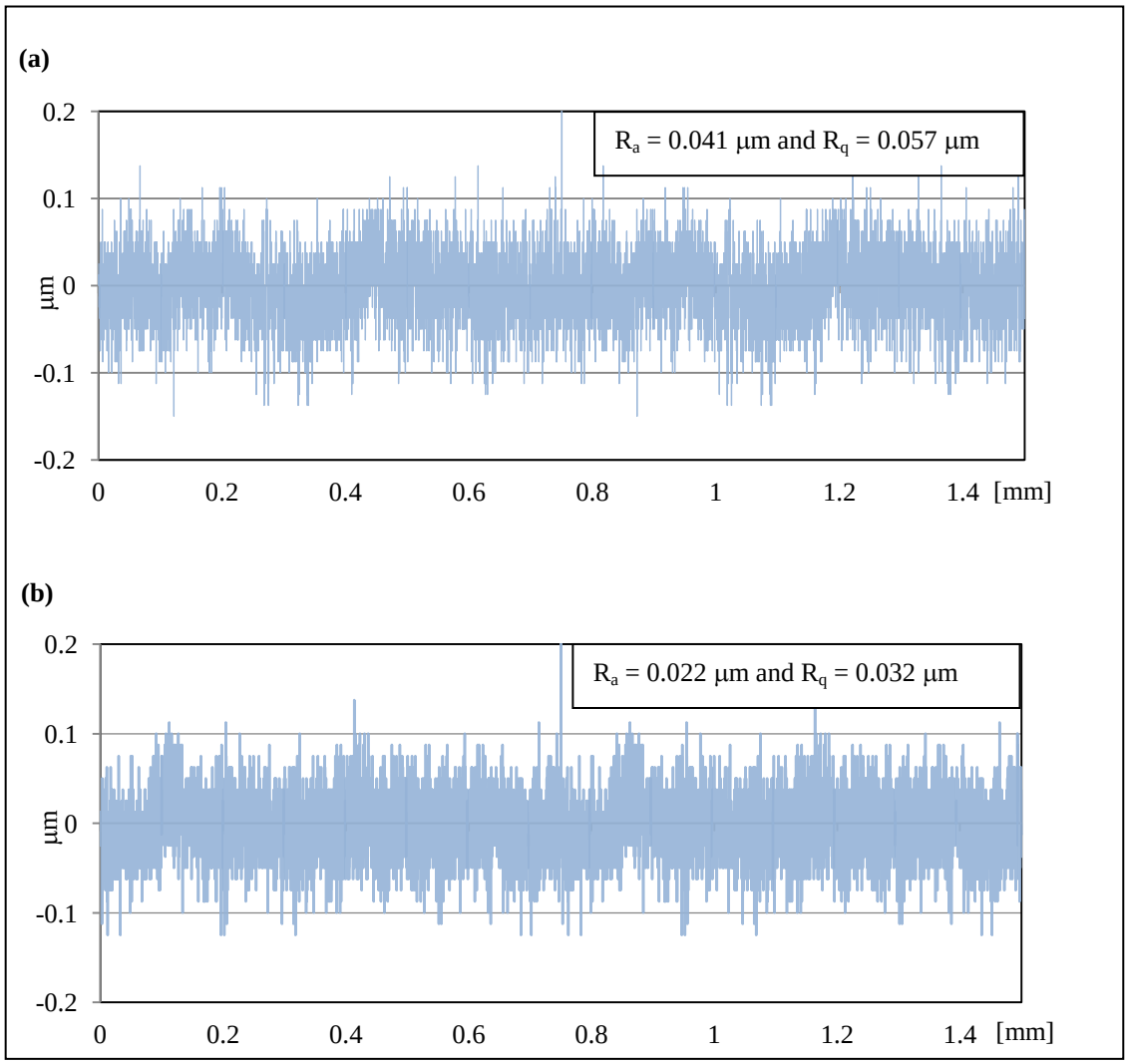

Fig. 4.10: Surface roughness profiles of (a) unfinished and (b) finished BK7 glass specimen at CeO_2 abrasives of 15 % by volume, magnetising current of 3 Amp, rotational speed of solid core tool of 300 rpm and working gap of 0.6 mm

To study and compare the surface morphology of unfinished and finished BK7 glass specimen, scanning electron microscopy (SEM) is performed. SEM images are taken at 6000× for unfinished and finished BK7 glass specimen as shown in Figure 12. The contrasted area in Figure 12(a) indicates the multiple number of debris that are visible on the surface of unfinished BK7 glass workpiece. Most of the debris are removed from the surface of BK7 glass workpiece by performing the magnetorheological finishing using solid rotating core tool at optimum finishing conditions. SEM image of finished BK7 glass workpiece is exhibited in Figure 12(b).

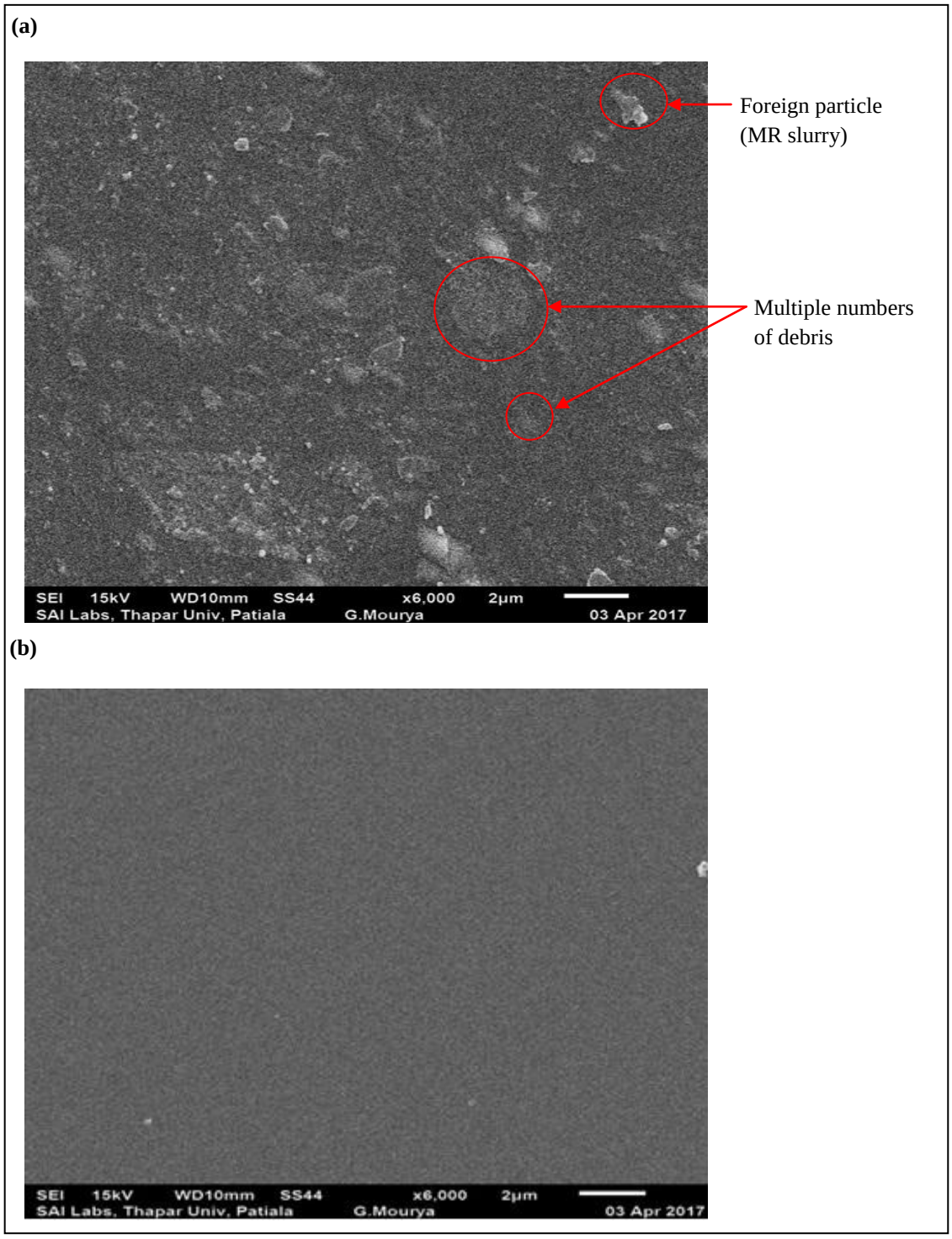

Fig. 4.12: Scanning electron microscope images taken at 6000× for (a) unfinished BK7 glass and (b) finished BK7 glass at CeO_2 abrasives of 15 % by volume, magnetising current of 3 Amp, rotational speed of solid core tool of 300 rpm and working gap of 0.6 mm

4.6 Conclusions

Nanofinishing of BK7 optical glass has been successfully performed using MRF process with solid core rotating tool. The task of material removal is profited by the proper concentration of CeO_2 abrasive particles and strongly performed as the key role in abrasion mechanism. Based on the results from the statistical study, the following conclusions were judged.

- A statistical study and surface response regression analysis has been performed well using Box-Behnken Design (BBD) with four factors and three levels.
- The working gap has been as a prominent parameter that affects the percentage in surface roughness ($\%\Delta R_a$) value with 44.42 % contribution on the improvement of surface roughness value.
- Out of 14 model terms only two interactions have been found significant, such as CeO_2 abrasives composition (% volume) with rotational speed of solid core tool (rpm) and magnetising current (Amp) with working gap (mm).
- Each and every CeO_2 abrasive particles were made functional in material removal mechanism of BK7 glass workpiece.
- Extended study on the concentration of CeO_2 abrasives in MR polishing fluid revealed the optimum value of 15 % by volume.
- The optimum finishing conditions were recorded at P = 15 % by volume, M = 3 Amp, S = 300 rpm and R = 0.60 mm.
- At the optimum finishing conditions, the final surface roughness value is obtained as low as 22 nm from the initial R_a = 41 nm of BK7 glass workpiece.

Chapter 5

Conclusions and Future Scope

5.1 Conclusions

In this thesis work, experiments on nanofinishing of BK7 glass and surface roughness profile tests with analysis of SEM are performed to understand the mechanism of material removal in MR finishing process on BK7 glass.

In chapter 3, the preliminary experiments are successfully conducted and reported. The Photospectroscopy test reveals that optical performance of the BK7 glass has been improved, by making the glass surface profile specular in nano-level range. The chemical and mechanical action material removal mechanism of BK7 glass has been presented and explained clearly.

Optical properties of BK7 glass such as absorbance, reflectance and transmittance are examined and overall good optical performance satisfied the materials standard of LARAMY-K optical lab for lens manufacturing. Further, a study has been performed on reduction of surface roughness values to the finishing time cycle. The lowest R_a and R_q values achieved after 90 minutes of finishing are 17 nm and 27 nm from 41 nm and 57 nm. Scanning electron microscopy showed improved results in surface morphology of finished BK7 glass at CeO_2 abrasives concentration of 10 % by volume, magnetizing current of 1 Amp, rotational speed of solid rotating core tool of 300 rpm and working gap of 0.8 mm. BK7 finds its relevance in transmissive optics of defense sector, as the application like long range binoculars.

In chapter 4, the role of MR finishing process including concentration CeO_2 abrasive powder, magnetizing current, rotational speed of solid core tool and working gap distance are studied and discussed. For the first time the investigation on these process parameters is done, which are applied for finishing BK7 glass with the MR finishing process using solid core rotating tool.

However, results of the response surface methodology illustrated that percentage contribution of working gap in the $\%\Delta R_a$ is found to be the most prominent factor. An extended study was performed to get the optimum value of abrasive concentration, where 15

% of CeO_2 is concluded as per this extended study. The optimum process parameters were obtained as CeO_2 abrasives concentration of 15 % by volume, magnetizing current of 3 Amp, rotational speed of solid core rotating tool of 300 rpm and working gap of 0.60 mm. Validation and confirmation of the experiments are analyzed, the % error for statistical designed model is found in range of -5.49 % to 1.48 % acceptable. The best surface roughness value at optimum conditions achieved is 22 nm from the initial of 41 nm in 30 minutes of finishing time.

5.2 Future Scope

- The nanofinishing of BK7 glass is a hard task as compared with other materials finishing. The work like handling and cleaning of BK7 glass workpiece requires a lot of special care, therefore development can be done on the devices like ultra sonic cleaner etc.
- A study can be done on finishing of same glass, by giving “Bi-directional motion” to the tool.
- Aspheric surface can be finished with addition of axis to the MRF setup.
- Effects of temperature, abrasive particle size and magnetized iron particle size on the percentage change in surface roughness value can be investigated using the same process and material.
- A study can be performed on the finishing of the same glass with opposite direction spins of both the workpiece and tool.

References

Baranwal, D.; Deshmukh, T.S. (2012) MR-fluid technology and its application - A review, International Journal of Emerging Technology and Advanced Engineering, 2, Issue 12.

Blaineau, P.; Andre, D.; Laheurte, R.; Darnis, P; Darbois, N.; Cahuc, O.; Neauport, J. (2015) Subsurface mechanical damage during bound abrasive grinding of fused silica glass, *Applied Surface Science*, 353: 764-773.

Belkhir, N.; Chorfa, A.; Bouzid, D. (2016) Compression behavior of polyurethane polishers in optical polishing process, *International Journal of Advanced Manufacturing Technology*, DOI:10.1007/s00170-016-8393-y.

Bennett, J.M.; Shaffer, J.J.; Shibano, Y.; Namba,Y. (1987) Float polishing of optical materials, *Applied optics*, 26: 696-703.

Bulsara, V.H.; Ahn, Y.; Chandrasekar, S.; Farris, T.N. (1998) Mechanics of polishing, *Journal of Applied Mechanics-Transactions of the ASME*, 65: 410-416.

Cheng, H.; Feng, Z.; Wang, Y.; Lei, S. (2007) Magnetorheological finishing of SiC Aspheric Mirrors, *Materials and Manufacturing Processes*, 20: 917-931.

Cook, L.M. (1990) Chemical processes in glass polishing, *Journal of Non-Crystalline Solids*, 120: 152-171.

Das, M.; Jain, V.K.; Ghoshdastidar, P.S. (2010) Nano-finishing of stainless-steel tubes using rotational magnetorheological abrasive flow finishing process, *Machining Science and Technology: An International Journal*, 14: 365-389.

Das, C.R. (2014) The reaction between borate glass and attacking agents-part III: equilibrium pH of the alkali borate glasses and their relationship with chemical durability and the glass composition, *Transactions of the Indian Ceramic Society*, 26: 155-158.

DeGroote, J.E.; Marino, A.E.; Wilson, J.P.; Bishop, A.L.; Lambropoulos, J.C.; Jacobs, S.D. (2007) Removal rate model for magnetorheological finishing of glass, *Applied Optics*, 46: 7927-7941.

Faberge, A.C. (1968) Polishing laps out of Teflon, *AIP-Review of Scientific Instruments*, DOI:10.1063/1.1683504.

Feng, J.; Chen, P.; Ni, J. (2012) Prediction of surface generation in microgrinding of ceramic materials by coupled trajectory and finite element analysis, *Finite Elements in Analysis and Design*, 57: 67-80.

Gan, S.; Zhou, Q.; Xu, X.; Hong, Y.; Liu, Y.; Fu, S. (2007) Study on the surface roughness of substrate with multi-fractal spectrum, *Microelectronic Engineering*, 84: 1806-1809.

Golini, D.; Kordonski, W.I.; Dumas, P.; Hogan, S. J. (1990) Magnetorheological finishing (MRF) in commercial precision optics manufacturing, *Proceedings of SPIE*, 3782: 80-91.

Guo, B; Zhao, Q; Fang, X. (2014) Precision grinding of optical glass with laser micro-structured coarse-grained diamond wheels, *Journal of Materials Processing Technology*, 214: 1045-1051.

Guo, H.; Wu, Y.; Lu, D.; Fujimoto, M.; Nomura, M. (2014) Effects of pressure and shear stress on material removal rate in ultra-fine polishing of optical glass with magnetic compound fluid slurry, *Journal of Materials Processing Technology*, 214: 2759-2769.

Hahimoto, F.; Yamaguchi, H.; Krajnik, P.; Wegener, K.; Chaudhari, R.; Hoffmeister, H.W.; Kuster, F. (2016) Abrasive fine finishing technology, *CIRP Annals – Manufacturing Technology*, 65: 597-620.

Harris, D.C. (2011) History of magnetorheological finishing, *Proceedings of the Window and Dome Technologies and Materials, SPIE*, DOI: 10.1117/12.882557.

Heinzel, C.; Rickens, K. (2009) Engineered wheels for grinding of optical glass, *CIRP Annals-Manufacturing Technology*, 58: 315-318.

Heslin, T.; Heaney, J.; Harper, M. (1974) The effects of particle Size on the optical properties and surface roughness of a glass-balloon-filled black paint, *NASA Technical Notes*, D, 7643.

Hoshino, T.; Kurata, Y.; Terasaki, Y.; Susa, K. (2001) Mechanism of polishing of SiO_2 films by CeO_2 particles, *Journal of Non-Crystalline Solids*, 283: 129-136.

Izman, S.; Venkatesh, V.C. (2007) Gelling of chips during vertical surface diamond grinding of BK7 glass, *Journal of Materials Processing Technology*, 185: 178-183.

Jacobs, S.D. (2007) Manipulating mechanics and chemistry in precision optics finishing, *Science and Technology of Advanced Materials*, 8: 153-157.

Jacobs, S.D.; Golini, D.; Hsu, Y.; Puchebner, B.E.; Strafford, D.; Kordonski, W.I.; Jacobs, S.D.; Arrasmith, S.A.; Kozhinova, I.A.; Gregg, L.L.; Shorey, A.B.; Romanofsky, H.J.; Golini, D.; Kordonski, W.I.; Dumas, P.; Hogan, S. (1999) An overview of magnetorheological finishing (MRF) for precision optics manufacturing, *ACERS 102: Ceramic Transactions*, R. Sabia, V.A. Greenhut, and C. Pantano, eds. (1999).

Jain, V.K. (2009) Magnetic field assisted abrasive based micro-/nano-finishing, *Journal of Materials Processing Technology*, 209: 6022-6038.

Jha, S.; Jain, V.K. (2005) Nano finishing techniques, *Micro manufacturing and Nano-Technology*, 171-195.

Jha, S.; Jain, V.K. (2008) Parametric analysis of magnetorheological abrasive flow finishing process, *International Journal of Manufacturing Technology and Management*, 13: 308-323.

Jiao, L.; Wu, Y.; Wang, X.; Guo, H.; Liang, Z. (2013) Fundamental performance magnetic compound fluid (MCF) wheel in ultra-fine surface finishing of optical glass, *International Journal of Machine Tools and Manufacture*, 75: 109-118.

Kordonski, W.I.; Shorey, A.B.; Tricard, M. (2006) Magnetorheological jet finishing technology, *Transactions of ASME*, 128: 21-26.

Kordonski, W.I.; Golini, D. (1999) Fundamentals of magnetorheological fluid utilization in high precision finishing, *Journal of Intelligent Material Systems and Structures*, 10: 683-689.

Kordonski, W.I.; Jacobs, S.D. (1996) Magnetorheological finishing. *International Journal of Modern Physics B*, 10: 2857-2865.

Kordonski, W.I.; Jacobs, S.D. (1996) Magnetorheological finishing, *International Journal of Modern Physics B*, 10: 2857-2865.

Kordonski, W.I.; Golini, D.; Dumas, P.; Hogan, S.J.; Jacobs, S.D. (1998) Magnetorheological suspension-based finishing technology, *Proceedings of SPIE*, 3326**:** 527-535.

Khurana, A.; Singh, A.K.; Bedi, T.S. (2017) Spot nanofinishing using ball nose magnetorheological solid rotating core tool, *The International Journal of Advanced Manufacturing Technology*, DOI: 10.1007/s00170-017-0166-8.

Lee, S.H.; Lu, Z.; Babu, S.V.; Matijevic, E. (2011) Chemical mechanical polishing of thermal oxide films using silica particles coated with ceria, *Journal of Materials Research*, 17: 2744-2749.

Lilienthal K.; Stubenrauch M.; Fischer, M.; Schober, A. (2010) Fused silica 'glass grass': fabrication and utilization, *Journal of micromechanics and microengineering*, 025017.

Maan, S.; Singh, G.; Singh, A.K. (2016) Nano surface finishing of permanent mold punch using magnetorheological fluid based finishing processes, *Materials and Manufacturing Processes*, DOI:10.1080/10426914.2016.1232823.

Manallah, A.; Bouafia, M. (2011) Application of the technique of total integrated scattering of light for micro-roughness evaluation of polished surfaces, *Physics Procedia*, 21: 174-179.

Malkin, S.; Hwang, T.W. (1996) Grinding mechanics for ceramics, *CIRP Annals – Manufacturing Technology*, 45: 569-580.

Miao, C.; Bristol, K.M.; Marino, A.E.; Shafrir, S.N.; DeGroote, J.E.; Jacobs, S.D. (2007) Magnetorheological fluid template for basic studies of mechanical-chemical effects during polishing, Proceedings of SPIE, 6671: 667110.

Miao, C.; Lambropoulos, J.C.; Jacobs, S.D. (2010) Process parameter effects on material removal in magnetorheological finishing of borosilicate glass," *Applied Optics*, 49: 1951-1963.

Montgomery, D.C. (Wiley, 2001) *Design and analysis of experiments*.

Onwuka, G.; Abou-El-Hossein, K. (2016) Surface roughness in ultra high precision grinding of BK7, *Procedia CIRP*, 45: 143-146.

Owen, J.D.; Davies, M.A.; Schmidt, D.; Urruti, E.H. (2015) On the ultra-precision diamond machining of chalcogenide glass, *CIRP Annals – Manufacturing Technology*, 64: 113-116.

Pa, P.S. (2009) Magnetic assistance in cylinder surface finish, *Materials and Manufacturing Processes*, 24: 819-823.

Pashmforoush, F.; Rahimi, A. (2015) Nanofinishing of BK7 optical glass using magnetic abrasive finishing process, *Applied Optics*, 54: 2199-2207.

Pattanaik, L.N.; Agarwal, H. (2014) Development of magnetorheological finishing (MRF) process for freeform surfaces, *International Journal of Advanced Mechanical Engineering*, 4: 611-618.

Prokhorov, I. V.; Fess, E.; Pietrowski, D.; Kordonski, V.W. (1995) Magnetorheological finishing: a deterministic process for optics manufacturing," *Proceedings of SPIE*, 2576: 372-382.

Rabinow, J. (1948) The Magnetic Fluid Clutch, *AIEE Transactions*, 67**:** 48-238.

Rahman, M.; Lim, H.S.; Neo, K.S.; Kumar, A.S.; Wong, Y.S.; Li, X.P. (2007) Tool-based nanofinishing and microfinishing, *Journal of Materials Processing Technology*, 185: 2-16.

Ravishankar, S.; Mahale, R. (2015) A study on magnetorheological fluids and their applications, *International Research Journal of Engineering and Technology*, 2: 2023-2028.

Rosenfeld, N.; Wereley, N.M.; Radakrishnan, R.; Sudarshan, T.S. (2002) Behavior of magnetorheological fluids utilizing nanopowder iron, *International Journal of Modern Physics B*, 16: 2392-2398.

Spaggiari, A. (2013) Properties and applications of magnetorheological fluids, *Frattura ed Integrità Strutturale*, 23: 57-61. DOI: 10.3221/IGF-ESIS.23.06

Shorey, A.B.; Jacobs, S.D.; Kordonski, W.I.; Gans, R.F. (2001) Experiments and observations regarding mechanisms of glass removal in magnetorheological finishing, *Applied Optics*, 40: 20-33.

Shorey, A.B. (2000) Mechanisms of material removal in magnetorheological finishing (MRF) of glass, PhD Thesis, University of Rochester, New York.

Sidpara, A.; Jain, V.K. (2011) Experimental investigations into forces during magnetorheological fluid based finishing process, International Journal of Machine Tools and Manufacturing, 51: 358-362.

Sidpara, A.; Das, M.; Jain, V.K. (2009) Rheological characterization of magnetorheological finishing fluid, *Materials and Manufacturing Processes*, 24: 1467-1478.

Sidpara, A,; Jain, V.K. (2012) Nano-level finishing of single crystal silicon blank using magnetorheological finishing process, *Tribology International*, 47: 159-166.

Singh, A.K.; Jha, S.; Pandey, P.M. (2011) Design and development of nanofinishing process for 3D surfaces using ball end MR finishing tool, International Journal of Machine Tools and Manufacture, 51: 142-151.

Singh, A.K.; Jha, S.; Pandey, P.M. (2012) Nanofinishing of a typical 3D ferromagnetic workpiece using ball end magnetorheological finishing process, *International Journal of Machine Tools & Manufacture*, 63: 21-31.

Singh, A.K.; Jha, S.; Pandey, P.M. (2012) Nanofinishing of fused silica glass using ball end magnetorheological finishing tool, Materials and Manufacturing Processes, 27: 1139-1144.

Singh, D.K.; Jain, V.K.; Raghuram, V. (2004) Parametric study of magnetic abrasive finishing process, *Journal of Materials Processing Technology*, 149: 22-29.

Singh, G.; Singh, A.K.; Garg, P. (2016) Development of magnetorheological finishing process for external cylindrical surfaces. *Materials and Manufacturing Processes*, DOI: 10.1080/10426914.2016.1221082.

Suzuki, H.; Moriwaki, T.; Okino, T.; Ando, Y. (2006) Development of ultrasonic vibration assisted polishing machine for micro aspheric die and mold, *CIRP Annals – Manufacturing Technology*, 55: 385-388.

Tsegaw, A.A.; Shiou, F.J.; Lin, S.P. (2015) Ultra-precision polishing of N-Bk7 using an innovative self-propelled abrasive fluid multi-jet polishing tool, *Journal of Mechanical Science and Technology*, 19: 262-285.

Wang, K.; Liu, S.; Chen, F.; Liu, Z.; Luo, X. (2009) Effect of manufacturing defects on optical performance of discontinuous freeform lenses, *Optics Express*, 17: 5457-5465.

Wang, J.; Meng, G. (2001) Magnetorheological fluid devices: principles, characteristics and applications in mechanical engineering, *Proceedings of the Institution of Mechanical Engineers, Part L: Journal of Materials: Design and Applications*, 215: 165-174.

Yokota, H.; Kinosita, K.; Sakata, H. (1969) Ellipsometric study of polished glass surfaces, *Japanese* Journal of *Applied Physics*, 3: 805-806.

Zhang, S.J.; To, S.; Wang, S.J.; Zhu, Z.W. (2015) A review of surface roughness generation in ultra precision machining, *International Journal of Machine Tools and Manufacture*, 91: 76-95.

Zhong, Z.W. (2008) Recent advances in Polishing of Advanced Materials, *Materials and Manufacturing Processes*, 23: 449-456.

Zhou, C; Zhang, Q.; He, C.; Li, Y. (2014) Functional liquid and tool wear in ultrasonic bound-abrasive polishing of fused silica with different polishing tools, *Optik*, DOI: http://dx.doi.org/10.1016/j.ijleo.2014.01.113.

List of Publications

SCI journal:

1. **Kumar, S.**; Singh, A.K. (2017) Magnetorheological nanofinishing of BK7 glass for lens manufacturing. *Materials and Manufacturing Processes*.
   Status: ***Accepted***
   Publisher: Taylor and Francis
   Impact factor: 1.419
2. **Kumar, S.**; Singh, A.K. (2017) Parametric analysis of magnetorheological nanofinishing process with solid core rotating tool on BK7 glass. *Applied Optics.*
   Status: ***Under review***
   Publisher: The Optical Society (OSA)
   Impact factor: 1.650

International Conferences:

1. **Kumar, S.**; Singh, A.K. (2016) Magnetorheological finishing techniques for optical glasses: a review. 4th International conference on production and industrial engineering, CPIE-2016, December 20, 2016 at NIT Jalandhar.
   Status: ***Published***